Department of Precision and Microsystems Engineering

Design and validation of a manoeuvering caging gripper for grasping in cluttered environments

Bart Friederich

Report no : 2022.010
Coach : Ir. A. E. Huisjes, Dr. Ir. V. van der Wijk
Professor : Prof. Dr. Ir. J. L. Herder
Specialisation : Mechatronic System Design
Type of report : MSc report
Date : 12/04/2022

TU Delft Delft University of Technology

Challenge the future

This page intentionally left blank.

Abstract

In this research, the problem of robotic grasping in dense clutter was analyzed from a mechanical engineering perspective. This has resulted in a prototype of an innovative new caging gripper for grasping in clutter, which was proven to be highly successful.

The research started with a literature review, in which the state-of-the-art of robotic grasping of difficult objects was analyzed, especially in the context of cluttered environments. It was concluded that a caging gripper is a universally good gripper for difficult objects, since it does not rely on friction and therefore has no minimum requirements on grasp force or object friction. However, it was also seen that for dense clutter, the caging gripper does not work, because it requires most of the object surface to be free for it to be reliably applied. The literature study concluded with the suggestion of redesigning the caging gripper so that it can mechanically deal with clutter. This is a novel approach compared to existing researches which try to solve the problem of clutter only in perception and planning.

Then, the functions behind caging grasping and caging grasping in clutter especially, were analyzed. This resulted in two additional sub-functions of the grasp manoeuvre which are relevant for minimizing the disturbance and forces on the object and surrounding clutter. Different fundamental strategies for these functions were analyzed, and it was found that by using object-following, forward propagating fingers, spatial disturbance during the grasp manoeuvre was minimized. Furthermore, by using everting surfaces on the propagating fingers, friction forces during this motion could be fully eliminated. Several concepts which implemented the above strategies were then conceived. A version using a flexible object-following backbone covered with zero-slip eversion belts was found to be the least complex to prototype.

Using this concept as a starting point, a prototype of the gripper was designed. The goal of this prototype was to first verify that a gripper with these functions could be built, and later demonstrate that the underlying new strategy of the concept indeed allows caging grasping in clutter. The designed gripper finger used a spring steel backbone, which was pre-curved to follow the object surfaces, and could be retracted into a channeled wrist-part. A system of pulleys was integrated into the backbone, to guiding two belts along the inner and outer contact surfaces of the finger backbone, which actively rolled out and retracted when the finger was exerted or retracted from the wrist. Three of these fingers were mount together on a hub to form a 3-fingered gripper for spherical objects.

The functions incorporated into the gripper were verified to be working using four different lab setups, which individually measured the object-following propagation path, the forces exerted on object and environment, and the holding force of the gripper. This showed that the gripper can set a sufficiently strong caging grasp by manoeuvering its fingers along the object surface, while only taking up the space required for the finger thickness. Furthermore, the forces exerted on the object and environment were shown to be negligible.

After the prototype was verified to be working properly, it was subjected to a practical test to demonstrate that this manoeuvering caging gripper indeed allows for grasping in dense clutter. For the practical test, the gripper was integrated with a robotic system consisting of a robot arm, a camera, and perception and planning software. Using this system, a cluttered pile of 32 tomatoes was successfully picked and placed one by one. The practical experiment showed that with little planning effort and no obstacle recognition, the gripper was able to successfully move all 32 tomatoes, most of which were obstructed by the cluttered pile from multiple sides, which is a task which could hitherto not be done with existing caging grippers.

Preface

Before you lies my thesis on the design of a novel gripper for the agri-food industry. The research project was conducted as conclusion of the masters degree of High-Tech Engineering, a track of the Mechanical Engineering Masters at the Delft University of Technology.

Throughout the majority of 2021 and the start of 2022, my full time and attention was spent on exploring this subject of robotic manipulation in the agri-food industry. The subject for this thesis was seeded by the FlexCRAFT project, a research initiative which has the goal to connect the agri-food industry with research institutes, among which the Delft University of Technology.

During a literature study at the start of the project, the proposal to design a new gripper for grasping in clutter was conceived. This subject proved itself an interesting one for the application of various subjects of the Mechanical Engineering master, including the High-Tech subject of compliant mechanisms and soft robotics, as well as general design methodologies taught over the years. In particular, the use of a structured problem analysis, resulting in new insights and the ideation of new useful mechanisms, is a skill that is not acquired in a single course, but over the many courses and design projects that the program at TU Delft offers. From all the skills and knowledge that the curriculum at TU Delft teaches, I hope that especially this is expressed in this final work of my educational career.

Thoughout the project, I have had the fortune of working closely with my daily supervisor, Ad Huisjes, who helped me define a great project, and gave me excellent guidance during the process of working on this relatively large and independent project. Our meetings have become increasingly collaborative in nature, resulting in new insights and for me, a stronger thesis. This way, I got to enjoy a fair share of teamwork and shared accomplishment in a year which had the chance to become a dull and lonely one, due to the COVID pandemic which had students working from home for most of the year.

Additionally, my thanks go out to my professor, Just Herder, who made time to attend the weekly meetings with the ”gripper group”, consisting of a rotation of students that were also working on grippers during the year. His advise and knowledge, whether about engineering details of mechanics and prototyping, or about more transcendent topics such as the higher objectives of a master research project and academic research in general, were very insightful.

The beauty of engineering

Before going deep down the rabbit hole of the subject of grasping in dense clutter and all the mechanical aspects involved, I would like to share a view on mechanical engineering which was not taught in a course or class, and that was not found in any book that I had to read. Nonetheless, it is one of the things that makes me the engineer that I am.

That view is that mechanical engineering is more than purely a functional thing, a method of solving problems and improving efficiency. Engineering may as well be a thing of beauty: a sort of art. As mechanical engineers and researchers, we are taught to look at our designs objectively and evaluate complex designs by means of some performance metrics. However, when looking at my most passionate peers, teachers, and others in engineering, I propose that the performance metrics and efficiency are not what brought them there. It is, in fact, the beauty of engineering.

I doubt that there is an engineer who has not at some point thought, while looking at some innovative piece of engineering: That's just beautiful. It could have been a complex machine with hundreds of parts meticulously designed and working in harmony like clockwork; or something lean and simple like an origami structure that unintuitively but intentionally unfolds to a different shape. It may be a prototype, it may be a graph or simulation, it need not be more than a formulated statement; in any case, engineering can, to the eye of the beholder, be beautiful.

Beauty is not always given a high priority in engineering. In my 5 years of education as a mechanical engineer, none of the concept choices included any factor to rate the designs aesthetically. In the grand scheme of things, however, I think it is precisely the beauty of engineering which attracts people with passion for engineering to do their work, and has a quite important function. A beautiful mechanism raises a curiosity into what it does, how it works, and for a maker: what more can be made. It inspires upon first glance, and instantly explains concepts, which in writing may take up an entire thesis to explain. It reminds me of a statement I read about a year ago, at the start of my thesis; it is one of the 10 rules of design by Dieter Rams, an influential industrial designer:

"Good design makes a product understandable. It clarifies the product's structure. Better still, it can make the product talk. At best, it is self-explanatory."

This statement might apply more readily to the design of consumer products than the industrial products that mechanical engineers are often concerned with. However, I believe that in some deep sense, many beautiful mechanisms fulfill it, which causes them to tickle our curiosity and inspire us. In other words, although it is hard to put a performance metric on it, beauty in engineering may serve a purpose.

Throughout the rest of this thesis, which is after all about engineering and not about industrial design, there will be no room for description of the aesthetics of the mechanisms as hideous or beautiful, which would not be very humble in any case. In fact, aesthetics have, other than the used colours, not had any direct influence on the design. Be that as it may, I still hope that some engineering beauty managed to find its way through the creative process, and that at the end of the thesis, the reader has learned a thing or two, but is also inspired. Inspired to find out more, inspired to make something. Because in the end, inspiration is what keeps us going.

Contents

Chapter 1

Introduction

In this report, a new strategy for grasping agri-food objects in clutter is conceived and validated by manufacturing and testing a prototype. The main content of this report consists of four researches, given in Chapters 2 to 5, which may be independently read.

First of all, in Chapter 2, the state-of-the-art of grasping agri-food objects in clutter is explored, showing that in cluttered environments grasping is not always successful. This leads to the proposal for a redesign of the caging gripper by making the grasp manoeuvre more suitable for clutter.

Following this proposal, in Chapter 3 the different strategies for improving the caging grasp manoeuvre are explored. The functions of a gripper caging gripper in general are expanded by new functions that are required when applying a caging gripper in dense clutter, resulting in a variety of new grasp strategies and accompanying concepts. Finally, one concept is suggested to have the highest potential for fast implementation into a prototype.

In Chapter 4, this concept is further developed and a prototype is manufactured. Using this prototype, the workings of the features that were introduced in the design are individually verified using different lab experiments.

In Chapter 5, the question whether the designed prototype and its underlying strategy actually improves the grasping success rate is answered by applying the gripper to a practical case, by picking and moving tomatoes from a dense cluttered pile.

Finally, in Chapter 6, the ideas and conclusions stated throughout the research are revisiting and connected.

Chapter 2

Robotic Grasping of Agri-Food Objects in Cluttered Environments: A review

2.1 Introduction

The agri-food industry is increasingly due for extensive automation, leading to new requirements for robotic systems to handle many of the complex tasks currently done by human labour. In this chapter, the state-of-the-art of robotic manipulation in the agri-food culture is examined, with a focus on the end-effectors (or grippers) used for grasping different difficult to grasp objects.

Whereas several reviews on the different gripper types for different objects already exist [Lien, 2013] [Birglen, 2015] [Bicchi and Kumar, 2000], this research tries to do so at a more fundamental level by only looking at the main physical principles of the gripper types and their limitations for individual object characteristics. Furthermore, where the reviews above stop at this relation between gripper and object, this review also tries to include the context (or: environment) of grasping tasks, showing that for cluttered environments, some grippers are difficult to use in practice.

Starting in Section 2.2, a brief introduction to the socio-economic motivations are given, which drive the innovation and automation in the agri-food industry. Then, in Section 2.3, the entire spectrum of agri-food tasks in which automation in the form of robotic manipulation plays a role is shown. The scope of this research is then narrowed down to the gripping task in the handling and harvesting processes. In Section 2.4, the different types of end-effectors used for manipulation are distinguished, and their suitability for different object types rated. In Section 2.6, research of manipulating agri-food objects in cluttered environments is reviewed and the problems and suggested solutions in form of other or new gripper designs are given. Finally, the findings of this review are discussed and concluded in Sections 2.7 and 2.8.

2.2 Socio-economic motivations for automation

The agri-food sector is already rapidly innovating and implementing automation. Automation (and technology as a whole) is not always inherently positive for the world, but it depends on its use. Below, it is shown that for agri-food, automation can be a solution to several problems that the world is facing or may be facing in the future, with regards to change in labour, providing (better) nutrition for the growing world population, and for mitigating problems arising from climate change.

2.2.1 Automation as a solution to labour shortage

The primary use for agri-food automation, is to replace human labour. This can be considered a good think, since generally, automation is used to replace labour that is considered dull and repetitive, which would in theory open up time for people to do more fulfilling tasks and work [Lin et al., 2011]. However, the question arises whether new, better labour exists. For different type of economies, this can be answered differently.

First of all, looking at high income countries, there is a trend of increasing shortage of labour, a solution currently solved by job replacement through immigration, which causes political tensions as a result [Christiaensen et al., 2021].

Secondly, middle-income countries that were previously suppliers of foreign labour, like the Central Eastern European countries were, are starting to face labour shortage as their economies too are growing and better jobs become available, and the population ages leading to a growth of health care and a decline in workforce [Astrov and Leitner, 2021]. In these economies, replacement of labour in the agri-food, albeit a relatively small sector, could well be provided by agri-food robotics and could solve labour problems in other sectors as well.

For low-income countries, the agri-food sector is a relatively much larger supplier of labour. However, as these countries develop, the interest in agri-food jobs is expected to drop rapidly as other emerging sectors provide better prospects, which in the future can cause the same labour shortage problems to arise [Christiaensen et al., 2021].

All in all, this shows that automation can provide a viable and important substitute for a changing global work force, from high-income countries at this point in time, all the way through low-income countries in the future.

2.2.2 Feeding the world of the future

Other than developments in the labour market, an important argument for automation is the fact that the ever-growing world population of the future will need to be fed. Although there is a net food surplus, economic inequality causes a large part of the world population to still go hungry [Tian et al., 2016]. Furthermore, the cost of food is only expected to rise with the rise of labour costs, which is only augmented by the fact that arable land becomes increasingly more scarce [Tian et al., 2016]. Moreover, as countries develop, the eating habits of the population changes from sustenance using staples to a more varying diet of high-value products like exotic fruits, vegetables, and meat which are much more labour-intensive to produce [Christiaensen et al., 2021]

In this aspect, agri-food automation can play an important role, by increasing productivity: Robots can run 24 hours a day, and do not suffer from productivity losses and costs due to regular relocation for season tasks like harvesting. Furthermore, robots can deliver a more consistent and higher quality of work with respect to human labour [Kootstra et al., 2021]. Finally, the decrease of labour costs of more nutritious foods can increase availability to low-income families, which can positively affect global health.

2.2.3 Mitigating in the adaptation to global warming

A modern challenge that the world is facing, is climate change. Although the impact of climate change on the agri-food sector is highly region dependent and can be both positive and negative for production yield, some regions of the world are at risk of running into poverty when productivity decreases [Hertel et al., 2010]. Some crops are at high risk of drastic productivity decrease with steep temperature increases expected to happen due to climate change [de Gorter and Drabik, 2013]. Aside from that, indirect developments that have to do with climate change policies, like the increasing use of food crops for biofuels [de Gorter and Drabik, 2013] may change the cost of these crops and increase the importance of labour intensive crops like individually picked fruit and vegetables. Furthermore, new methods of cultivation may be required in regions where the productivity of current cultivation methods will start to decrease.

In all of these issues, agri-food automation may play a role in the future. By increasing productivity and lowering labour costs, yield decreases and price increases may be offset, and innovations may help making different cultivation methods possible in areas where climate breaks the status-quo.

2.2.4 Conclusions

All in all, automation of labour in the agri-food industry can be a good development in a changing world where labour becomes increasingly more expensive, and labour shortage currently experienced in high-income countries is expected to become an increasing and spreading problem. With the ever increasing world population, arable land will become scarce, and the increased productivity that automation can offer can play a role in keeping the world fed. Furthermore, the decrease of labour costs and advanced productivity for human labour intensive nutritious foods like individually picked fruits and vegetables, will make nutritious food more widely available, increasing global health. Lastly, in facing the challenges that climate change will inevitably cause in terms of a changing agri-food sector, automation can play a role in keeping food prices low and can mitigate in shifting the cultivation methods to suitable methods for the changing climate.

2.3 Focus on the task of grasping high-value products

The agri-food industry, being responsible for a wide variety of products, also has a wide variety of production methods. In certain sectors, robotic automation has already been widely implemented, for instance in bulk processes like crop and grain harvesting [Gifford, 1992, p. 10], or in milk production [Global, 2015]. Furthermore, food processing has been mechanized for a long time already, with machines being implemented for specific processing steps like handling and palletizing [IFT, 2022].

A more recent development is the use of robotics in individual handling, harvesting and processing of delicate and difficult to grasp products like fruits, vegetables and fish, meat and poultry, for which a number of tech companies are coming up with new end effectors to handle the products (e.g. Festo, Blueprint Automation, Marell, Lacquey, etc.) and mechatronic systems which can use sensor inputs, perception and planning algorithms to make handling these objects possible in the complex environments (e.g. DENSO Robotics, Demcon, ABB, Aris) of the agri-food industry. Although there are all of these companies specializing on manipulation individual food products, plenty of tasks can not yet be performed by robots. Especially improvements in the grasping task are necessary, and they would have a wide impact since any individual manipulation task requires some form of grasping.

Throughout the rest of this review, the focus will therefore be on reviewing the state-of-the-art of grasping with the goal of manipulating high-value agri-food products. This will be done by first looking at the different types of end-effectors (grippers) which are available for these types of products, and then widening the scope to find out in which ways research and industry are dealing with the problems that arise when applying grippers in the complex contexts (environments) in which the tasks must be performed.

2.4 Gripper types for handling agri-food products

The use of grippers for handling products was kick-started in the 70's [Gasparetto and Scalera, 2019]. During that time, advances in robotic manipulator design made industrial use of robotic manipulation possible. In these early days, grasping was only performed on pre-programmed repetitive tasks without using any sensory inputs, and the object types that could be picked up were limited. However, as robotics expanded through various industries, many new types of grippers were developed using a variety of grasping methods to be able to grasp different object types. In this section, the main categories of gripper types and their underlying principle are explained. Then, the qualities required for grasping agri-food objects specifically are given, by which the suitability of the existing grippers for different object types is rated.

2.4.1 Pinching grippers

One of the most prevalent grippers in industry is the pinching gripper, which is characterized by the fact that it uses 2 or more opposing fingers to generate normal forces on an object, which in turn results in grip (friction forces) to control objects [Lien, 2013, p. 152]. Therefore, a minimal pinch force is required to ensure grip. Examples of these types of grippers are the parallel grippers by industrial leading companies like SMC and Schunk (Figure 2.1). The main grasping principle is the use of *friction* between fingers and object.

2.4.2 Caging grippers

Another principle used in grippers is caging; a principle in which the gripper spatially encompasses the object so that there is no way for escape. This type of grip in principle makes use of the normal forces at multiple contact points around the object, instead of friction forces [1], as shown in the example in Figure 2.2. Included in this category are also compliant shape-based grippers like the Festo Finray gripper, although these also rely on friction to keep hold of the object. The main grasping principle is the use of *normal forces* and *shape* around the object.

2.4.3 Pneumatic grippers

Another popular gripper is the pneumatic gripper. Generally, these use a suction cup which uses vacuum [2] to keep the object surface against the gripper, while resulting normal forces and friction forces constrain the object from sliding off or rotating [Lien, 2013, p. 158]. There is a wide variety of suction cups available with various shapes and applications, with a large number of companies that produce them. Examples of the suction cups produced by Festo are shown in Figure 2.3 along some of their other end effector lines. The main grasping principle is the use of *friction and normal forces.*

[1] Often, there is an overlap between pinching grippers and caging grippers, where for instance the movement perpendicular to the fingers is constrained in a caging way, while the object is constrained in the longitudinal direction via friction. Furthermore, frictional and encompassing constraints may even work together at constraining a single degree of freedom of the object, where the friction enhances the caging function.

[2] Variations also exist in the form of Coanda and Bernoulli grippers which makes use of high flow and the accompanying pressure drop to hold on to the object. These are however not very common for the relatively heavy objects of the agri-food industry [Lien, 2013, p. 162]

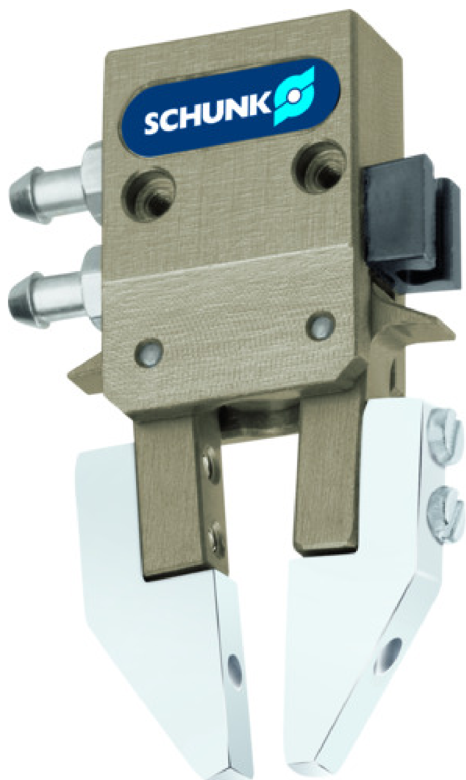

Figure 2.1: An industrial parallel gripper, consisting of two opposing parallel finger on a centering prismatic join. Retrieved from [Schunk, nd].

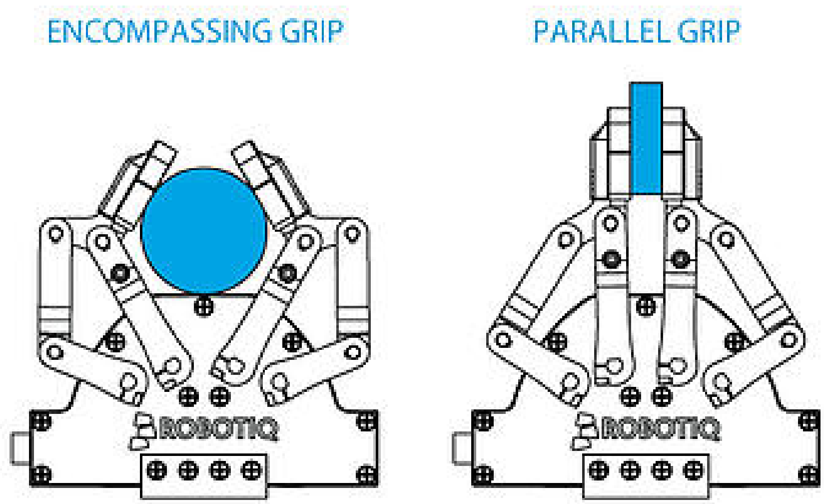

Figure 2.2: Illustration of the difference between a caging and pinching grip, where the caging grip spatially constraints the object from moving upwards out of the gripper, and the pinching grip only does so by friction forces. Retrieved from [Robotiq, nd].

2.4.4 Needle grippers

In some sectors, like in the meat industry, grippers can use the puncturing of objects using needles under different directions, effectively constraining the objects' movements [Lien, 2013, p. 154]. A disadvantage is that the object gets damaged, which for many objects decreases its value, or can introduce pathogens to otherwise unexposed areas. An example of a needle gripper by the company SINTEF is shown in Figure 2.4. The main grasping principle is the use of *normal forces and shape* of the gripper.

2.4.5 Temporary adhesion

There are also different principles available for using temporary adhesion to stick the object to the gripper, for instance by using a freezing element on the object, which is commonly used in the meat industry [Lien, 2013, p. 168]. However, these methods are very specific to the types of objects that can be grasped. The main grasping principle is the use of *surface adhesion.*

2.4.6 Other gripper types

There is still a range of gripper designs which cannot so easily be placed in a category since they combine different grasping modes of the above categories. These include granular jamming

Figure 2.3: The product range of end effectors made by Festo. In the foreground, several suction cups are shown. Retrieved from [FESTO, nda].

[Amend et al., 2012] or rheological [Pettersson et al., 2010] grippers, which do not use translating fingers but a pouch whose stiffness can be changed, so that it can deform around the object in soft state and then be stiffened, resulting in a combination of suction, normal forces and friction that lift the object. Other designs combine different gripper types more obviously, like mounting suction cups on flexible fingers to be able to grasp a diverse range of objects [Huang et al., 2020]. Finally, there is a world of research on grippers based on anthropomorphic hands which can apply many grasp modes [Gama Melo et al., 2014], but these devices are generally too complex and costly for industrial applications. Although all these uncategorized grippers do provide important benefits, these qualities can individually be traced back to the main principles in the categories named above, so that the analysis of gripper qualities which will be done below, can easily be applied to these uncategorized grippers as well.

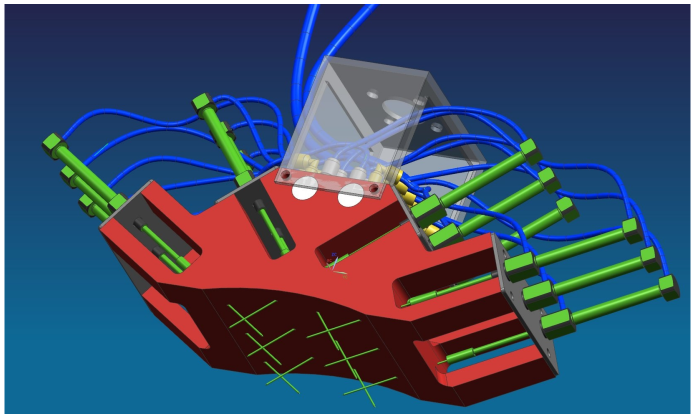

Figure 2.4: Design for a gripper making use of angled needles to hold objects. Retrieved from [SINTEF Raufoss Manufacturing, nd].

2.5 Different Qualities of Gripper Principles

As a gripper is a complex system on its own, there are many aspects involved in determining the gripper quality, e.g. how well it performs at a certain task. Additionally, there is an endless amount of object types in various shapes and with various properties and requirements. Hence, quantifying and comparing the performance between all different grippers types for all tasks is a feeble effort. Instead, in this research, a mapping is made which shows the inherent suitability of the different gripper types to handle difficult object characteristics. This mapping is done, based on the main mechanical principles of the gripper types, and their relation to the object characteristics.

2.5.1 Object Characteristics

Above, it was suggested that different grasping principles might perform inherently better or worse for different object characteristics. It requires no convincing that grasping something fragile with needles, or that grasping something slippery by using friction forces is difficult. Using this same approach, a list of object characteristics which are deemed inherently difficult for various gripper types is given, and the suitability of each gripper type is given based on the fundamental merits on the underlying mechanical principles. These results are summarized in Table 2.1.

- **Fragile:** Many objects need to be treated with care as to not damage them by application of excessive forces, which would devalue the product. Examples are high-value fruits meant for retail, which may not be left with punctures or bruises.

  A caging gripper (++) is inherently gentle, since it does not require any forces other than opposing the acceleration forces during movement, which can easily be divided over a large contact area. Pinching grippers (+) and suction cups (+) score a bit less, because they require an additional normal force for grip, in addition to the acceleration forces that need to be opposed, but when designed with care, can still be used for fragile objects. (−−) Finally, the needle gripper scores the worst, since it inherently damages the objects objects by puncturing. For temporary adhesion grippers (~), no conclusive answer can be given since this is highly specific to the method of adhesion and object.

- **Deformable:** When an object is deformable, its shape will change upon gripper/acceleration forces being applied. For different gripper types, this can have disadvantages.

  A needle gripper (++) scores well, since the angled needles actually provide the object with a structure acting as a skeleton. Temporary adhesion grippers (++) score fine as well, since the bond between object and the gripper will locally keep the object's shape, regardless of further object deformation. The caging gripper (++) scores well too, since the gripper can easily be designed so that the object cannot escape, even in its deformed shape. Furthermore, the deformations are limited to those caused by gravity and acceleration. Suction cups (+) can be used with deformable objects as well, although their use becomes more difficult because peeling effects may cause a sudden loss of vacuum when the object deforms under gravitational forces. Furthermore, excessive deformations in the vacuum cup can decrease the effectiveness of vacuum forming. Finally, pinching grippers (−−) perform poorly for deformable objects since they require a minimal normal force to obtain a grip, which become unpredictable due to the large deformations of the object.

- **Slippery:** Some objects are inherently slippery, like wet objects or fatty meat.

  Temporary adhesive grippers (++) provide a good solution since the bond is not friction dependent. Both needle grippers (++) and caging grippers (++) are based on normal forces and shape of the objects and independent of friction, so these work well for slippery objects too. Suction cup grippers (−) and pinching grippers (−−), however, depend highly on friction, where the suction cup grippers perform slightly better because the highly concentrated contact pressure can still increase grip..

- **Rough:** The surface roughness of some objects can provide both advantages and disadvantages.

  For caging grippers (++) and needle grippers (++), surface roughness plays no role because they do not depend on surface parameters. For pinching grippers (++), surface roughness only helps in obtaining grip. However, for temporary adhesion grippers (−), the surface roughness decreases the effective surface area, decreasing its force. For suction cup grippers (−−), surface roughness can inhibit vacuum forming altogether.

- **Irregular:** Due to organic nature of agri-food objects, their shapes and surfaces might be irregular, like sweet peppers which can differ wildly in shape, or tomatoes which may have creases and a deep dimple at their stem.

  Needles grippers (++) have little problems with this since they can penetrate deeply into the object so that the irregularities in shape are irrelevant. Caging grippers (+) can perform well, although since it is a shape-based grasping method, irregularities should fall within the range for which the caging gripper is designed. Suction cup grippers (+) and temporary adhesion grippers (+) require at least a regular area to be applied, though this can be fixed with extra care in planning and perception. Finally, pinch grippers (−) require more advanced pose estimation for irregular objects so that the gripper can be applied at two (or more) correct opposing surfaces to obtain the required normal forces for grip but can be be used.

Table 2.1: Gripper principles rated on their the ability to handle difficult object characteristics

Gripper type	**Object characteristics**				
	Fragile	**Deformable**	**Slippery**	**Rough**	**Irregular**
Pinching	+	–	– –	++	–
Caging	++	++	++	++	+
Pneumatic	+	+	–	– –	+
Needles	– –	++	++	++	++
Adhesion	~	++	++	–	+

2.5.2 The caging gripper as a universal gripper

As can be seen in Table 2.1, due to the variety of gripper principles that exist, for all characteristics some solutions exist. For instance, slippery objects can ideally be picked up by needle grippers, caging grippers or adhesion grippers, and rough objects by piching, caging or needle grippers. In practice, the problem is however, more difficult, since a typical agri-food object may have several of these difficult features at once. A chicken fillet for instance is both very deformable and very slippery, and in case it is destined for sale in a supermarket, should not be damaged so should be treated as fragile. For these combined cases, finding a usable gripper is a more difficult. Looking at the gripper types, however, it can be seen that the caging gripper is in principle a very universal type, since it does not rely on friction or the accompanying high normal forces required to establish friction, making it suitable for all different object types.

One of the issues it does suffer with, is the use with irregular shapes, since the it is basically a shape-based grasping method. In literature, this problem is being addressed using compliant or underactuated grippers, which are able to adapt to different object shapes, examples being the Festo Finray gripper (2.5a) or the underactuated gripper by Lacquey (2.5b), so that this issue does not really limit its use. Still, in practice, the caging gripper has a major disadvantage that prevent it from being used in many agri-food contexts. In the next section, these contexts (environments) and issues that arise are addressed.

(a) Compliant Finray gripper designed by Festo. Retrieved from [FESTO, ndb].

(b) Underactuated finger gripper designed by Lacquey. Retrieved from [Lacquey, nd].

Figure 2.5: Different caging grippers from industry which are designed to handle irregular shapes

2.6 Grasping in cluttered environments

In Section 2.5.2, it was shown that for the wide range of object characteristics, many gripper types have been developed. However an aspect of grasping which was not addressed, and is often omitted in reviews on grippers, is the context in which the manipulation tasks must be performed. Especially in research on gripper design, the grippers are often tested in ideal settings, where the objects are manually placed in the grippers [Zhong et al., 2019] or taken from an otherwise obstruction-less [Wang et al., 2017] surface or already neatly separated collection of objects [Wang et al., 2020]. Therefore, once environments become cluttered and complex, the behaviour of these grippers is unknown.

An analogy can be seen in the industry, where in most process lines objects are being singulated beforehand by separate machines such as the Marel SingleFeed [Marel, nd] so that the grippers only have to deal with separated objects, leading to a causality dilemma in which grippers do not need to work with cluttered environments and conversely are not designed to handle cluttered environments.

Still, there are cases in which clutter around the object cannot be avoided and it cannot be separated easily in a separate process step, for instance in harvesting of fruit from inside a trees canopy [Ji et al., 2016] or from fruit clusters [Xiong et al., 2020a] or bin picking diverse objects [D'Avella et al., 2020]. Furthermore, if grippers can be made to handle objects in clutter, this could eliminate singulation elements from or ease the task for singulation elements in processing lines.

In most research on gripper design, clutter does not take a prominent place, but there is still a lot of research being done on manipulation in clutter, even in the agri-food industry specifically, yielding over 50 researches on the subject in the past since the year 2000. In the rest of this section, a classification of the different types of clutter as found in research on agri-food manipulation is made [3], showing which types of clutter are relevant for grippers specifically. The different strategies that these researches employ are then categorized.

2.6.1 Classifications of clutter

Some examples of cluttered environments have already been given above, but their characteristics vary widely; for instance, when manoeuvering through a tree canopy, the branches are rigid and will not give way, but the space is open enough to manoeuvre. Conversely, when picking a tomato from the middle of a bin of tomatoes, the surrounding clutter is dense and leaves no room to freely manoeuvre around the object, but the clutter can comply to being pushed aside.

From these two examples, two important characteristics of clutter come to light, by which clutter can be characterised, being the clutter density and the clutter compliancy. Using these characteristics, the list of papers from the search query are placed in different categories based on the

[3] The search was done in Scopus, using the query: TITLE-ABS-KEY (("manipulation" OR "manipulating" OR "grasping" OR "grasp" OR "picking") AND ("clutter" OR "pile" OR "bin" OR "obstacles") AND ("agri-food" OR "agri" OR "food" OR "fruits" OR "fruit" OR "vegetables" OR "vegetable" OR "meat" OR "fish" OR "poultry")) AND (LIMIT-TO (PUBSTAGE , "final")) AND (LIMIT-TO (SUBJAREA , "AGRI") OR LIMIT-TO (SUBJAREA , "ENGI") OR LIMIT-TO (SUBJAREA , "COMP")) AND (LIMIT-TO (LANGUAGE , "English")). This yielded 152 results which were manually filtered to 34 results that were deemed relevant, including some additional results which were referenced in the resulting papers

combination of whether they are dense or open, and compliant or stiff. The environments are considered open if tasks and motions can freely be performed without needing to move or modify obstacles, and considered dense otherwise. Environments are considered compliant if moving or modifying obstacles (e.g., deforming/compressing) can be done without damaging them, and rigid if this is not possible. The list showing these papers and classifications is given in Table 2.2.

Open clutter (both stiff and compliant)

Looking at environments that are considered open, and the associated problems that are addressed in the papers, most cases have little to do with grasping, regardless of whether they are stiff or compliant. The cases of open clutter generally have to do with obstacle recognition and avoidance in the harvesting context, where robotics must reach through canopies and plants, as well as avoiding other rows of crops during harvesting [Ge et al., 2019] [SepúLveda et al., 2020] [Bac et al., 2016], [Hemming et al., 2014], a problem familiar from obstacle avoidance and collision sensing in industrial robots [Khatib, 1985] [Popov et al., 2017]. In line with this is the design of redundant manipulators to increase reachability in the open clutter [Van Henten et al., 2010]. An important observation that is made with respect to grippers is that the success rate in finding correct grasping manoeuvres can be dramatically increased with smaller grippers [Bac et al., 2016], though it was not specified whether this has to do with manoeuvering the gripper through the plants, or with finding a suitable grasp position.

Dense stiff clutter

For the quadrant of dense and stiff clutter, no cases could be found in the context of manipulation in agri-food. This is basically an unsolvable case in the sense that if the object cannot be reached due to obstacles, and the obstacles also cannot be moved or modified, the case becomes essentially unsolvable with a robotic gripper. An example of such a case can be found outside of agri-food in the task of urban search and rescue in earthquake debris [Tadokoro et al., 1999] [Jha et al., 2020], where manoeuvering through the clutter is done only for search operations, and manipulation is carried out by careful excavation controlled manually.

Dense compliant clutter

Instead, for grasping, problems arise with dense cluttered environments immediately around the object, in which the object cannot be grasped without interaction, such as the example of bin-picking fruit and vegetables, where the success rate in grasping decreases with the amount of clutter due to the grippers colliding with surrounding objects [Mnyusiwalla et al., 2020]. In several of the cases concerning harvesting through plants and canopies, such as when harvesting sweet peppers [Hemming et al., 2014] and strawberries [Xiong et al., 2020a], the clutter is in fact open only at a macro scale, but can be considered dense and compliant at the fruit clusters where the fruit must be picked and some papers state that these clusters and obstacles near the fruit negatively impact success rate [Davidson et al., 2016] [Bac et al., 2017].

2.6.2 Limitations of solving clutter using grasp planning

A trend that was seen in the papers above is that the subject of grasping in clutter is primarily seen as an obstacle detection and avoidance problem for which solutions are sought in control. This works

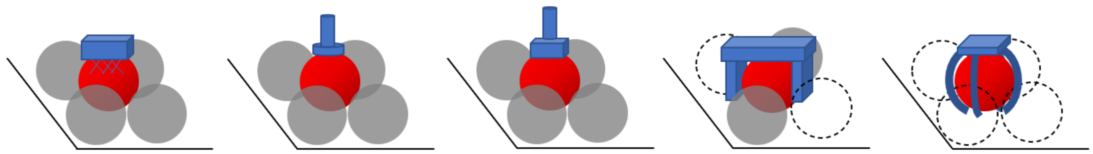

Figure 2.6: Schematic presentation of the allowable obstructed sides for certain gripper types. Needle grippers (a), suction cup grippers (b), adhesion grippers (c) require only one surface to be free to grasp. Pinching grippers (d) require the top an two opposing sides to be free. Caging grippers (e) require the top and all sides to be free to set a grasp.

well at the macro scale of harvesting, where a robot arm is moving through open clutter to reach the object. However, at the local scale, clusters and other obstacles make obstacle-avoidance impossible, which contributes to a large part of failure rate. For instance, in the robotic apple harvester by [Silwal et al., 2017], 13% of the grasp failures were caused by unwanted contact between the gripper and obstacles. For increasing robustness, the paper suggests improvements in obstacle detection and grasp planning, but the step from obstacle avoidance to interaction may not be trivial. An example of a step towards obstacle interaction, is the strawberry robot by [Xiong et al., 2020a] which interacts with obstacles by pushing them aside to reach an obstructed strawberry. However, this solution is complex and the mechanics of the case of strawberries are very specific. Although these advances are being made in grasp planning in dense clutter, the problem of obstacle detection and planning is becoming increasingly more complex. Instead solving the problem in control by including obstacle interaction, the problem and the solution of grasping in dense clutter might also be found in the gripper design, which will be explored below.

2.6.3 Suitability of gripper types in relation to clutter

Some grippers are inherently more suitable grasping in clutter. Looking at the gripper types of Section 2.4 in relation to grasping in clutter, one important new gripper characteristic can be added, which is the number of surfaces used around the object for a certain gripper, shown schematically in Figure 2.6. The importance of this characteristic for clutter follows directly from the observation that when grasping in dense clutter, the requirement for obstacle avoidance inhibits the gripper from being applied to objects that are partly obstructed. Hence, a low number of surfaces required for grasping will provide more freedom in grasp planning and thus increase the amount of objects that can be grasped.

As can be seen, there is actually a group of grippers which require not more than one surface to attach, being the needle, adhesion and suction grippers. For cluttered environments, these grippers would be very suitable. Pinching grippers require at least three surfaces to be empty if only two fingers are used, and a caging gripper requires all sides and the top of the object to be free.

Even though caging grippers appear to be the least suitable for clutter, in the research presented in Table 2.2, the grippers which were most used were actually caging grippers. A suggested reason for this is that in choosing a gripper for these tasks, the capabilities of handling clutter play no or no significant role, compared to the consideration of the grippers capability of handling the object type. Caging grippers were shown to be in general a good choice (see Section 2.4), and the ability to handle the object makes or breaks the success rate of the robotic system. However, this means that inherently, the systems using caging grippers will not be able to reach 100% grasp rates without much more advanced perception and planning.

2.6.4 The need for an improved caging gripper

Rather than improving perception and planning to handle more advanced interaction with clutter and improve grasp rate, we suggest a mechanical approach, in which caging grippers are redesigned so that they can be applied even though the object is partially obstructed.

Looking at the way that caging grippers are designed, the closing manoeuvre generally consists of the fingers sliding perpendicularly onto the object, or finger that pivot at their base. This takes up a lot of free unnecessary space around the object during the grasp manoeuvre. Instead, if the fingers were designed so that they remain in close proximity to the object surface, less displacements and accompanying unpredictable interactions with the clutter are required.

Secondly, since a caging gripper will have to be moved through the clutter to reach all sides of an obstructed object, these motions will be accompanied by several interacting forces between the moving gripper structure and the object and clutter. To avoid miss grasps and damages, these interacting forces should be minimized.

2.6.5 Manoeuvering mechanisms for clutter

Outside of the agri-food industry, several examples of manoeuvering mechanisms for cluttered environments could be found, which may provide a solution to the problem of setting a caging grasp in clutter.

First of all, there are several researches about design and modelling of redundant or continuum manipulators, which allows manoeuvering through constricted spaced [Bulut and Conkur, 2021]. These have applications at a small scale for surgery [Eastwood et al., 2020] [Henselmans et al., 2019], grasping small objects from confined spaces [Mazzolai et al., 2019] or inspection devices for jet engines [Wang et al., 2019b], but may also be used at a much large scale, for instance for performing tasks in dangerous hard to reach environments [Ma et al., 1994].

Whereas the manipulators named so far did not explicitly involve the interacting forces with the environment, there are also several maneuvering mechanisms which do. First of all, there are several mechanisms which use alternating anchoring points, to actually use friction with the environment for manoeuvering [Wang et al., 2019a] [Breedveld, 2006]. In other cases, rolling contacts are used to propagate the mechanism further [Breedveld et al., 2008].

Another line of research, involves tip-growing mechanisms, where new material is 3D-printed [Sadeghi et al., 2017] or fed through the core of the mechanism and inflated, and thereby no sliding during manoeuvering occurs [Do et al., 2020] [Blumenschein et al., 2020].

These manoeuvering mechanisms, especially those which are designed for interaction with the environment, can provide a basis for improving the caging manoeuvre mechanically, which is so far not done in gripper design.

Research	Clutter Density	Clutter Stiffness	Gripper type	Strategy for solving clutter	Placement motivation
[Gong et al., 2022]	High	Low	Caging	Avoidance/planning	Macro-scale: plant with stems
[Gong et al., 2022]	High	Low	Caging	No	Local scale: clusters/plant obstacles
[Xiong et al., 2021]	High	Low	Capturing	Clutter manipulation	Local scale: clusters/plant obstacles
[Lin et al., 2021]	Low	High	Caging	Avoidance/planning	Macro-scale: plant with stems
[Lin et al., 2021]	High	Low	Caging	Not mentioned	Local scale: clusters/plant obstacles
[He et al., 2021]	Low	Low	Pinching	Avoidance/planning	Macro-scale: plant with stems
[He et al., 2021]	High	Low	Pinching	Grasping whole bunch	Local scale: clusters/plant obstacles
[Nemlekar et al., 2021]	Low	Low	Pinching	avoidance/planning	Macro-scale: plant with stems
[Fu et al., 2020]	High	Low	No gripper given	Not mentioned	Local scale: clusters/plant obstacles
[Xiong et al., 2020a]	High	Low	Capturing	clutter manipulation	Local scale: clusters/plant obstacles
[Mnyusiwalla et al., 2020]	High	Low	Caging/pinching	Not mentioned	Piles in bins
[Xiong et al., 2020b]	High	Low	Capturing	Not mentioned	Local scale: clusters/plant obstacles
[Sarabu et al., 2019]	Low	High	Pinching	Avoidance/planning	Macro-scale: plant with stems
[Yang et al., 2020]	Low	High	Caging	Avoidance/planning	Macro-scale: plant with stems
[Joffe et al., 2019]	High	Low	Suction cup	Avoidance/planning	Piles in bins
[Ge et al., 2019]	Low	High	Capturing	Avoidance/planning	Macro-scale: solid structures
[Davidson et al., 2016]	High	Low	Pinching	No	Local scale: clusters/plant obstacles
[Cao et al., 2019]	Low	High	Pinching	Not mentioned	Macro-scale: plant with stems
[Cao et al., 2019]	High	Low	Pinching	Avoidance/planning	Local scale: clusters/plant obstacles
[Moli, 2018]	Low	High	No gripper given	Avoidance/planning	Macro-scale: plant with stems
[Silwal et al., 2017]	High	Low	Pinching/caging	Avoidance/planning	Local scale: clusters/plant obstacles
[Bac et al., 2017]	High	Low	Pinching	Avoidance/Modifying crop	Local scale: clusters/plant obstacles
[Bac et al., 2017]	High	Low	Suction with lip	Modifying crop	Local scale: clusters/plant obstacles
[Davidson et al., 2017]	Low	High	Pinching	Avoidance/planning	Macro-scale: tree
[Xue, 2017]	Low	High	No gripper given	Avoidance/planning	Macro-scale: tree
[Zhang et al., 2016]	High	Low	Pinch	Avoidance/Modifying crop	Local scale: clusters/plant obstacles
[Bac et al., 2016]	High	Low	Suction with lip	Avoidance/planning	Local scale: clusters/plant obstacles
[Bac et al., 2016]	Low	Low	Suction with lip	Avoidance/planning	Macro-scale: plant with stems
[Jianjun et al., 2012]	Low	Low	No gripper given	Avoidance/planning	Macro-scale: plant with stems
[Cheng et al., 2012]	Low	High	No gripper given	Avoidance/planning	Macro-scale: plant with stems
[Baur et al., 2012]	Low	High	No gripper given	Avoidance/planning	Macro-scale: plant with stems
[Guo et al., 2010]	Low	High	Caging	Avoidance/planning	Macro-scale: tree
[Guo et al., 2010]	High	Low	Caging	No	Local scale: clusters/plant obstacles
[Scarfe et al., 2009]	Low	Low	Caging	Avoidance/Modifying crop	Macro-scale: solid structures

Table 2.2: Table showing the list of research on manipulation of agri-food objects in clutter.

2.7 Discussions

Unlike other reviews, in this review an attempt was made to not only look at the suitability of grippers for different objects, but also at the suitability of grippers for different cluttered environment, which agri-food objects are often subjected to. Below, these two subjects are individually discussed.

In Section 2.5, a mapping was made which showed the inherent suitability of different grippers for different object types. Although this mapping gives some key insights into the fundamental principles and limitations of the grippers, the field of gripping is huge. Hence, variations on all gripper types exists so that each fundamental limitation can, with some additional design features, individually be overcome. Still, for coming up with a lean gripper solution, it is believed that it would be most feasible to use a gripper that is fundamentally suitable for the object types, and in that respect, the caging gripper is expected to be very universally applicable.

In Section 2.6, the context in which grasping must be performed was explored, by first looking at a comprehensive list of research on manipulation in clutter in the agri-food industry. From this, it was shown that at a local scale around the object where gripping is done, problems arise due to obstacles preventing some grippers from being placed. This research suggests that the problem is caused and may be solved by gripper design, either by choosing gripper grippers more suitable for clutter, or redesigning grippers that are not, such as redesigning the caging gripper so that its grasp manoeuvre better interacts with the clutter. In research, however, the focus is on improving perception and grasp planning to better find grasp poses and even interact with the environment. A more broad vision on the problem of grasping in clutter is that both the gripper design and perception and planning should be advanced, where a better gripper design will relieve some of the constraints for grasp planning, so that together, even more difficult edge cases can be solved.

The research finishes with the problems that arise when applying a caging gripper in clutter, to draw analogies with other research outside of the agri-food industry, which also deals with clutter. The fact that these researches exist and are successful in manoeuvering through clutter should be interpreted as a motivation and inspiration to look into improving the design of the caging gripper for clutter. However, applying these researches on caging grippers is not straight forward, since caging grippers have additional functional requirements that may directly oppose those present in the examples provided. For instance, for manoeuvering with minimal interaction, the mechanisms need to be soft, while gripper fingers should in general be stiff to transfer forces. Still, through the combination of several functions, for instance stiffening the eversion tube of [Takahashi et al., 2021] with a continuum mechanism as a backbone, or adding additional features, for instance adding rollers onto a redundant manipulator, these problems can in principle be overcome.

2.8 Conclusions

In this research, the state-of-the-art of grasping in the agri-food industry was reviewed in terms of the suitability of grippers for different objects, and the suitability of grippers for different cluttered environments.

Five different characteristics were identified which make agri-food objects difficult to grasp, with objects being fragile, deformable, slippery, rough, or irregular or a combination of these characteristics. It was found that for every difficult characteristic individually, well performing grippers were found. However, since most objects have a combination of these characteristics (e.g., being both soft and fragile), a more universally applicable gripper is found in the caging gripper. This type of gripper does not rely on friction and it therefore has no problems with different surface characteristics (slippery/rough objects) or a minimum normal force to obtain friction which may result in unpredictable grasps (deformable objects) or damaging grasps (fragile objects).

By looking at research on grasping in clutter in the agri-food industry, it was found that for grippers, especially the dense clutter immediately near the object posed problems. These problems were found to be caused by the grippers not being able to reach the object without unwanted interaction with the environment, which caused miss-grasps or prevented the perception and planning from finding a viable grasp position.

It was concluded that, contrary to the trend in state-of-the-art research to solve the problem with better software, a viable solution might be found in a more suitable gripper choice or special gripper design. Especially a redesign of the caging gripper so that it is able to be applied regardless of the object being obstructed from multiple sides, has a high potential for solving hard-to-grasp objects in dense clutter in the agri-food industry.

Although better gripper design is expected to simplify the problem of grasping in clutter, a combination of advancements in gripper design and software is required to be able to grasp even the most difficult cases.

Chapter 3

Issues of, and Mechanical Strategies for Caging Grasping in Dense Cluttered Environments

3.1 Introduction

As stated in the previous chapter, if a gripper could be designed which is able to form a caging grip around an object, even when it is surrounded by dense clutter, this would have high potential as a gripper for all kinds of difficult objects in difficult grasp cases. In this chapter, the functional requirements and the design space for such a gripper are explored. This will result in several fundamental strategies of solving the issues inherent to grasping in dense clutter, and a list of concepts to implement these strategies. Finally, the concepts will be analyzed in terms of development complexity leading to a choice for a concept which can be developed into a prototype at a later stage.

3.2 Caging gripper functions

Before looking into the issues of grasping in clutter, and the new functions that arise, the caging gripper in its traditional form is analyzed. This is done by looking at the tasks that a caging gripper must perform.

Robotic grippers are generally part of a bigger robotic system, consisting at least of some robotic manipulator (arm), a perception and control module that can take inputs from the environment, and an end effector (or gripper) which is mounted at the end of the robot. In Figure 3.1, the process steps of a typical manipulation are illustrated, and explained below:

- **Figure 3.1a: Identify object** First, the robotic system must determine the location of the object so that the path towards the object can be planned. This can be done using computer vision, or it can be pre-programmed if the location of the object is predictable.
- **Figure 3.1b: Positioning** Then, the gripper must be placed in position for the grasp manoeuvre. Up to this point, contact between the gripper and the object/environment is generally avoided by the robotic system since it could cause damage and disturbances.
- **Figure 3.1c: Grasping manoeuvre** After the gripper is placed in position, it performs the grasping manoeuvre. For different gripper types, the methods of engagement differ. For a caging gripper, however, engagement in principle consists of actuating and closing the caging structure around the object so that there remains no sufficiently large opening for the object to escape.
- **Figure 3.1d: Manipulate object** After the gripper has engaged, the manipulator arm will start the manipulation of the object, consisting of a variety of translations and rotations of the end of the robot arm. The gripper is responsible for transferring these translations and rotations and corresponding forces and moments to the object. In a caging gripper, this is primarily done by normal forces of the grippers contacts with the object surface opposite to the object accelerations. The caging structure must lead these normal forces to the gripper's connection with the robot arm.
- **Figure 3.1e: Releasing gripper from object** After the robotic manipulator has finished its movement, the object should be released by disengaging the gripper. In most grippers, this can simply be performed by reversing the grasping manoeuvre.

Looking at the tasks above, it can be seen that there are only three tasks in which the robotic gripper performs a function. Explicitly, these functions are the **grasping manoeuvre**, the **force transferring**, and the **release manoeuvre**, and they are functions that any caging gripper must possess. However, with these functions alone, the issues of grasping in clutter specifically are not yet addressed.

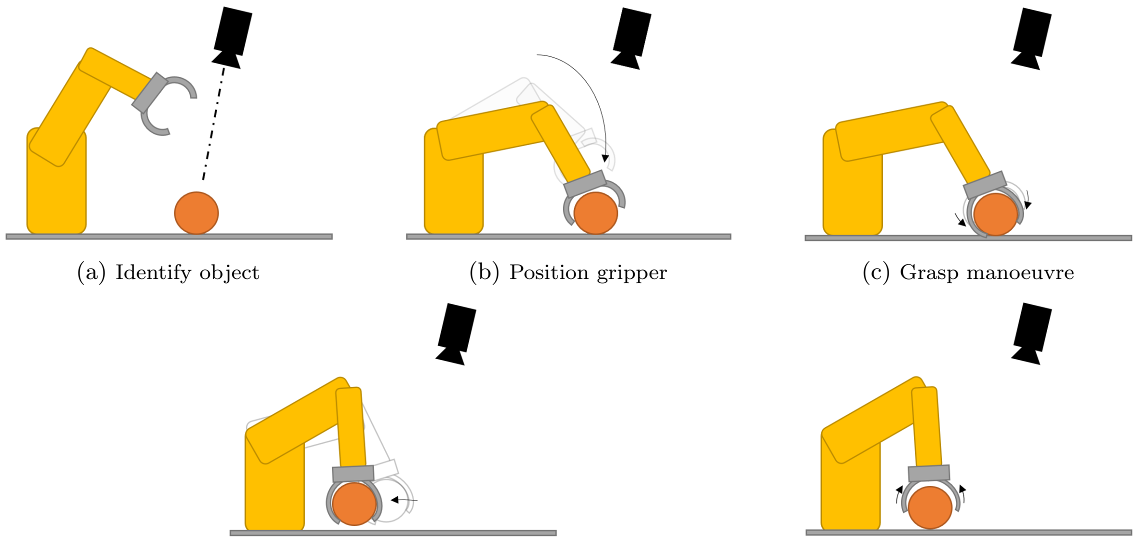

(a) Identify object (b) Position gripper (c) Grasp manoeuvre (d) Manipulate object (e) Release manoeuvre

Figure 3.1: A basic robotic manipulation, consisting of five sub tasks

3.3 Grasping in clutter

In clutter, some new issues and accompanying functions for caging grippers arise. These will be explored here.

3.3.1 Limited space

When grasping in clutter, the available space around the object is limited. Therefore, with traditional hinging or prismatic caging grippers, positioning the gripper (Task C of Figure 3.1) without collisions is not possible. This leads to a sub-function which is added to the **grasping manoeuvre** function, being that the caging structure should engage with an **object following motion**, thereby requiring only a small free surface of the object during positioning. Furthermore, by following the object surface, spatial disturbance of the environment during the grasp is limited only to the volume of the gripper structure.

3.3.2 Limited allowable friction forces

The clutter is initially kept together, be it through gravity or other forces, and insertion of a gripper structure may increase these forces further. These normal forces can cause friction during the grasp manoeuvre, which will damage or disturb the object and environment. This leads to another sub-function of the **grasping manoeuvre** function, being that the moving caging structure should incorporate a method to **reduce friction**. Together with these additional sub-functions the full functional requirements for a caging gripper for dense clutter can thus be described by the chart in Figure 3.2:

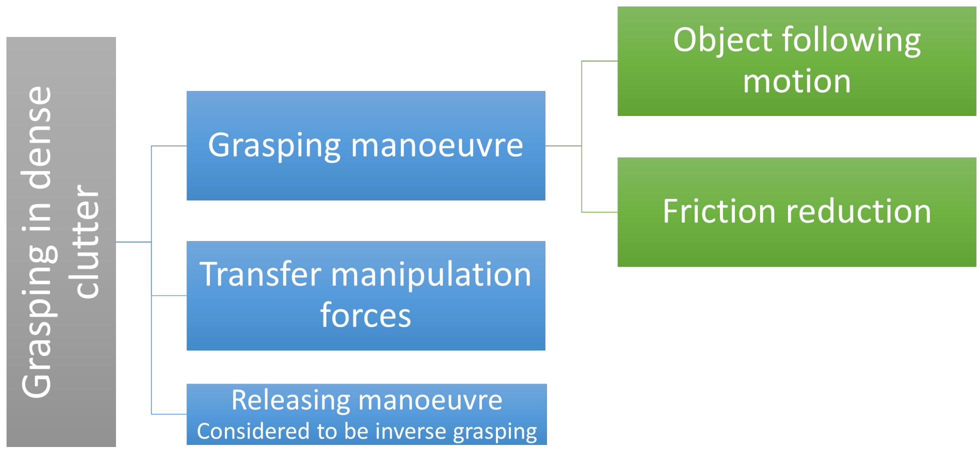

Figure 3.2: Schematic showing the functions of required in a caging gripper for dense clutter.

3.4 Strategies for the clutter-specific functions

With the definition of these new sub-functions that are required for the grasping manoeuvre, new gripper designs can be conceived to implement these functions. To direct further design efforts to the research paths with the highest potential, first the different fundamental strategies that can be used are analyzed in terms of the theoretically achievable performance.

3.4.1 Object following motions / strategies

Several strategies exist for closing the caging structure around the object, while following its surface. In essence, they can be divided into two groups, being the ones where the gripper fingers or structures propagate sideways to their length, and those where they propagate forwards. 3.3.

The principles are described in more detail below:

- **S-path propagation:** The gripper structure approaches the object from a single line going through the center of the object. At the object surface, the structure makes an s-curve so that it follows the object surface while requiring a minimal free space/footprint.
- **Helical propagation:** The gripper structure makes a helical/screw motion around the object and through the clutter, thereby only requiring the entry-point of the screw to be free during the grasp manoeuvre.
- **Building propagation:** The gripper structure is built up during the grasp, thereby generating a structure (instead of transferring/deforming a structure) during the manoeuvre.
- **Virtual hinge points:** Instead of simple hinges or prismatic joints at the wrist, a virtual hinge point is created so that the caging structure rotates around the center of the object, thereby leaving no free space during the grasp manoeuvre.
- **Radial hinging:** Instead of the above methods, where the structure propagates forwards along the object surface, the structure can also propagate sideways, for instance by using a hinge which is aligned radially from the object.

3.4.2 Friction reduction strategies

To reduce friction, several strategies exist as well, which are shown in Figure 3.4. The strategies can be divided into three basic categories, which are based on reducing the three different factors that contribute in work performed by friction:

- **Reducing normal forces:** For friction to occur, a normal force on the surface is necessary. As was said, a normal force between the object and the surrounding obstacles is expected to be present in a dense cluttered environment. However, minimizing the gripper thickness, or designing it as a wedge, may reduce the additional normal force that is caused by insertion of the finger. Still, with this method, the preexisting normal force can not be avoided.
- **Reducing friction coefficients:** Another factor that can be influenced is the friction coefficient between the object and environment. However, these solutions would be very object specific and may inhibit the universality and friction-independence of the caging gripper principle. Furthermore, although the friction can this way be reduced, it cannot fully be eliminated.

- **Reducing relative slip:** Lastly, for the friction force to do work and cause damage or disturbance, a relative motion between the surfaces of the gripper and object/environment is necessary. By reducing or even eliminating this relative motion, the work caused by slip can be reduced or eliminated, without altering the friction between the gripper and the object/environment.

3.4.3 Fundamentally most feasible strategies

Some of the strategies above have some inherent limit on how well they are able to perform their functions. To choose which strategies have the highest potential and are most interesting for further investigation, they are individually rated on several criteria following from the issues of grasping in clutter.

Criteria for object following motion strategy

For the object following manoeuvre, two different criteria come into play when looking at how well the strategies can possibly perform in clutter, which are evaluated below. The results of this evaluation are summarized in Table 3.1.

- **Required free object surface:** First of all, to allow grasping when the object is severely obstructed, the required free surface for positioning should be minimal. Looking at the different gripper designs, it is assumed that the S-path propagation (++), Helical propagation (++) and Building propagation (++) have no theoretical limit on how large the free area must be, since the wrist from which the fingers propagate may be very small. However, for the Virtual Hinge propagation (−−) and the Radial hinging (−−), a large entire length of the fingers/structure is already wrapped over the object at the start of engagement, therefore requiring a large section of the object to be free before engaging the gripper.
- **Object shape universality:** Another aspect, which follows from the need for a rather universal gripper for the variety of agri-food objects, is that the gripper design should be adaptable for a variety of shapes. For most grippers, the design does not change much with for instance cylinders or spheres. However, the Spiralling propagation (−−) and Radial hinging methods (−−) rely on the object being roughly spherical making them less broadly applicable.

Table 3.1: Table showing the criteria, and the scores of the individual strategies based on the underlying physical principles.

Criterion	Sideways propagation	Forward propagation			
		S-path	**Helical**	**Building**	**Virtual hinge**
Required free angle	−	++	+	++	−−
Object universality	−	++	−	++	−

Criteria for friction reduction strategy

For the several friction reduction strategies, two aspects are important for determining the limitations of their feasibility. They are analyzed below the results of which are summarized in Table 3.2.

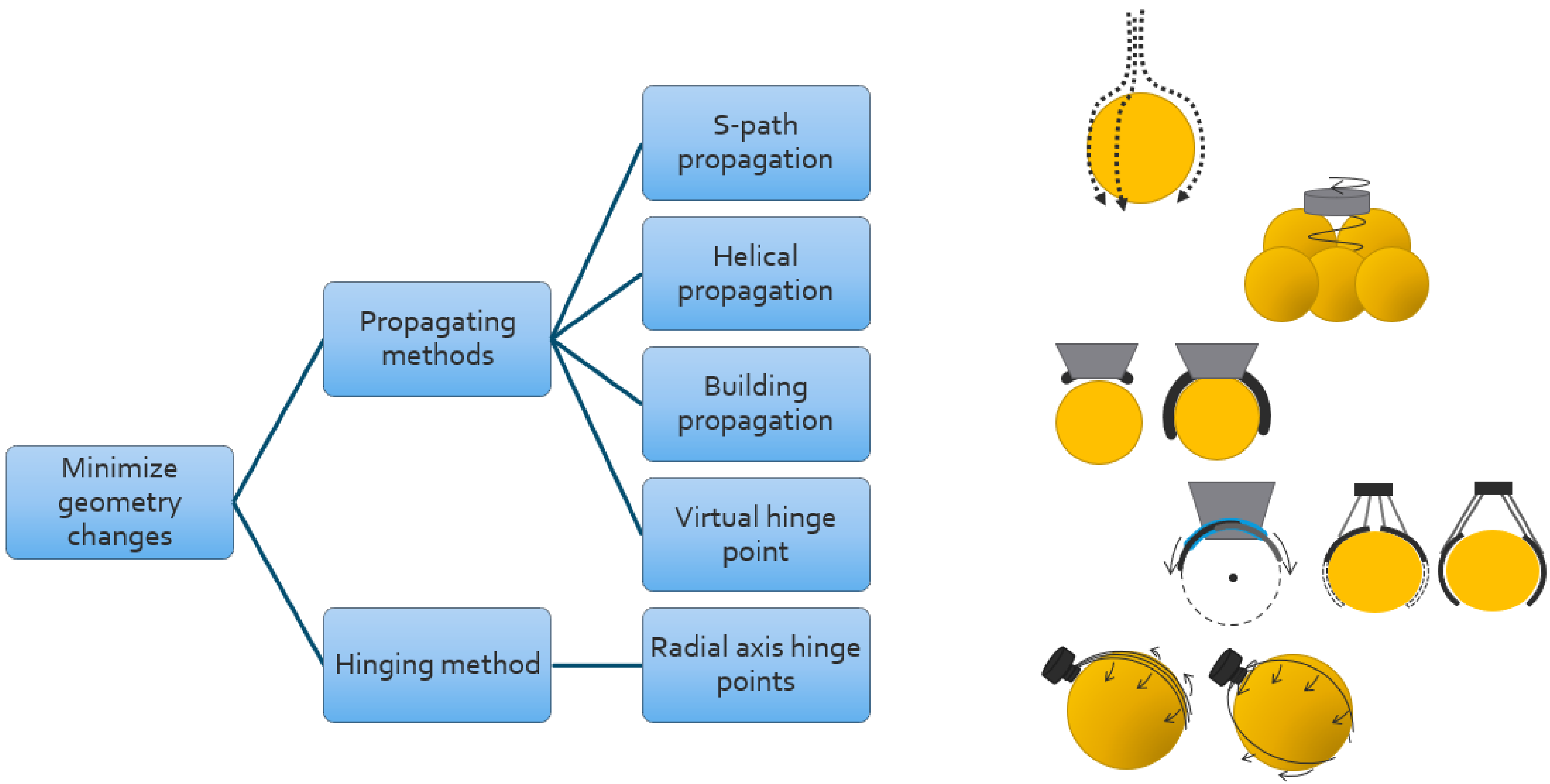

Figure 3.3: Different strategies for manoeuvering from the wrist to underneath the object to establish a caging structure

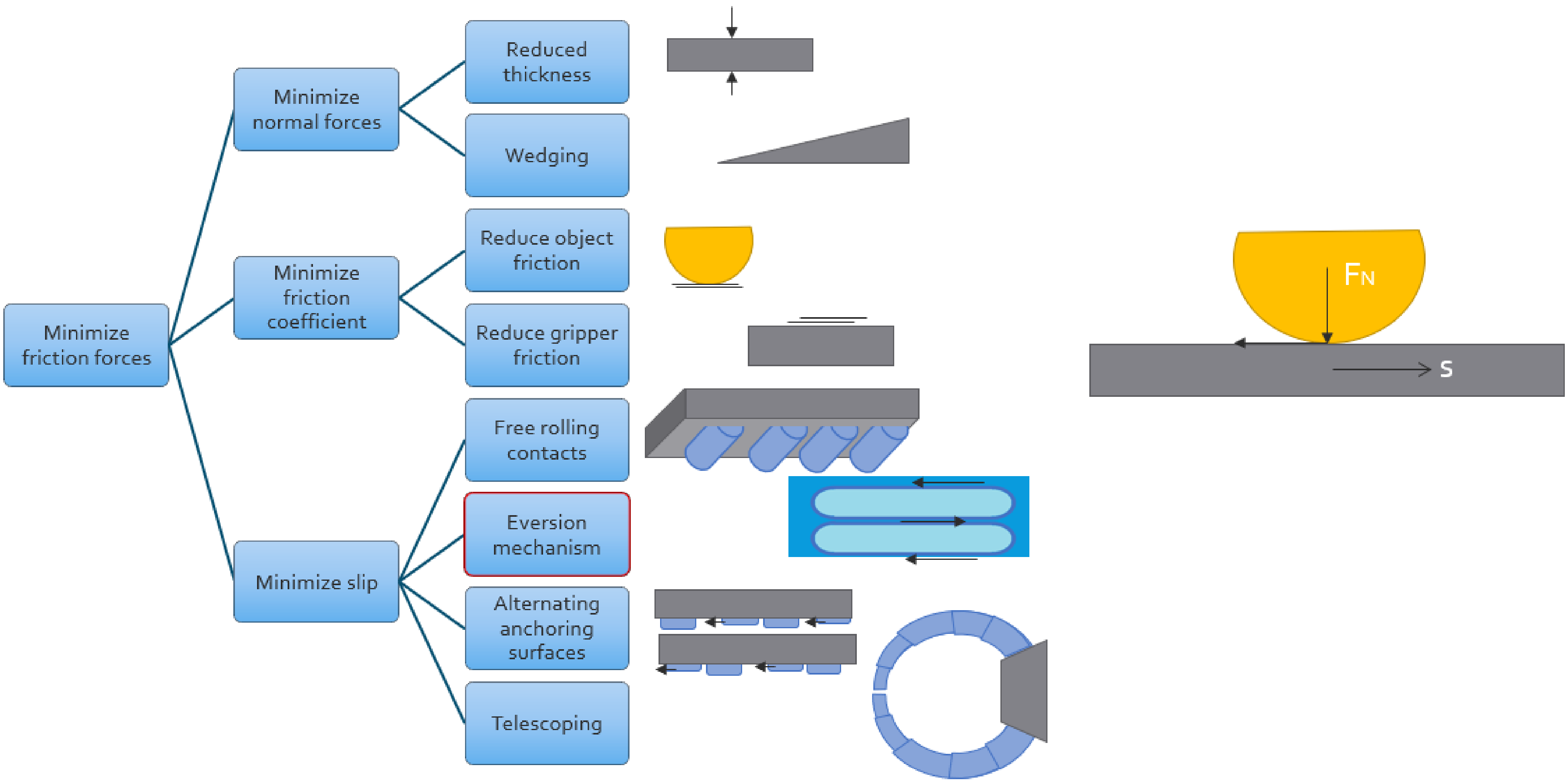

Figure 3.4: Different strategies for reducing the effects of friction while manoeuvering the caging structure along the object

- **Remaining friction force:** First and foremost, the level of reduction of fricton is defining for which strategy is best. Most strategies cannot fully eliminate existing friction forces, like reducing normal forces (−−) and friction coefficients (−−). For the slip reduction methods, not all methods fully eliminate slip. The telescoping strategy for instance still has slip at the surface of the part which is extending at that time (−), though the already-extended part remains still. The use of free-rolling contacts does fully eliminate slip, but some forces may still be present due to friction in the mechanism (+). The other methods, being eversion (++) and walking (++), can fully eliminate slip and friction forces.

- **Potential traction force:** Upon further inspection of these friction reduction strategies, another aspect that may have potential advantages is that some methods may instead of eliminating friction, use it to their advantage by applying "traction" through the manoeuvre. For this to work, the strategy should *actively* eliminate slip, so that the contact surfaces will remain still with respect to the object and can still transfer friction forces onto the gripper structure. This is not the case for either normal force reduction (−−) or friction coefficient reduction (−−). The free-rolling contact strategy (−−) does eliminate slip but does not allow traction since the free rolling contacts cannot effectively transfer the friction forces to the gripper structure. The other slip-reducing strategies however do allow for traction, where the eversion (++) and walking (++) strategies could yield better results since their entire contact surfaces can provide traction during the grasp, while for telescoping (+) there will at least be some section which moves with respect to the object surface during the manoeuvre.

Table 3.2: Table showing the criteria, and the scores of the individual strategies based on the underlying physical principles.

Criterion	**Normal force reduction**	**Friction coef. reduction**	**Slip reduction**			
			Free rolling	**Eversion surfaces**	**"Walking" contacts**	**Telescoping**
Remaining friction force	−−	−−	+	++	++	+
Potential traction force	−−	−−	−−	++	++	+

Most feasible strategies

Looking at Tables 3.1 and 3.2, for both problems during the grasp manoeuvre (reducing space and reducing friction), several strategies have some inherent limitations, and others do not. For the object-following motion, the s-path propagation and building propagation are expected to require a minimal free angle around the object initially, while they could also in theory be adapted universally for different object shapes. For friction reduction, both everting surfaces and walking contacts can potentially fully reduce slip, and more so even employ friction to allow traction for the grasp manoeuvre.

Together, a combination of these strategies is expected to eliminate unwanted disturbances during the grasp manoeuvre. Therefore, a gripper with these features could be applied to cluttered environments much more easily. However, the strategies are still very abstract and the question whether they can be physically combines is not trivial. Therefore, below, some concepts employing these strategies will be given, using which a prototype could be built to put the proposed strategies for improving grasping in clutter to the test.

3.5 Concepts for a maneuvering zero-slip gripper

To be able to verify the claim that a gripper with these features could improve grasping success in dense clutter, a prototype must eventually be made to perform practical testing.

Below, a collection of concepts is shown that implement the most feasible strategies mentioned above. Since they are still just concepts, their precise implementations vary so that the sections below could be considered to describe groups of concepts rather than specific concepts.

Eversion tube based mechanisms

One important group of concepts, is those which employ an eversion tube, or some adaption of it, to eliminate slip. Its propagation can be considered a "building propagation", since the structure is actually built up from the tip onwards. A new issue when using this for making gripper fingers for instance, is the fact that it must have a certain bending stiffness to transfer forces. Several methods can be employed, ranging from using (high) pressure inside the tube (Figure 3.5a), reïnforcement in the tube using a backing with axial stiffness, e.g. spring steel sheet (Figure 3.5b), an axially stiff but bendable backbone which additionally have to follow the S-path manoeuvre (Figure 3.5c) or even some origami-structure designed with the appropriate path/motions, for instance based in self inverting structures (Figure 3.5d).


(a) (b) (c) (d)

Figure 3.5: Different implementations for using an eversion mechanism with some sort of method for increasing bending stiffness. Figure (d) was adapted from [Lee et al., 2013].

Self-inverting u-profile mechanism

Another concept makes use of an origami U-profile which makes a 180°turn at the tip and travels backwards through itself (Figure 3.6). By placing the parallel sides of the u profile at the contact surfaces, slip at the contact surfaces is eliminated while new material is fed through the core. Since the "backbone" of the u-profile only needs to bend in its plane-perpendicular direction, the planar stiffness can be used for transferring grasp forces. By designing the u-profile in a curve, it can even follow the object surface.

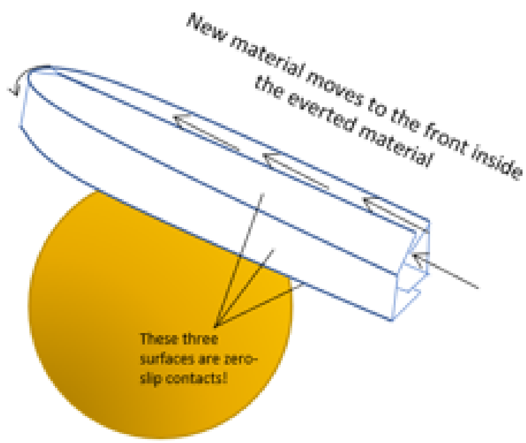

Figure 3.6: Concept for a zero-slip manoeveuvering gripper using self-inverting profile, perpendicular to the manoeuvre direction

Unrolling mechanism

Another concept is based on the unrolling tongue of a butterfly [Lee et al., 2019], which also minimizes slip at any point other than the unrolling "spool" (Figure 3.7). Stiffness can be gained by inserting a backbone into the spool, by pressurizing the tongue tube, or even by wrapping different tongues (fingers) over one-another.

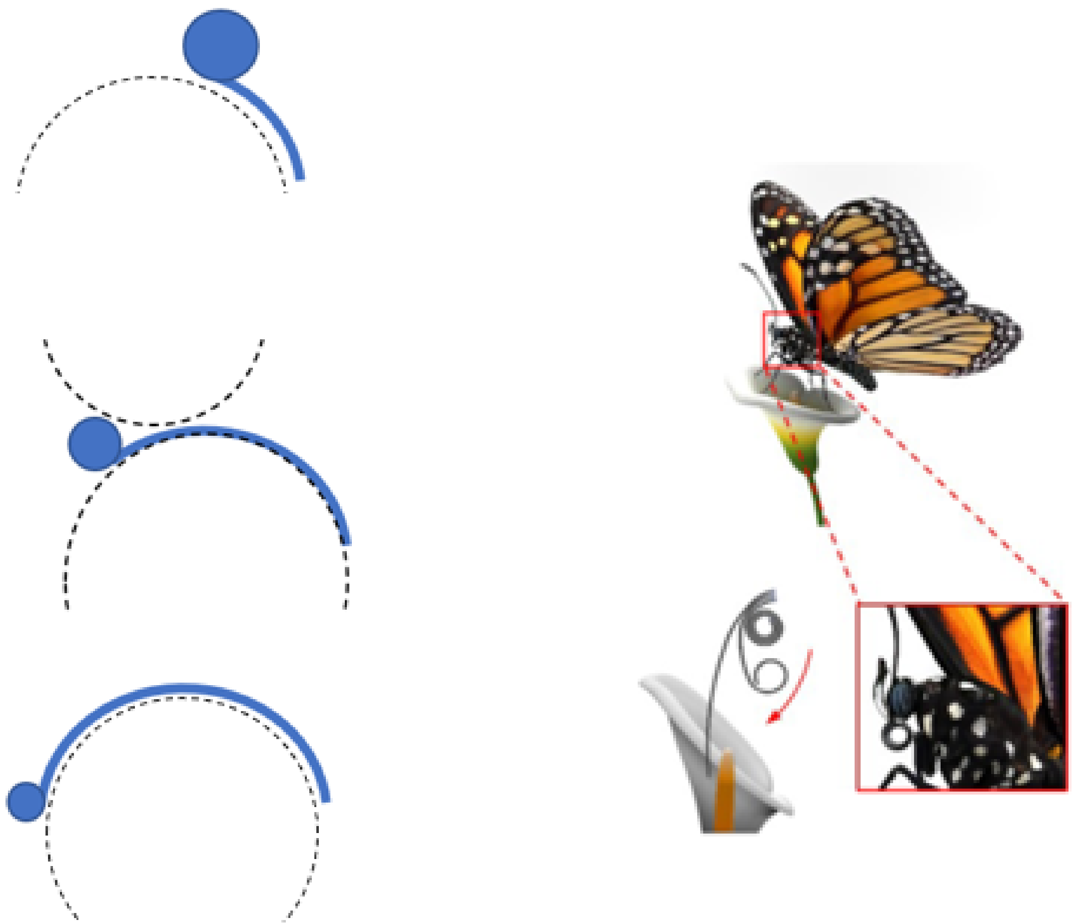

(a) (b)

Figure 3.7: Concept for a zero-slip manoeuvering gripper using an unrolling mechanism. Figure (b) was adapted from [Lee et al., 2019],

2D eversion-based mechanisms

Finally, another range of concepts make use of belts and rollers which perform the effect of the eversion mechanism at the inside and outside contact surface of different fingers around the object. For this approach, a solid backbone manoeuvering in an s-path is used for bending and axial stiffness of the finger. Different variations can be employed, for instance using a combination of one belt so that only the object-contacting surface has eliminated slip (Figure 3.8a), a belt at both the inside and outside surface eliminating all slip (Figure 3.8b) or the use of actively driven rollers (Figure 3.8c).

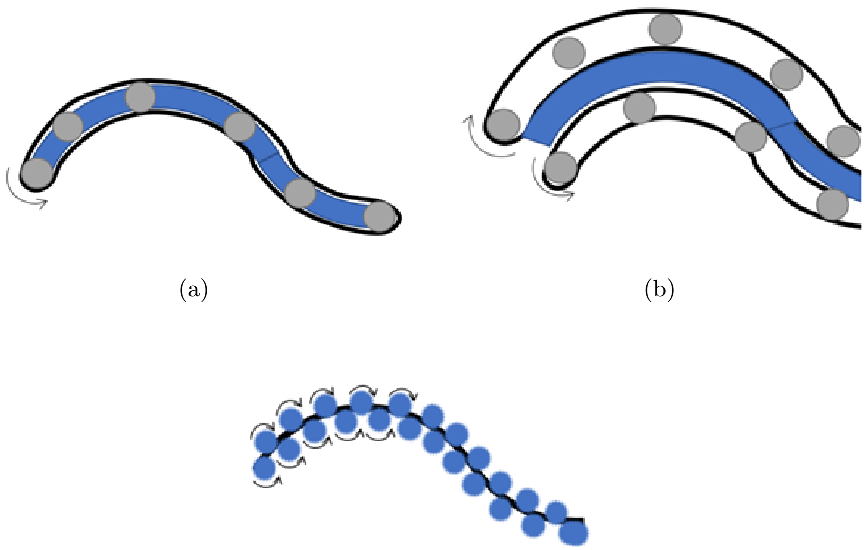

(a) (b)

(c)

Figure 3.8: Different implementations for using belts or rollers to implement a 2D eversion mechanism around a stiff backbone.

3.5.1 Concept choice for an easy to develop prototype

To further investigate whether the clutter problem can be solved with the strategies named above, a prototype will be designed and tested. Here, the choice and reasoning of a concept which is estimated to be easiest to develop into a fully functional one is given.

To make a choice out of the concepts above, the presence or absence of certain concept aspects which were deemed to be complex for development, design and manufacturing, was estimated. If such a complex aspect is present, a + is given. Consequently, the concept with the least number of +'s can be considered to be physically less difficult to develop. It must be noted that this analysis is subjective and that some techniques might be perceived as less complex for the reader than for the author. The aspects that were used for the rating were as follows:

- **Complexity of deformations**: If there are deformations present in the mechanism, if they are in 3D or otherwise expected to be complex to model, this is expected to make a working prototype with all functions much more difficult. For any eversion tube mechanisms (++), deformations are 3D and therefore complex to mode. This is the case at the turning point of the U-profile (++) as well. For the rolling mechanism (+), deformations are present but can be described in 2D. This holds for the 2D eversion mechanisms (+) as well.
- **Level of deformations**: If the deformations present are very large, non-linear behaviour will occur which significantly complicates modelling and may also make material choice and behaviour complex. This is the case for any of the eversion tube mechanisms where the tip deformations will involved folding and wrinkling (++) as well as the unrolling mechanism (++) which should have a very tight rolling radius at its tip. Only the pressure-based eversion tube mechanism (+) is specifically expected to be somewhat less difficult because its tube material requires no stiffness, and can therefore be very thin, eliminating high strains during bending. For the 2D eversion mechanism (+) the belts can be very thin so that deformations are not very extensive. Depending on the way the u-profile is implemented, for instance by more of an origami structure from very thin material, deformations can also be relatively small (+).
- **Realms of physics:** Another aspect is the amount of realms of physics involved. If a solution is either purely mechanical or purely pneumatic, this is expected to make development easier, since no multi-physics modelling and design is required. In fact, only the example of the pressure-based eversion mechanism (++) suffers from this aspect.
- **Difficult production processes:** Although very subjective, some production processes like sewing and (silicone)casting are considered difficult processes because they are labour intensive and require specific (design) skills. For the eversion tubes (++), it is estimated that the thin-walled tubes need to be made fabricated and joined somehow, and that at least some complex manufacturing techniques for this will need to be employed for this.

Looking at the total of complex aspects present for the different concepts, the 2D implementation of an eversion mechanism seems to have the least complex design aspects. This is because all the deformations happen in 2D, and the parts which must provide stiffness for grasping (the backbone) are decoupled from the eversion contacts which are can therefore be highly flexible and have low strains (deformations). Furthermore, because it is purely mechanical, no difficulties with pressure systems, leaks, seals etc. will be involved.

Table 3.3: Table showing the expected ease of development and manufacturing for different concepts

	High-pressure eversion	**Eversion with stiff components**	**Self-inverting u-profile**	**Unrolling mechanism**	**2D eversion mechanism**
Complexity of deformations	++	++	++	+	+
Level of deformations	++	++	+	++	+
Realms of physics	++	−	−	−	−
Difficult production processes	++	++	−	+	−
Total	8	6	3	4	2

3.6 Conclusions

In this research, the issues of, and strategies for setting caging grasps in dense clutter were analyzed. It was found that, in addition to the general tasks (or: functions) of a caging gripper, being the grasp manoeuvre and transferring of forces from object to the wrist during manipulation, two new subfunctions could be attributed to the grasp manoeuvre when dense clutter was concerned.

First of all, since the free space is limited or nonexistent around the object due to the surrounding obstacles, during the grasp manoeuvre, the motion has to closely follow the object surface. Secondly, since forces keeping the obstacles to the object are expected to be present, friction forces will be involved during the motion which will cause further disturbance, hence these friction effects should in some way be minimized.

Several fundamental strategies for these subfunctions were analyzed and it was found that using a growing or an S-propagating, object-following motion with zero-slip surfaces would be the most optimal for decreasing disturbance or damage during grasping.

Different concepts that implemented these strategies were conceived, showing that there is a wide design space that is not yet explored.

From these concepts, one concept was concluded to have the best potential to be turned into a prototype, for verifying the underlying theory that an object-following grasp manoeuvre, combines with zero-slip surfaces will indeed improve grasping capabilities of caging grippers in dense clutter.

Chapter 4

Design and validation of an object following zero-sliding gripper

4.1 Introduction

In this chapter, a novel design of a caging gripper for cluttered objects in the agri-food industry is designed and its workings validated.

The research follows the suggestion from Chapter 3 to use a caging grasp, where the object is manipulated primarily by the normal forces on the gripper surfaces surrounding the object. This method of grasping was explained to be very widely applicable to agri-food objects, since it does not rely on friction, making it suitable for a variety of object surface types. The independence from friction also means that this grasp method does not require a minimal normal force to establish friction, making it very suitable for deformable or fragile objects as well. However, so far the caging gripper has had a major drawback, being that it has to encompass the object during the grasp manoeuvre. This makes grasp planning difficult when the object is partially obstructed by surrounding clutter. Common approaches are using more advanced planning and perception to still make grasping possible, however this remains a complex problem and does not guarantee success.

In this chapter, a mechanical approach is implemented to make caging grasps possible in clutter, based on the concept of Chapter 3 which is shown schematically in Figure 4.1. The concept makes use of fingers that follow the object surface and everting surfaces to eliminate relative sliding between gripper fingers and the object/environment during the grasp manoeuvre. This way, the disturbance and damage to the object and environment are reduced, preventing damage and miss grasping. A prototype for grasping tomatoes will be designed and manufactured, and the correct working of the functions incorporated in the gripper will be individually validated by using four different lab experiments.

The chapter starts off with an explanation of the functional requirements and design parameters that are relevant for this new type of gripper, in Section 4.2. Then, in Section 4.3, the division of the gripper functions over the gripper elements and their workings are shown. In Section 4.5 the detailed design, manufacturing materials and processes used for the prototype are elaborated. In Section 4.6, the setups used for measuring the performance of the gripper, in terms of its individual functions are shown. The results are given in Section 4.7, and discussed in Section 4.8, which also leads to several recommendations. Finally, in Section 4.9, the conclusions on the gripper design and validation are given.

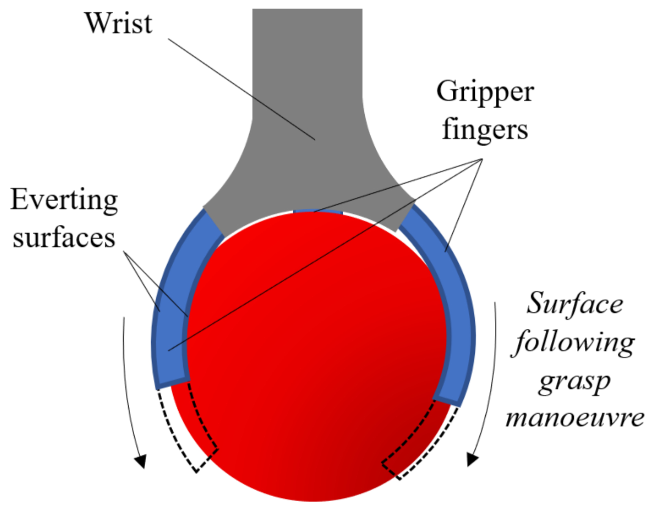

Figure 4.1: Simplified sketch of the proposed gripper concept. The gripper wrist is placed on the object, after which the fingers emerge from the wrist and follow the object. The fingers are fitted with everting surfaces that have zero relative sliding with respect to the object and environment.

4.2 Gripper functions and parameters

The gripper that is to be designed needs to carry out a number of functions, consisting of some basic gripper functions present in any caging gripper, but also functions related to the specific method of grasping in clutter. Furthermore, the gripper faces some constraints (or design parameters) based on the task of grasping tomatoes, both due to object size and weight, and due to the characteristics of the cluttered environment in which the task is performed. In this section, these functions and design parameters are disambiguated and quantified.

4.2.1 Gripper Functions

In principle, any caging gripper performs three basic functions, being:

- **Grasp manoeuvre:** After the robotic system puts the gripper in the correct grasping position, the gripper performs a closing manoeuvre so that it will encompass the object. In this concept, this is done by propagating three gripper fingers from the wrist along the surface of the object, where the fingers fingers are naturally curved and kept at the surface by reaction forces from the object surface.
- **Transfer manipulation forces from wrist to object** After closing, the robotic system performs some manipulation tasks by moving the wrist of the gripper, which transfers the manipulation forces onto to object. For this gripper, normal forces of the finger surfaces surround the object must thus be transferred to the wrist of the robot by means of the structural stiffness in the fingers.
- **Release manoeuvre*** After manipulation, the object needs to be released from the gripper again. In this gripper, this is performed by the reverse operation of the closing manoeuvre and not considered a separate function in the design.

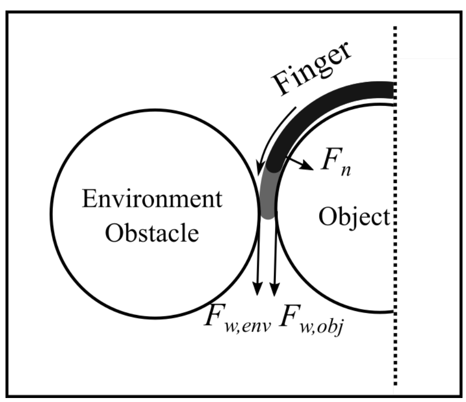

Figure 4.2: Friction forces exerted by the finger on the object ($F_{w,obj}$) and on the environment obstacles ($F_{w,env}$) when inserting a finger between two objects in a cluttered environment. A normal force F_n may push symmetrically on each side of the object.

When performing the object following closing manoeuvre in dense clutter, several forces come into play due to interactions with the clutter and object, as illustrated in Figure 4.2. These forces may disturb the object or environment, resulting in miss-grasps or damage, which are mitigated by the following subfunctions:

- **Friction/sliding elimination:** Due to forces present in the clutter e.g. the gravitational forces and in a stack or bunch of tomatoes, friction forces $F_{w,env}$ and $F_{w,obj}$ would act when inserting a finger between object and environment. To mitigate the negative effects of friction (e.g. damage / missgrasps) sliding between the finger surfaces and the object/environment must be eliminated, thereby eliminating the effects of these friction forces.
- **Initial tangential finger guiding:** When following the object surface, the fingers exert a small normal forces at the object surface. The horizontal components balance out, but the vertical components result in a net vertical force $F_{net,norm}$. To minimize this force and minimize pushing the object away, an additional subfunction is introduced for initially guiding the fingers tangentially onto the object so the normal forces are negligible until they are well past the top surface of the object.

4.2.2 Design parameters and constraints

For the design, several parameters are relevant, which follow from the objects to be picked up, being roma/pomodori tomatoes. The tomatoes are expected to have a mean diameter of $D = 60$ mm, with a variety in size within +/- 10 mm.

First of all, the required holding force F_{hold} force follows approximately from the diameter, since most agri-food products are largely made up of water, meaning that the weight can be approximated by multiplying the volume of a sphere of diameter D with the volumetric mass of water $v_{water} \approx 1000$ kg/m^3 according to Equation 4.1, resulting in a weight of $m_{tomato} = 180$ gr for a tomato with the maximum diameter of $D = 60 + 10 = 70$ mm.

$$m_{tomato} = \frac{\pi D^3}{6} v_{water} \tag{4.1}$$

Assuming that the gripper will be used to vertically lift the tomatoes, this means that the minimal manipulation force that the gripper should apply is $F_{hold} = m_{tomato} \cdot g_{earth} \approx 1.8$ N, where the Earth's gravity g_{earth} is approximated by 9.81 m/s^2.

Next, two parameters related specifically to grasping in clutter are important, which become apparent from the schematic representation of clutter in Figure 4.3. These are as follows:

- **Free angle around object θ_{free}:** Before the gripper performs its object-following grasp manoeuvre, it already requires the object to have some free surface, represented by the free angle θ_{free} so that the gripper can approach the object without interacting with the environment. To be able to grasp any object that which can be approximately identified from a top view, the gripper should not require more than a quarter of the object, or 90°of the top surface, to be free.
- **Finger thickness t_{finger}:** When inserting the finger between two objects, each object would compress by about $t_{finger}/2$. The allowable compression of tomatoes is about 10% [Li et al., 2013] before visual damage occurs [1], which means that the finger thickness should be at most $t_{finger} = 20\% \cdot D_{tomato} = 12$mm before damage to the tomato occurs.

[1] In practice a 10% compression will result in internal damage, which will impact shelf life of the product, but for this research visual damage is used as the limit since it is easily verifiable during experimentation.

Table 4.1: Design parameters for a caging gripper for tomatoes

Name	**symbol**	**Constraint**	**Source**
Object diameter	D	50 mm $< D <$ 70 mm	Expected object population for example case
Manipulation force	F_{hold}	$>$ 11 N	Corresponds to lifting a sphere with object diameter D comprised entirely of water
Finger thickness	t_{finger}	$<$ 12mm	Surrounding objects will never be strained beyond the allowable 20% strain
Free angle	θ_{free}	$< 90^{\circ}$	Any object which can approximately be identified from a top view, can be grasped

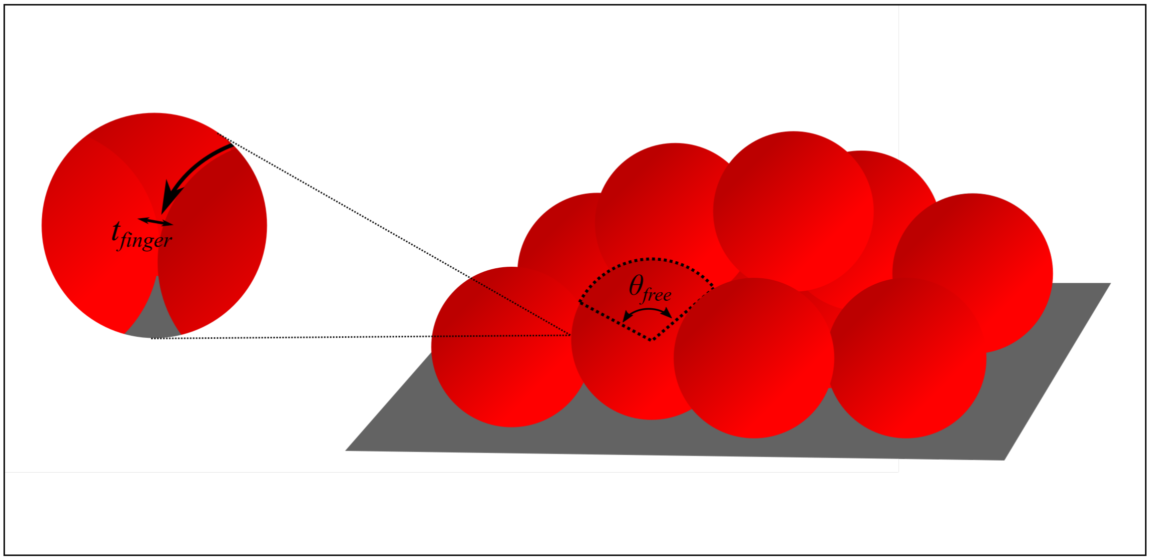

Figure 4.3: Schematic representation, showing the relevant parameters for grasping in clutter: The required free space around object θ_{free} during the approach and the displacements during maneuvering of the gripper fingers into the clutter, equal to the finger thickness t_{finger}.

4.3 Gripper design

To validate the concept and underlying principles working, the functions named above need to be implemented into an integrated gripper design and manufactured into a prototype. In this section, the division of functions over the gripper parts, and the kinematics and mechanics of the design and subsequent design choices are explained.

4.3.1 Functional division between gripper parts

A schematic presentation of the parts of the gripper is shown in Figure 4.4. The gripper consists of three identical fingers mounted on a middle hub, in which the functions named in Section 4.2 are incorporated as follows:

- **Grasp manoeuvre**: To allow forward propagation of the finger during the grasp manoeuvre, the middle hub and actuator provide the linear motion of the finger inside the wrist, while the backbone of the finger provides axial stiffness to transfer this motion through to finger outside of the wrist up to the finger tip.
- **Friction/sliding elimination**: To counter disturbance and damage due to the friction forces $F_{w,env}$ and $F_{w,obj}$, the zero-slip belts covering the finger roll out during grasping with the same speed as the finger is propagating forward, eliminating slip at the contact surfaces between the finger and the object and environment.
- **Initial tangential finger guiding**: To allow the finger to approach and follow the object during the grasp manoeuvre, and minimize the net normal forces $F_{net,norm}$ on the object, the

backbone is made flexible and pre-shaped to the curve of the object surface, and the wrist is fitted with a shaped channel to direct the backbone tangentially onto the surface of the object.

- **Transfer manipulation forces:** To transfer normal forces from the finger to the wrist, the fingers have a bending stiffness, which is provided by a combination of tensile forces on the inner zero-slip belts, and compressive forces in the backbone.

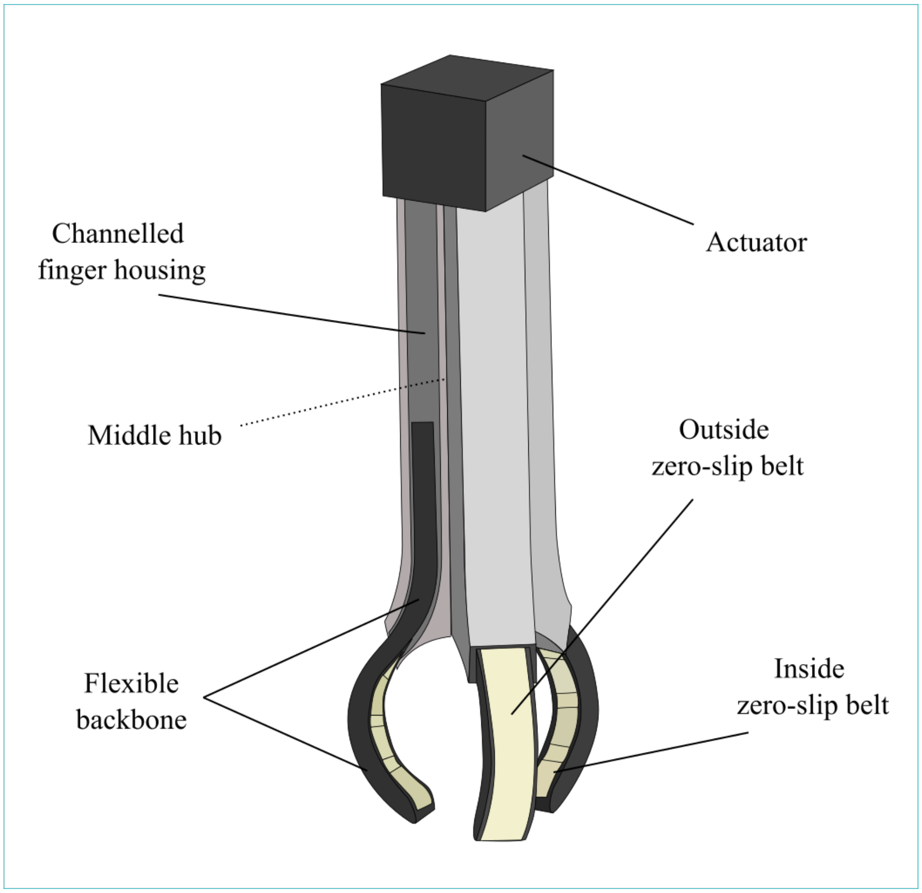

Figure 4.4: Schematic presentation showing the parts of the gripper in different colours. The middle hub is hidden behind the finger modules and cannot be seen.

4.3.2 Forward propagating flexible backbone

The finger consists of a spring steel backbone which is able to slide in and out of a channel in the wrist. This channel has a long straight section, directed through the object center. Near the object, this channel makes a sharp bend so that the backbone ends tangentially to the object surface.

The spring steel backbone is pre-shaped before insertion in the channel to the radius of the object. This way, while the backbone is pushed out of the channel, it will first follow the curved channel-end, directing it tangentially to the object, and then reassume its pre-tensioned shape as soon as it leaves the channel, thereby following the object surface.

4.3.3 Zero relative sliding surfaces

The in- and outside surfaces of the gripper fingers are covered by belts which actively roll out of the finger tip while it propagates from the gripper wrist. The configuration resembles a 2D-implementation of the pneumatic eversion mechanisms known from literature [Do et al., 2020] [Hawkes et al., 2017] [Blumenschein et al., 2020], an example of which is shown in Figure 4.5. In the designed implementation, shown schematically in Figure 4.6, most of the features present in Figure 4.5 can be found in another form. The belts replace the tube and are fixed at their outside ends at the wrist[2] of the gripper, like the tube was in the eversion mechanism. However, instead of air pressure, a sheet-metal backbone with rollers is used to push forward the finger and push out (evert) new belt material. Furthermore, instead of the circumferential tension in the tube, which keeps the in- and outside of the tube together, pull-in rollers are used on the inside of the finger to keep the belt near the finger. Instead of the reel from Figure 4.5, a rubber band is used to retract the belts through the core of the finger. Finally, the linear actuator performs the mechanical work and control that the pump used to perform.

4.3.4 Modular wrist system

Due to the complex assembly and high part count of each individual finger, it is important that the fingers can be individually built, tested, and even be replaced easily. To achieve this, the gripper is divided into several modules, being:

- *3 identical finger modules,* each of which consists of a housing containing the guiding channel, and a gripper finger
- *The linear actuator,* consisting of a stepper motor with a non-captive spindle, meaning that the spindle translates with respect to the motor when actuated
- *The middle hub,* which forms the connection between all other parts, by providing mounting points for the actuator and finger module housings, and by providing a guided sliding block connects the actuator spindle to each of the sliding fingers in the finger modules

[2] The inner belt is mounted after the curve, so that the pull-in rollers can pass up to there.

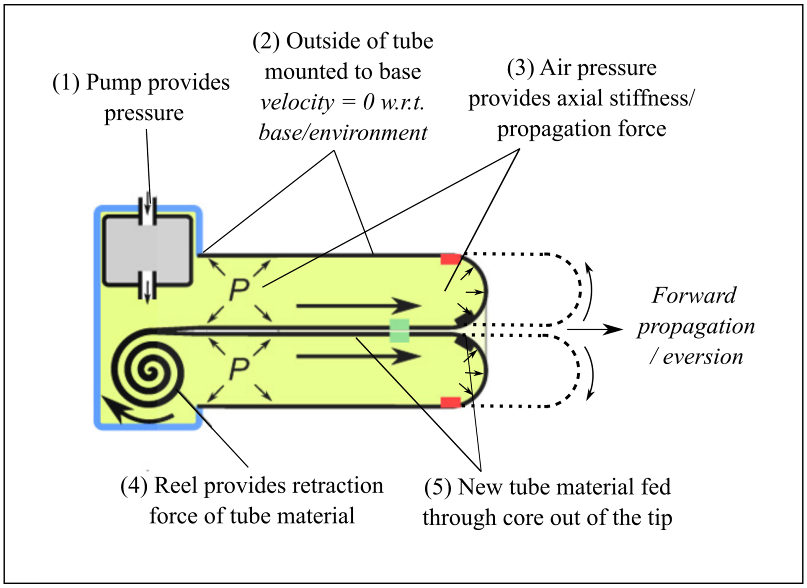

Figure 4.5: Schematic section view of an eversion tube mechanism, adapted from [Hawkes et al., 2017]. The eversion tube is able to easily propagate through tight spaces while the outside surface of the tube remains still with respect to the environment because it is fixed to the base.

4.4 Mechanical analysis of key features of the gripper

Some elements of the design required a thorough mechanical analysis to establish the correct dimensions and determine the expected behaviour. In this section, the methods and results of these mechanical analyses are shown.

4.4.1 Maximimum backbone thickness to allow S-bend

To prevent fatigue failure in the spring steel backbone in the long term, no excessive deformations may occur during the S-shaped manoeuvre. The S-shaped curve consists of two opposite curves: The first is the bent part in the wrist, with a radius of $R_{backbone,wrist} = 25$ mm, and the second part is the one following the object, with a radius of $R_{backbone,object} = 42$ mm at the backbone of the finger. The radii of curvature are several orders of magnitude larger than the thickness of the backbone, due to which the backbone can be approximated as a thin film. Therefore, the maximum strain can be calculated by applying the difference between the relaxed and strained curvatures, $R_{backbone,object} + R_{backbone,wrist} = R_{effective} = 67$ mm in the bending Equation 4.2 for the resulting max strain η_{max}. Combining with Equation 4.3 then shows the maximum backbone thickness for a given material Young's Modulus $E_{backbone}$ and allowable stress $\sigma_{allowable}$ as Equation 4.4:

$$\eta_{max} = \frac{t_{backbone}}{2R_{effective}} \tag{4.2}$$

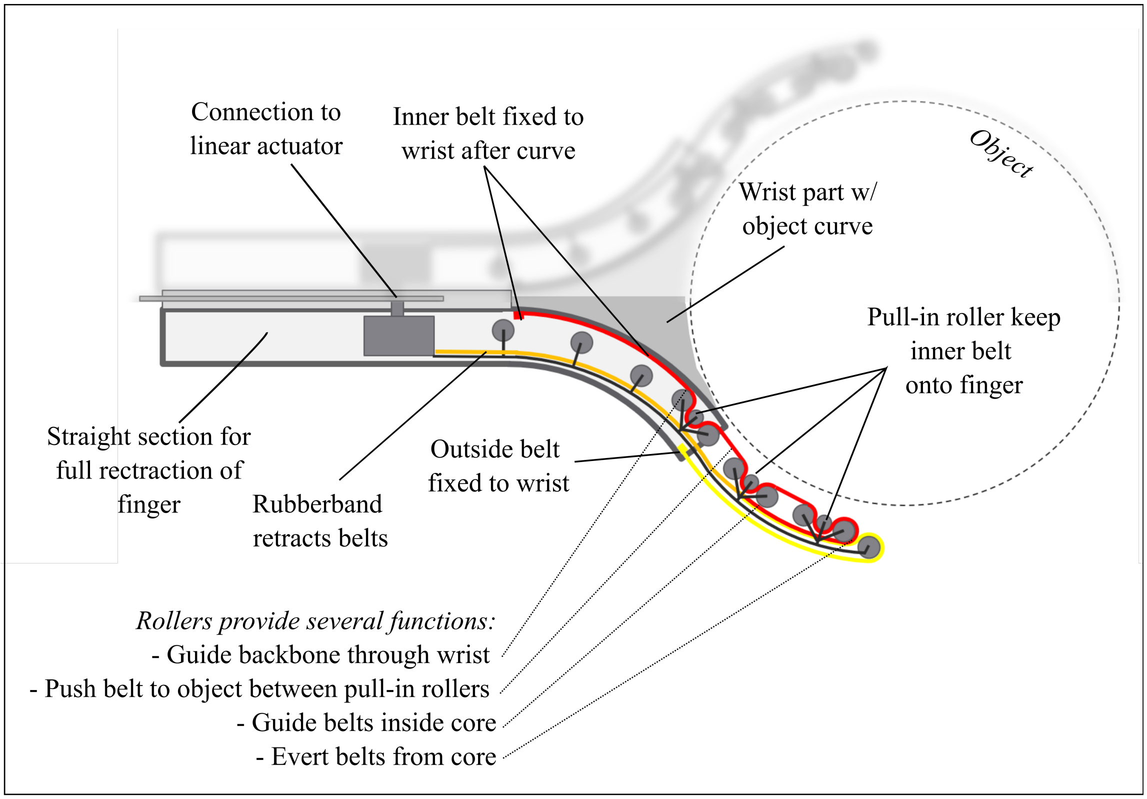

Figure 4.6: Schematic description of the configuration of belts and roller inside each finger.

$$\eta = \frac{\sigma_{allowable}}{E_{backbone}} \tag{4.3}$$

$$t_{backbone,max} = \frac{2(R_{effective}\sigma_{allowable}}{E_{backbone}} \tag{4.4}$$

For the backbone, C100S spring steel is used. Like most steels, it has a Young's Modulus of about E_{young} = 210 MPa, but more importantly, it has a relatively high σ_{yield} of at least 1600 MPa [h+s Präzisionsfolien GmbH, 2017]. Assuming an endurance limit of $\sigma_{allowable} = 0.5\ \sigma_{yield} = 900$ MPa, and entering this in Equation 4.4, this gives a maximum backbone thickness $t_{backbone,max} = 0.5$ mm. In practice, it was found that for this thickness, the required actuation forces would drastically increase, and that bending operations would become difficult. Therefore, a final backbone thickness of 0.20 mm was chosen, for which the strains remain well below the endurance limit.

4.4.2 Analysis of the belt friction

Because the belts go through a series of pulleys under different wrapping angles ϕ, with a certain friction, as shown in Figure 4.7, the belt tension will decrease throughout the pulley system. To verify that the rubberband, which has a force of F_{rub} = 1.5 - 4.5 N depending on the elongation (see Appendix E), has sufficient tension, the spare belt tension throughout the pulley system is calculated. This is done, by first setting up the equations for friction loss in a single pulley, and then iterating this calculation over all pulleys for a single belt. For the belt to retract, there should be a significant spare tension F_{spare} at the end of the belt so that even with additional forces on the belt (e.g. viscoelastic friction due to belt deformation, or an unexpected contact with the object or otherwise), the belt still retracts.

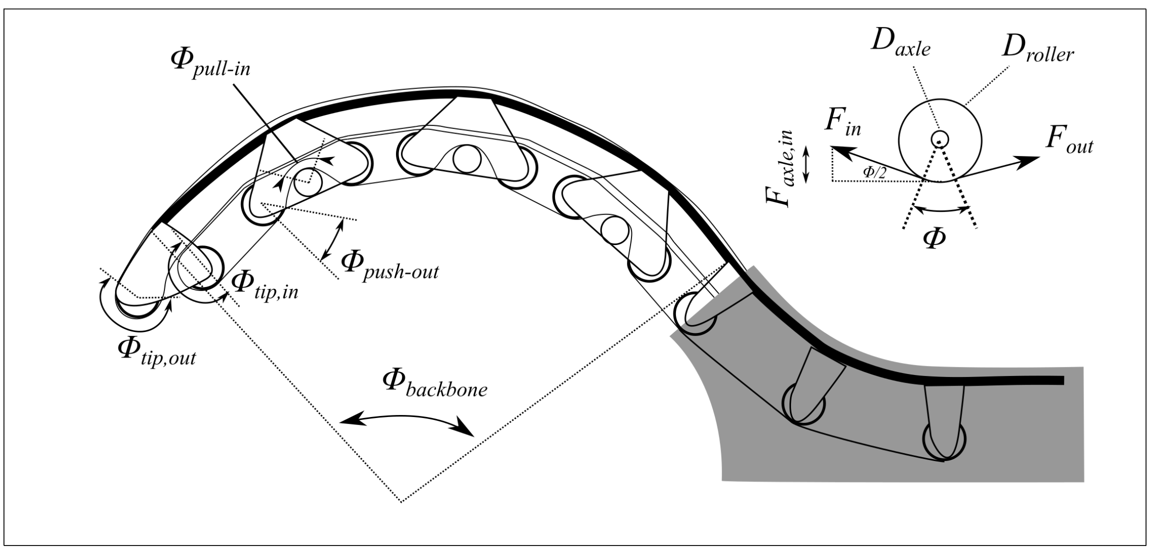

Figure 4.7: Schematic showing the relevant wrapping angles ϕ and dimensions of the belt and pulley system.

Friction for a single pulley

Each time the belt wraps a certain angle around a pulley, a part of the belt tension is lost as friction:

$$F_{out} = F_{in} - F_w \tag{4.5}$$

Calculation of this friction force is done by first finding the net force that F_{in} and F_{out} apply on the roller axle, and multiplying it by the effective friction coefficient of the rollers μ_{eff}. Since the friction loss at each individual roller is small, the force F_{out} can be approximated by F_{in} when calculating the force on the axle [3]. This way, it is reduced to a symmetric goniometric problem, as shown in the top right of Figure 4.7, so that the net force can be written as:

$$F_N = 2 \cdot F_{in} sin(\phi/2) \tag{4.6}$$

The effective friction coefficient for the axle is calculated as the friction coefficient at the sliding axle surface, multiplied by the ratio of the axle diameter over the roller diameter:

$$\mu_{eff} = \mu_{axle} \frac{D_{axle}}{D_{roller}} \tag{4.7}$$

Then, using Equations 4.6 and 4.7, the friction force F_w can be calculated, so that F_{out} is found:

$$F_w = F_N \cdot \mu_{eff} \tag{4.8}$$

$$F_{out} = F_{in}(1 - 2\mu_{eff} sin(\phi/2)) \tag{4.9}$$

Resultant spare tension at inside belt end

The belt tension was calculated using a python script, which is given in Appendix B. The final belt tension at the end of the pulley system was calculated by starting at the foremost pulley with $F_{in} = F_{rub}$ and calculating F_{out}. The resulting F_{out} was used as F_{in} for the next pulley, and this process was iterated until the last pulley was reached[4]. Using this calculation, the expected belt tension at the end of the belt is expected to be about $F_{spare,in} = 2.4$ N, which is expected to be sufficient considering the low friction losses expected.

[3]Note that an analytic approach to this problem is available; however for the desired accuracy of calculating F_w for this gripper design, this simpler approach is deemed sufficient.

[4]The friction at the surfaces in the core of the finger are herein neglected since the total wrapping angles are low, and the axle pressure increase mostly counters the axle pressure on the roller cause by the belt running on the opposite side of that same roller

Resultant spare tension at outside belt

For the outside belt, the friction actually consists only of the friction caused by the tip roller, and the friction cause by the sliding between the backbone and the belt. For the tip roller friction, equation 4.9 can be used again. For the backbone friction, the Capstan equation (4.10 is used resulting in the combined Equation 4.11:

$$F_{out} = F_{in} e^{-\mu_{back}\phi_{back}} \tag{4.10}$$

$$F_{spare,out} = F_{rub}(1 - 2\mu_{eff} sin(\phi_{back}/2))e^{-\mu_{back}\phi_{back}} \tag{4.11}$$

In the same script of Appendix B, this calculation is shown, which resulted in a spare tension of $F_{spare} = 1.6$ N. which is again deemed sufficient.

4.4.3 FEA analysis of the grasping force

To determine whether the grasping force of the gripper is sufficient, the reaction force of the fingers of the object, which should be overcome to pull an object out of the gripper, is retrieved from a simulation in the SolidWorks Simulations FEA add-on, with a simplified model of a single gripper finger.

Object

The object is simulated by using a half cylinder of the expected object diameter of 60 mm, which is kept in place with respect to the gripper with a fixed constraint. The resultant horizontal reaction force on this object by the finger can then be retrieved, which gives an adequate measure for the force that needs to be overcome to displace the object out of the gripper.

Non-penetrable contact

For simplification of the model, a single point of contact, being the outermost inside roller (or: the fingertip), is assumed. The contact is assumed to be frictionless, which is a conservative approach since the gripper should also be able to work for slippery objects. Furthermore any friction force would oppose slip, and is thus expected to only aid in improving the holding force.

Backbone

The backbone of the finger is modelled as being fixed from the point it emerges from the wrist, which is used as a Fixed Geometry constraint. The rest of the finger will be modelled linearly, which is allowed due to the thin sheet characteristics of the backbone. In the simulation, a Young's Modulus of 210 GPa, a Shear Modulus of 79 GPa and a Poisson Ratio of 0.28 were set as material properties.

Relevant belt forces in simulation

Including the entire mechanics of the belts, rollers and rubber bands would be too complex. Instead, an estimation is made, based on the effective tensile forces that the belts exert between some key points of the finger structure. To do this, the belt tension of each belt will be modelled as constant throughout the finger [5], and equal to the tension in the rubber band that occurs when the finger is in its initial shape [6], where the rubber band is stretched to 130 mm, corresponding to a tension of $F_{belt} = F_{rubberband} \approx 3$ N.

In Figure 4.8, the distinct parts of the belt are noted. Many of these can be neglected, since they work in parallel to much stiffer parts of sheet metal:

- **(1) Outside belt, outer surface:** This section of the belt is in parallel and almost coincident with the sheet metal backbone, which is several orders of magnitude stiffer, so that omitting this section will not significantly impact the model.
- **(2) Outside and (3) Inside belt, tip section:** Up to the first inside roller, these sections of the belt are structurally in parallel with the sheet metal tip tabs, which are expected to be several orders of magnitude stiffer than the belt.
- **(4) Outside and inside belt tab sections:** at the tabs where the pull-in rollers are placed, the belts act parallel to the sheet metal triangular tabs which are several orders of magnitude stiffer than the belt.
- **(5) Effective sections:** The rest of the belt sections, marked by the solid lines, can each be seen to individually connect between two of the push-out rollers. These sections can actually do work by pulley the rollers against one another and are therefore the only relevant sections for the simulation.

Modelling belts as pre-tensioned springs between rollers

Another effect of disregarding friction is that no net moments can be applied to any of the rollers, meaning that only the net forces applied to each roller need to be taken into account. This allows for a simplification, being that these sections of the belt can now be modelled by a constant force between two rollers, equal to $F_{rubberband}$. In the Solidworks Simulations Add-on, this can be done by adding constant forces between two flattened surfaces extruded from the rollers, with a force of $n \cdot F_{belt}$ where n is the number of sections between the two rollers. The resulting model, with constraints and springs added, is shown in Figure 4.9.

FEA results

In Figure 4.9, the resulting model of the finger deflecting under the tendons tension can be seen. The reaction force on the object was retrieved to be 0.97 N in x-direction (horizontal in the figure). Since this is the holding force of only 1 finger, the total holding force is expected to be at least $F_{hold,FEA} = 2.91$ N.

[5] In practice, the friction forces will cause the belt tension to vary throughout the finger. However, since friction forces always oppose motion, the friction forces will in principle only decrease deflection of the finger and thus increase holding force.

[6] This rubber band tension would only increase during deflection of the finger since the total path length of the rubber band would increase, this is also a safe approach to determining $F_{hold,min}$

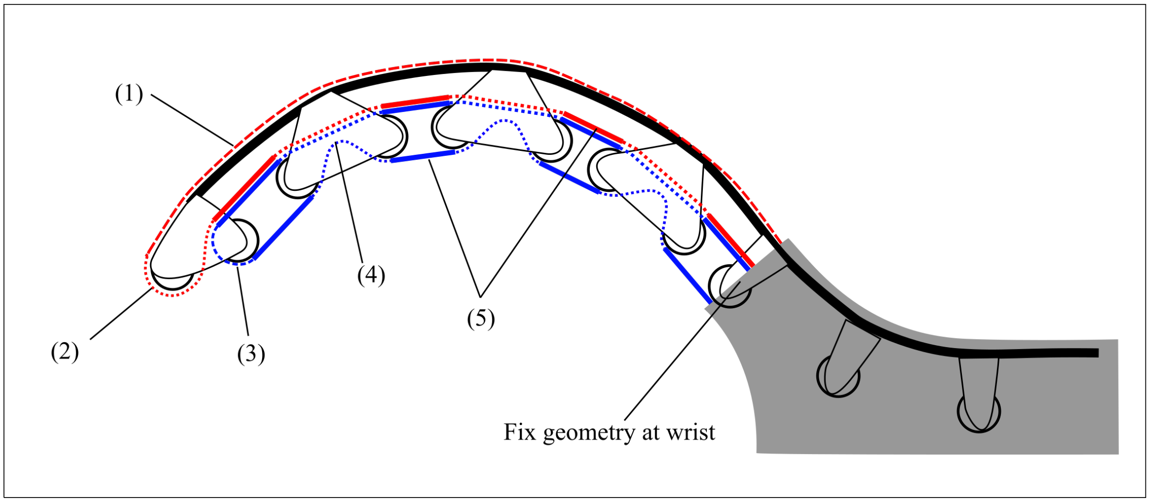

Figure 4.8: Different sections of the belt of a finger marked by numbers. Only the solid lined pieces significantly contribute to the finger stiffness.

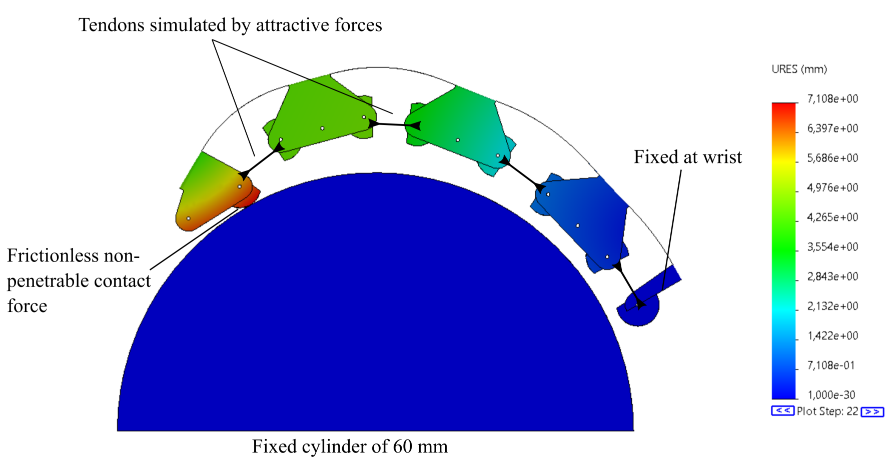

Figure 4.9: Result of FEA model for determining reaction force on on object of a flexible finger. The finger is cut where it emerges from the wrist, where a Fixed Geometry Constraint is added. The tensile forces of the belts are modelled by constant forces between the pushout-rollers.

In Section 4.2, the total required holding force F_{hold} was determined to be 1.8 N for the largest object size, which is much lower. Therefore the gripper is expected to hold even the heaviest objects with a safe margin.

4.5 Detailed design and manufacturing

In this section, the detailed design of, and manufacturing processes used for making the gripper are shown using several photos from the prototype in various states of assembly.

4.5.1 Finger backbone fabrication

The finger backbone, shown in Figure 4.10, is made of hardened spring steel sheet[7], which is cut out using a CO2 laser cutting machine at the lowest allowable speed to prevent unwanted annealing which reduces the yield strain of the backbone[8]. Conversely, the roller tabs on the side of backbone need to be bent at a sharp bending radius at a 90 degree angle, which is not possible at the hardened state of the spring steel. Therefore, these tabs are individually heated using a small torch and slowly cooled to locally lower the hardness, allowing them to be plasticly bent without breaking. More details on this process can be found in Appendix A. The edges of the backbone are individually filed to remove rough edges for the rollers and objects to get caught. The finger is then pre-shaped to the s-shape when the finger is engaged, as can be seen in Figure 4.10.

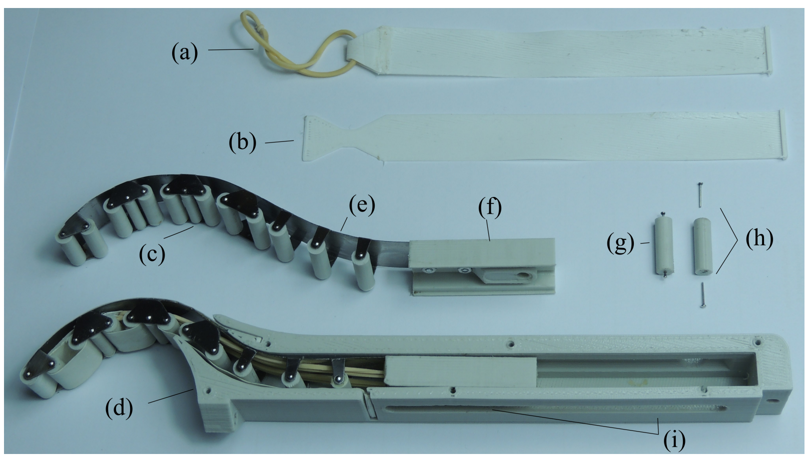

Figure 4.10: A single finger module in various states of assembly. The labeled parts as are follows: (a) Belt with rubberband (b) Unwelded belt (c) Finger with guide rollers (d) Complete finger module with wrist part and belts mounted (e) Pre-shaped backbone (f) Finger sliding block (g) Assembled roller (h) Disassembled roller and pin axles (i) Slot for actuator connection.

4.5.2 Tensioned belts with guiding rollers

The completed finger module at the bottom of Figure 4.10, is shown in the extended state. In white, the inner and outer belts can be seen, which are individually 3D-printed in flexible TPU. Each belt is printed in 3 layers of 0.2, 0.1, and 0.1 mm thickness respectively, at alternating infill directions of +15°and -15°with respect to the longitudinal axis of the belt, to achieve longitudinal stiffness but still some weaving strength. Tabs were printed at the end of the belts which slide and

[7]Known as: C100S, 1.1274, AISI 1095

[8]The used settings for laser cutting are given in Appendix F. Note that this settings are an indication only and will differ for each part and machine used.

lock into slots in the wrist. Furthermore, at the other end of the belt, a foldable tab was added which could be welded to the back of the belt, resulting in a loop for the retraction bands to mount to[9]. The retraction bands are made of rubber bands with an unstressed cross-section of 1.2x1.2mm, which are cut and tied at a total loop length of 56 mm. The force response of the resulting loops, when pulling between two points, rises from 1.5 N at 70 mm length to 4.4 N at 150 mm length[10].

4.5.3 Guiding rollers

The rollers, shown in the right of Figure 4.10, consist of a plastic cylinder at either end of which a small (0.5 mm diameter) steel pin can be inserted which is kept in place by an interference fit and acts as an axle. The roller are 3D-printed in 0.1 mm layer thickness using PLA. The used pins are re-purposed headpins which are commonly used in sewing. The head of the pin acts both as a stop to keep the roller centered in the backbone, and as a sliding surface for the sides of the finger inside the wrist channel. The pins are individually cut at a length of 8 mm, and the points sharpened using a grinding tool, which is necessary to get the pins in the interference-fit holes of the rollers.

4.5.4 Finger module housing and middle hub

The finger module housings, shown in Figure 4.11, are 3D-printed in PLA at 0.1 mm layer thickness. Each housing consists of a bottom part in which the finger is placed, and a lid. Instead of a PLA lid, a transparent acrylic lid can also be mounted, which allows demonstration and inspection of the inside workings of the gripper finger.

The middle hub consists of a hollow triangular bar through which a slider can glide up and down. This slider has 3 protrusions, which connect to the sliding fingers in each of the finger modules. On each side of the triangular bar, a long slot is left open, which corresponds to a similar slot in the finger module housing, to allow the mentioned protrusions to slide up and down. The parts are connected using 16 mm M3 screws, which are screwed directly into slightly undersized holes in the PLA material. Furthermore, during assembly, all sliding surfaces are lubricated with bearing grease.

4.5.5 Linear actuator

The used actuator is a NEMA 17 non-captive spindle motor, with a holding torque of 0.26 Nm and a spindle pitch of 2 mm. The motor is powered using an A4988 stepper driver connected to an Arduino. The motor is driven at a maximum speed of 700 steps per second or about 233 RPM. For mounting the spindle on the middle hub slider, the hole was printed slightly undersized, and the spindle was heated to 100 °C before screwing it into the plastic slider. The fully assembled gripper, including the actuator, can be seen in Figure 4.12 through 4.15.

[9] Welding the tabs was done by clamping the folded tab between two thin strips of steel sheet, and gently heating the steel sheet with a soldering iron until the tab melted and fused with the rest of the belt.

[10] For the characteristics of the rubber bands, see Appendix E

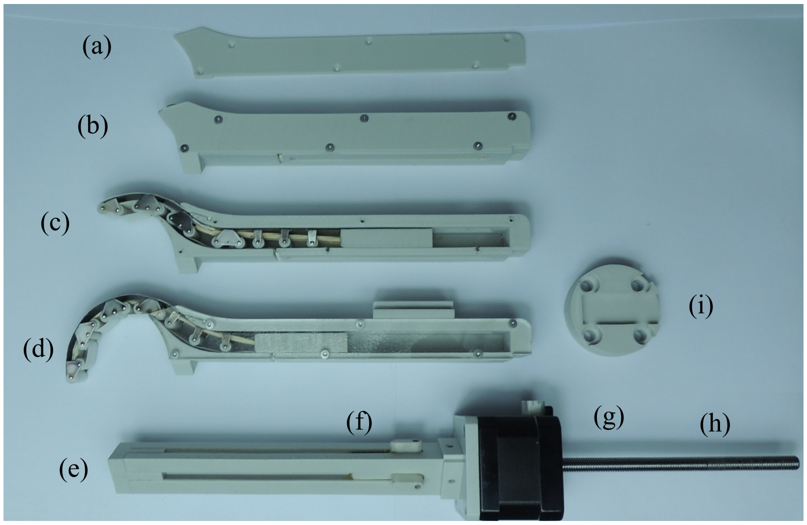

Figure 4.11: Disassembled gripper, showing the separate finger modulus in various extension states and different covers. Parts and modules are labeled as: (a) PLA cover (b) PLA-covered completed fingermodule (retracted) (c) Open finger module (partially engaged) (d) Transparent-covered completed finger module (engaged) with arm-connector block (e) Triangular middle hub (f) slider block with protrusions (g) Actuator (h) spindle (i) arm-connector plate.

Figure 4.12: Prototype of the designed gripper, in its fully assembled and functional form.

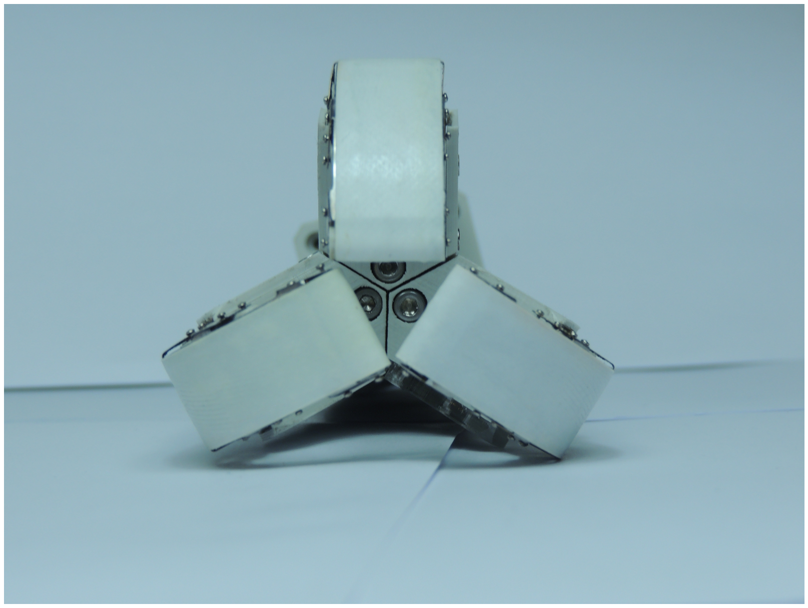

Figure 4.13: Prototype of the designed gripper, in its fully assembled and functional form.

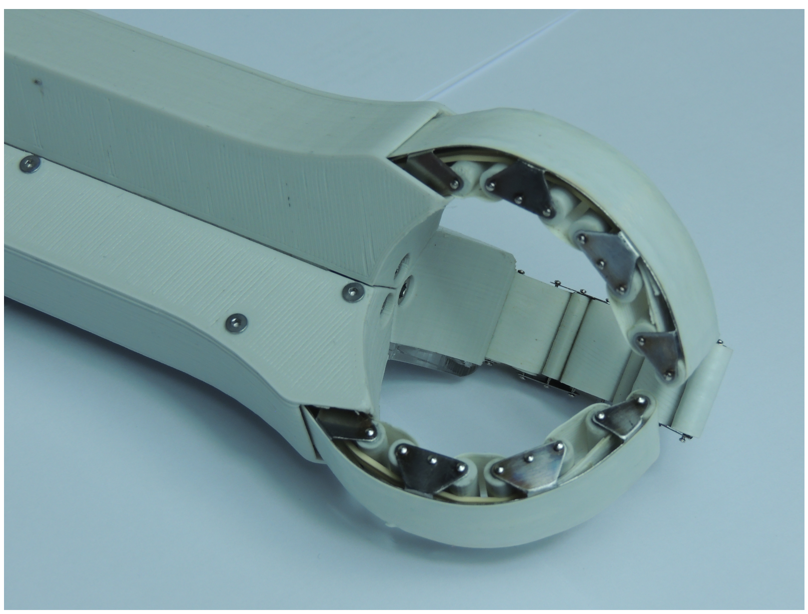

Figure 4.14: Prototype of the designed gripper, in its fully assembled and functional form.

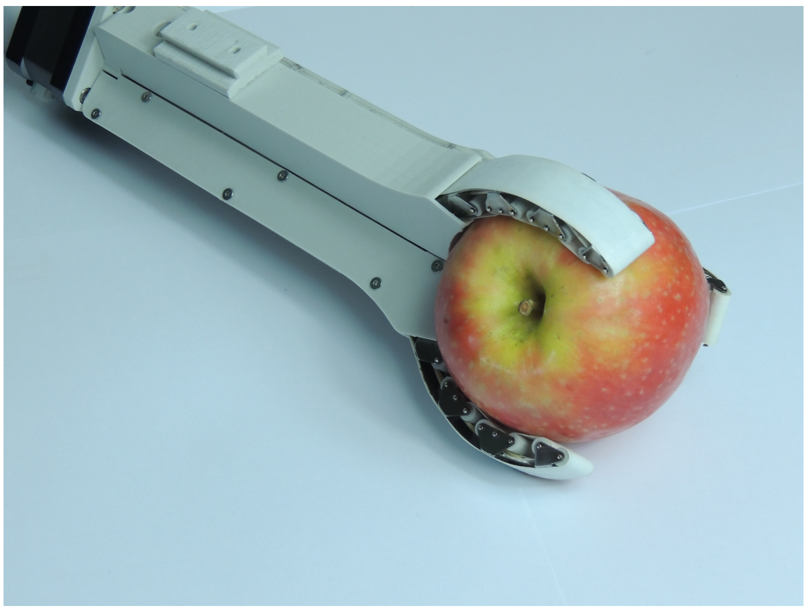

Figure 4.15: Prototype of the designed gripper, in its fully assembled and functional form, holding an apple.

4.6 Measurement/verification of gripper functions

In theory, the chosen design should exhibit certain mechanical behaviours that should improve success rate in grasping in clutter. Using a combination of measurements, it can be verified that the designed mechanical behaviour is indeed present. This is done in four measurements: The propagation deviation, the holding force, the friction force/work, and the net force exerted by the gripper. These measurements act as performance metrics for the four corresonding functionalities that were defined in Section 4.2: Grasp manoeuvre, transfer of manipulation forces, friction/sliding elimination, and initial tangential finger guiding.

4.6.1 Measuring propagation deviations

The finger is designed to propagate forwards along the surface. To verify that the fingers perform the desired motion, the motion of a finger during the grasp manoeuvre is recorded, and the intermediate states graphically compared with the final state. This way, potential deviations from the ideal object-following (and thereby disturbance-minimizing) path can be found.

4.6.2 Measuring holding force

In Section 4.4, the holding force of the gripper, when pulling an object out in the direction of the grippers axis was calculated to be at least $F_{hold,min} = 3.21$ N. To find the holding force in practice, a setup was made in which the force to pull an object out of the closed gripper could be estimated.

Setup

In the setup, the gripper was mounted vertically upwards. A spherical object of 60 mm was placed in the gripper. Using a spring scale with a hook, the object could be manually pulled vertically upwards with an increasing tension which could be read from the spring scale. By subtracting the weight of the object (which was 50 grams), the holding force of the gripper, could then be calculated.

Measurement plan

Using a video recording of the experiment, the maximum exerted force before disengagement could be determined up to a precision of 25 gr. For a more accurate estimation, this step was repeated 7 times to calculate an average holding force $F_{hold,average}$.

4.6.3 Measuring friction force and frictional work

The designed mechanism is expected to give no relative slip at its inside and outside contact surfaces. In effect, this means that the designed gripper should exert no force and no work by friction when moving between two objects. To verify this effect, a setup was made consisting of two cylinders that can rotate and are rotationally centered by springs in between which the gripper finger can be inserted. The resulting rotation of the cylinders could then be directly converted to the frictional force and work that the fingers have exerted on the object. The performance of the designed finger was compared to two exemplary gripper fingers that do have not have zero-slip belts, one of which also follows the object-following path.

Setup

In the measurement setup, shown in Figure 4.16, two cylinders were mounted on individual carriages that run on a linear guide so that they could freely move sideways. On each cylinder, an indicator was mounted so that the angle of rotation $\Delta\theta$ could be measured. A tension spring held the cylinders together. The effective force of this spring was measured to be $F_{norm} = 7$ N when the cylinders were separated 12 mm, which was the nominal thickness of the gripper fingers.

Using a combination of a pulley, wires and two opposing tension springs, the cylinders were kept in a neutral position with an effective torsion spring coefficient κ_{eff}, which were measured as $\kappa_{eff,L} = 0.642$ mNm / degree and $\kappa_{eff,R} = 0.666$ mNm / degree for the left and right cylinder respectively. Measurement and calibration of the setup can be found in H.

Using these spring coefficients, the exerted moments on the cylinders could be calculated, and thus the net friction force exerted at the cylinders surface at $R_{cyl} = 30$ mm:

$$M_{fric} = \kappa_{eff}\Delta\theta \tag{4.12}$$

$$F_{fric} = M_{fric}/R_{cyl} \tag{4.13}$$

Finally, the total exerted work on the cylinders could be calculated as the work stored in the spring system:

$$W_{fric} = \tfrac{1}{2}\kappa_{eff}\Delta\theta^2 \tag{4.14}$$

Non-zero-slip fingers for comparison

To determine whether the designed zero-slip belts were indeed responsible for the decrease in frictional work and force, two benchmark fingers were used, shown in the top left of Figure 4.17. Both fingers were 3D-printed using the same material as the belts of the zero-slip fingers, so that differences could not be attributed to different friction coefficients. The first finger was simply a straight bar of TPU, of the same width and height as the cross section of the zero-slip finger. Since the zero-slip finger curved around the object resulting in more contact points and it also had contact with the object at the wrist, a straight finger might not have given a good comparison. Therefore, a second finger was designed, consisting of a compliant structure that follows the same object following motion when inserted and exerted in the same wrist channel as the designed zero-slip finger.

Measurement plan

For each of the three fingers, the finger was slowly inserted and retracted from the two cylinders using the actuator, which was repeated 10 times. Then, using video material of the experiment, the maximum rotation of each cylinder during each insertion was noted. Finally, using the mean of these rotations θ_{ave}, the exerted F_{fric} and W_{fric} were calculated.

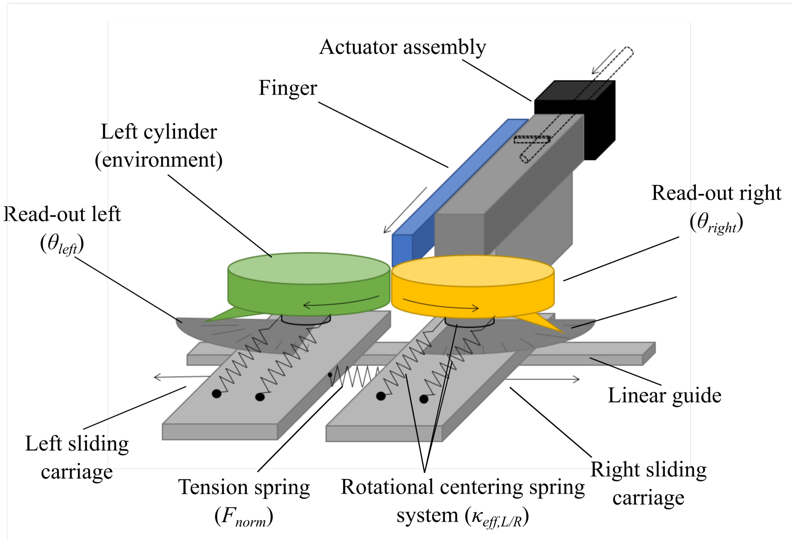

Figure 4.16: Schematic describing the setup used for determining the rotation and force caused by friction when inserting a gripper finger between two cylinders.

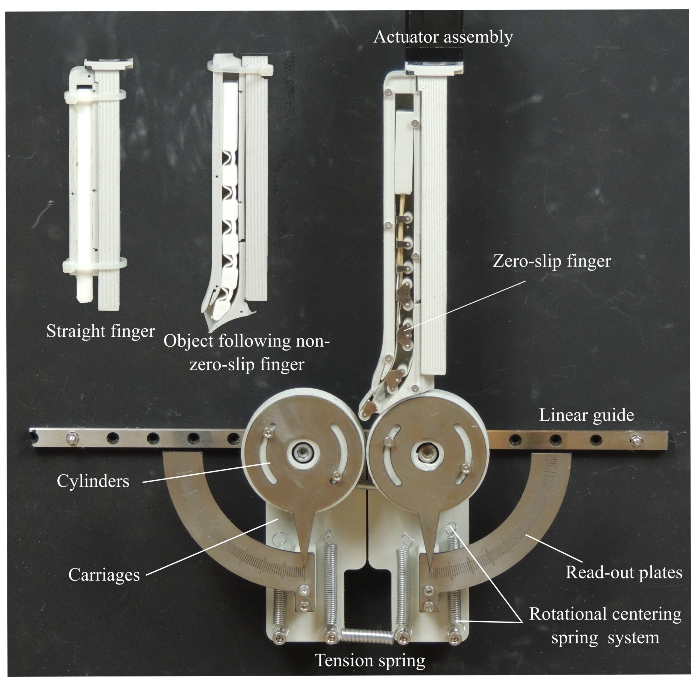

Figure 4.17: Measurement setup used for determining rotation and force caused by friction. In the left upper corner, the non-zero-slip fingers used for comparing the mounted zero-slip finger are shown.

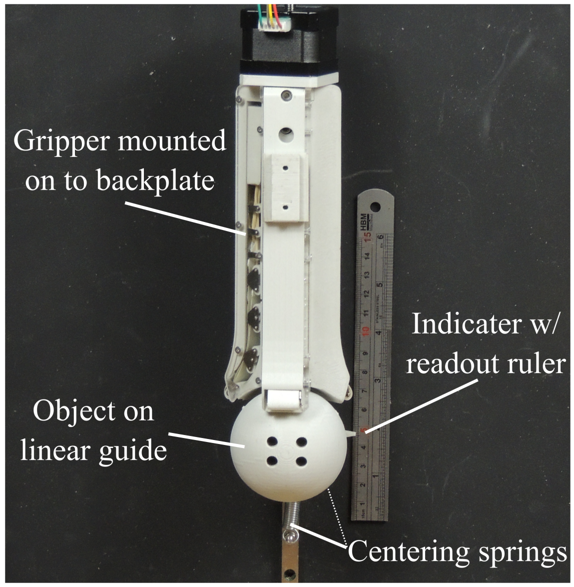

Figure 4.18: Setup used for measuring the net force the gripper exerts during the grasping manoeuvre.

4.6.4 Measuring net force during grasp

The wrist of the gripper has a curved section that is supposed to make sure the gripper finger approaches the object surface tangentially. The function of this curve is to reduce normal forces on the object at the start of the grasping manoeuvre, the net sum of which could cause the object to be pushed from the gripper before the grasp is completed. To determine this net force F_{net}, another measurement setup was made.

Setup

The setup consisted of a linear guide along which a spherical object could move, as shown in Figure 4.18. The gripper was mounted horizontally, parallel to the linear guide and in line with the object. The object was kept in a neutral position by two opposing tension springs, which together had an effective spring constant k_{eff} that was measured to be 0.1875 N/mm. The calibration and determination of k_{eff} can be found in Appendix H. Using an indicator at the object, and a ruler mounted next to the linear guide, the displacement u_{obj} of the object could be determined with a precision of 0.25 mm, which together with the k_{eff} could be used to measure the maximum force F_{net} that was exerted during the grasp manoeuvre:

$$F_{net} = k_{eff} u_{obj} \tag{4.15}$$

Measurement plan

The gripper was placed so that the palm of the gripper was at a 2 mm distance from the object surface while the gripper was in open position. The gripper was then slowly engaged and disengaged

10 times using its actuator, and the resulting maximum displacement u_{obj} of each attempt was retrieved from a video recording of the experiment, from which the exerted force could then be calculated.

4.7 Results

Below, the results obtained with the experimental setups are shown separately for each setup. The tables with data are found at the end of this section.

4.7.1 Forwards object-following propagation

In Figure 4.19, several intermediate states retrieved from the recording of the motion a single finger are overlayed. The bound of the final finger state is traced in red. As can be see, the finger closely follows the bounds of the final finger position, meaning that the finger successfully propagates forward. Furthermore, the finger closely follows the object surface from the moment it makes contact, which is 10 mm after leaving the wrist. For the first centimeter, the finger is separated from the object only by a maximum of 3 mm or 25% of the finger thickness. The separate stills used in the overlay of Figure 4.19, can be found in Appendix G.

4.7.2 Measurement of holding force

In Table 4.2, the measured forces and the effective holding forces when correcting for the object weight, are shown. The average holding force that was measured, was $F_{mean} = 3.7$ +/−0.4 N (95% confidence interval). When comparing this result with the FEA estimation of Section 4.4 ($F_{hold,min}$ = 2.91 N), the FEA underestimated the holding force by 13%.

4.7.3 Friction force and fce by rictional work

In Table 4.3, 4.4, and 4.5 the maximum rotations θ_L and θ_R measured during the experiments for each finger type are given, as well as the $\Delta\theta_L$ and $\Delta\theta_R$ corrected for the offsets of the left and right cylinder being $\theta_{0,L} = 1.3$ degrees and $\theta_{0,R} = 0.2$ degrees. For data on the calibration of the setup, see Appendix H. In Table 4.6, these means values of these rotations are used to calculate the exerted friction forces and friction work by Equations 4.12, 4.13, and 4.14. As can be seen, the force during insertion of the finger has largely been eliminated, with a decrease in force of at least 91% for the inside (right) cylinder, and 97% for the outside (left) cylinder when comparing the everting finger to the other fingers. Furthermore, in regard to the work exerted by the friction forces during insertion, there is a decrease of 97 % for the inside (right) and 99 % for the outside (left) cylinder.

4.7.4 Net force during grasp manoeuvre

The measurement results of object displacement and calculated net force that the gripper exerted during grasping are shown in Table 4.7. The displacement Δu is calculated by substracting the measured position from the initial position $u_0 = 39.6$ which resulted from calibration (See Appendix H). As can be seen, the measurement results were consistent within the precision of the measurement setup, resulting in a measured force of $F_{net} = 0.11$ +/- 0.08 N (95% confidence interval), where the uncertainty follows from the limited precision of the setup.

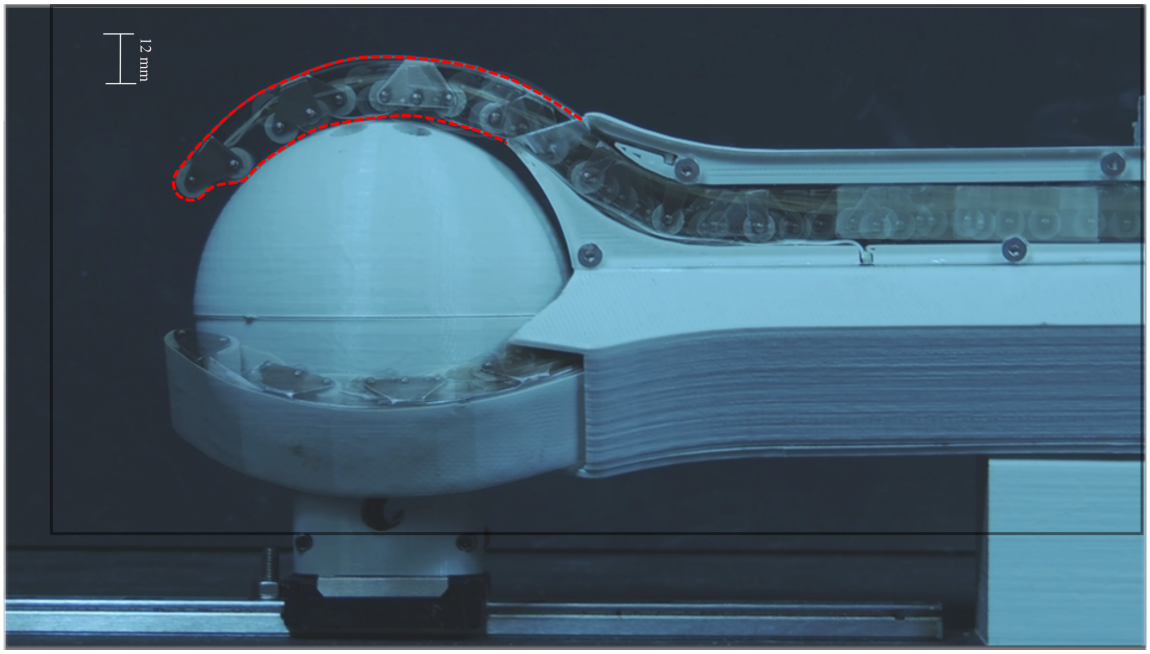

Figure 4.19: Overlaid intermediate states of the grasping manoeuvre, showing how the finger closely follows the object while it propagates forwards.

Table 4.2: Measured holding forces F and effective holding forces F_{corr} of the robotic gripper. Below, the mean value and standard deviation of the samples is given.

F **(gr)**	F_{corr} **(gr)**	F_{corr} **(N)**
450	400	3.9
425	375	3.7
450	400	3.9
425	375	3.7
400	350	3.4
425	375	3.7
400	350	3.4
	Mean	3.7
	Stand. Dev.	0.2

Table 4.3: Measured maximum angles of cylinders during inserting of a solid TPU finger.

Solid finger			
$\theta_{max,L}$	$\Delta\theta_{max,L}$	$\theta_{max,R}$	$\Delta\theta_{max,R}$
37	35.7	33	32.8
37	35.7	32	31.8
37	35.7	33	32.8
37	35.7	33	32.8
37	35.7	34	33.8
36	34.7	34	33.8
36	34.7	34	33.8
37	35.7	34	33.8
37	35.7	34	33.8
37	35.7	34	33.8
37	35.7	35	34.8
Mean:	35.5	-	33.5
Standard Deviation:	0.4	-	0.8

Table 4.4: Measured maximum angles of cylinders during inserting of a flexible TPU finger.

Flex finger			
$\theta_{max,L}$	$\Delta\theta_{max,L}$	$\theta_{max,R}$	$\Delta\theta_{max,R}$
40	38.7	18	17.8
40	38.7	19	18.8
44	42.7	22	21.8
41	39.7	19	18.8
40	38.7	20	19.8
42	40.7	18	17.8
42	40.7	20	19.8
39	37.7	18	17.8
43	41.7	20	19.8
40	38.7	20	19.8
42	40.7	18	17.8
Mean:	39.9	-	19.1
Standard Deviation:	1.5	-	1.3

Table 4.5: Measured maximum angles of cylinders during inserting of a TPU finger with everting surfaces.

Everting finger			
$\theta_{max,L}$	$\Delta\theta_{max,L}$	$\theta_{max,R}$	$\Delta\theta_{max,R}$
3	1.7	2	1.8
3	1.7	1	0.8
3	1.7	1	0.8
5	3.7	0	-0.2
2	0.7	1	0.8
4	2.7	0	-0.2
4	2.7	1	0.8
5	3.7	0	-0.2
8	6.7	1	0.8
7	5.7	0	-0.2
5	3.7	0	-0.2
Mean:	3.2	-	0.5
Standard Deviation:	1.8	-	0.7

Table 4.6: Exerted friction force F and performed frictional work W as calculated for each of the fingers and each rotations, and the accompanying standard deviations.

		$\Delta\theta$ **(deg)**		F **(N)**		W **(mJ)**	
		Mean	**Std. Dev.**	**Mean**	**Std. Dev.**	**Mean**	**Std. Dev.**
Solid finger	**L**	35.5	0.4	0.76	0.01	7.06	0.16
	R	33.5	0.8	0.74	0.02	6.5	0.3
Flex finger	**L**	39.9	0.15	0.854	0.003	8.91	0.07
	R	19.1	1.3	0.42	0.03	2.1	0.3
Everting finger	**L**	3.2	1.8	0.07	0.04	0.06	0.06
	R	0.5	0.7	0.01	0.02	0.001	0.004

Table 4.7: Measured positions u, displacements Δu when correcting for the initial position u_0 and calculated net force F_{net} for 10 different engagements of the gripper around the object.

u **(mm)**	Δu **(mm)**	F_{net} **(N)**
39	0.6	0.11
39	0.6	0.11
39	0.6	0.11
39	0.6	0.11
39	0.6	0.11
39	0.6	0.11
39	0.6	0.11
39	0.6	0.11
39	0.6	0.11
39	0.6	0.11

4.8 Discussions

4.8.1 Measurement results

The overlayed stills of Figure 4.19 showed that the mechanism only takes up the minimal space of the finger thickness during the grasping manoeuvre and propagates forward. Only at the start of the motion, the finger deviates from the object surface, albeit by only a very small amount. This is caused by the wrist of the gripper being over-dimensioned. This in turn allows the gripper to also work for slightly larger objects.

The average holding force of $F_{mean} = 3.7$ N was slightly higher than the calculated hold force $F_{hold,min} = 3.21$ N from 4.4. A reason for this might be that the friction forces between the gripper finger and the object contribute a significant amount of additional holding force, so that the experimentally determined force would closer resemble the calculated $F_{hold,min}$ if very slippery objects were used. Furthermore, in practice, the tension in the belts is expected to be higher due to friction, which could have a positive effect on the holding force by increasing finger stiffness.

The measured friction forces exerted during insertion of the fingers were nearly eliminated by the zero-slip belts (a decrease of at least 93%). The effect is even more pronounced when looking at the frictional work (a decrease of at least 97%), which is a better measure for the disturbance in compliant clutter since it also includes in the movement of the belt surfaces. Still, some small disturbances were present even with the zero-slip fingers. These are expected to be caused by the non-ideal initial contact between finger and rollers, when the finger is "seeking" the middle between the rollers. This also explains the relatively high uncertainty in measured forces for the eversion finger. However, the resulting forces do not further increase after initial contact, showing that over all, the zero-slip surfaces do their work well.

Finally, the net force that the gripper exerted during the grasp manoeuvre, was measured to be 0.1 N. Compared to both the holding force and the weight of the objects that the gripper should manipulate, this force is negligible and is not expected to damage or disturb the object and environment.

4.8.2 Design

The gripper that was designed consisted of integrated functions with one function leading to another. For example, the object-following forward propagation immediately caused the requirement for zero-slip surfaces. On the other hand, there were also functions which had conflicting requirements. For example, the object-following propagation required compliancy, while the required holding force asked for finger stiffness. Because of these integrated functions, finding quantify-able performance metrics on which to optimize the design proved difficult, so the design was iteratively designed, adjusting part parameters and changing the design until the gripper worked.

Additionally, the mechanical analysis done on the belt friction done in Section 4.4, turned out to be inaccurate resulting in too high friction in the inner belts. Therefore, during the experiments, a modification to the pulley system had to be done, where the last pull-in roller was removed to reduce friction. It is expected that the high friction is caused by visco-elastic losses during deformation of the belt over the pulley system. From measuring friction on a single pulley (see Appendix I), it was indeed found that such an additional friction force exists and is of significant magnitude to explain the problems with friction.

4.8.3 Verification of functions

The different functions of the gripper work together and their contributions are hard to split up. The main feature of the concept, was that it was designed to "minimize disturbance" to the object and environment by a) reducing frictional work (the eversion belts) and b) reducing work by normal forces (tangential finger approach to minimize initial normal forces, forward propagation to minimize spatial disturbance during grasp). These features were measured individually, which showed at least that the mechanism only takes up the minimal space (only the finger thickness) during manoeuvring, and that the friction forces present will cause negligible disturbance. However, the low net force that the object exerts during the grasp manoeuvre cannot with confidence be attributed to the initial tangential finger approach of the object alone, since the eversion belts may actually provide some friction *preventing* the object from being pushed out of the gripper. The same goes for the measured holding force: here, the eversion belts also provide some friction, which may help in holding the object.

The fact that the friction in the eversion belts may actually help improving grip, as well as prevent disturbance during grasping by keeping the object and environment in place, could be seen as a design feature, which will prove helpful in a range of specific tasks. However, it also means that the design verification as done above, only holds up for objects that have a similar friction coefficient as the objects used for testing, so that the holding force and net force exerted on the object may differ if for instance a very slippery object would be grasped.

Other than that, the above tests were done using the PLA spheres of the nominal object diameter for which the gripper was designed. Running the same experiments on objects of different dimensions and more irregular shapes, may yield different results.

4.9 Conclusions

Throughout this chapter, a prototype for a novel grasping principle, based on a concept conceived in earlier research, was designed and its functions validated. The novel grasping principle used manoeuvering fingers which follow the object surface, to allow setting a caging grip in dense clutter. The main goal of this research was to show that such a gripper could be designed and manufactured, and to verify whether the implemented functions behaved as required.

In the Section 4.2 the novel grasping principle was disambiguated, leading to a few functions and design parameters specific to the context of grasping in clutter. Using these functions and parameters, in Section 4.3 it was shown that these functions could be united into an integrated gripper design. The important mechanics required for successful implementation were analyzed in Section 4.4, showing that the grasp force was theoretically expected to be sufficient, and that the belts should have been able to properly extend and retract when accounting for the friction present in the rollers. Together, this lead to the detailed gripper design which was manufactured and shown in Section 4.5.

A combination of four different lab experiments were proposed, the setups and measurement plans of which were given in Section 4.6. Using these setups, the theorized behaviour was validated to work in Section 4.7 using several tests which showed that the designed gripper fingers could closely follow the object, and do so without exerting excessive normal or friction forces on the object or surrounding clutter. Furthermore, the gripper was shown to have a sufficient holding force for the task of manipulating agri-food objects.

From this, it can be concluded that the principle, being a manoeuvering caging gripper, can be implemented into a prototype whose interaction in terms of forces and movements with respect to the the environment is minimized. However, the task is still left to verify that this new grasping principle indeed performs well when grasping in dense clutter.

Chapter 5

Demonstration of gripper performance in a realistic environment

5.1 Introduction

In Chapter 4, a novel gripper design for grasping in dense clutter was presented, making use of manoeuvering fingers with everting belts at their contact surfaces so that they can manoeuvre around a target object and between its surface and the surrounding clutter while causing minimal disturbance. It was verified that the novel gripper design is able to closely follow a spherical object surface with negligible slip and friction force on the object and surroundings during the grasp manoeuvre, and that the gripper exerts only a very low net force on the object during grasping. Furthermore, the gripper was shown to have a holding force that is sufficient for manipulation tasks.

In this chapter, the claim that these properties allow grasping in dense clutter is put to the test. This is done by mounting the gripper to a robot system and automatically manipulate and move a pile of tomatoes to another table one-by-one, which is a task that hitherto can not be reliably performed by caging grippers. Furthermore, to substantiate that the resulting success is not attributed to the robotic system but rather the gripper itself, relatively simple perception and planning is used, which does not use obstacle recognition or grasp pose planning.

5.2 Success rate and damage rate as performance metric

The task of grasping from clutter was not generally considered a gripper problem in literature, but rather a problem for path planning and perception algorithms. Therefore, no benchmark for determining gripper performance in this context could be found. In this research, a new benchmark is suggested, being the success rate of grasping and moving objects from a cluttered pile with some clearly determined and relatively simple perception and grasp planning algorithms. The success rate will herein be defined as the percentage of manipulation attempts that were successful at picking up and manipulating the object.

An important factor when manipulating fragile objects, is that they should not be damaged during the manipulation. In this experiment, the tomatoes are considered damaged when the skin is at some location punctured, which can be easily verified visually. Importantly, both the object tomato and the surrounding tomatoes in the pile may not be damaged during each grasp. Therefore, rather than checking for damage after each manipulation, and potentially inadvertently influencing the experiment, the entire set of tomatoes is checked after the entire experiment has run, giving the total sum of damaged tomatoes by both direct (gripper to goal object) and indirect (gripper to surrounding object) damage.

5.3 Measurement setup

The used measurement setup consisted of several elements, which are described below.

5.3.1 Robotic system

The robotic system is shown in Figure 5.1 and 5.2. It consists of an ABB IRB 1200 robot arm, which is controlled via ROS and guided using computer vision and perception. The robotic system is programmed to detect and aim at the center of a random tomato and direct the gripper to a pre-grasp position about 5 cm above the object. Then the system applies the gripper vertically so that the object is centred and in the middle of the wrist curve. Graphically, the inaccuracy of the robotic system position was estimated to be +/−5 mm in the horizontal axes, and +/−5 mm for the vertical axis, as seen in Figure 5.3. This corresponds to 8% of the object diameter, which is comparable to state-of-the-art researches on the centroid positioning error of object localization [Jidong et al., 2016] [Li et al., 2022].

5.3.2 End-effector connection

The designed gripper can be mounted via a sliding dovetail connection on the side of the gripper, onto a connector plate. The slightly loose fit of the dove tail connection works as a safety mechanism: In case the robotic system performs an incorrect movement, e.g., placing a tomato on top of another tomato, the gripper will slide from the robotic arm without damage. A power cable is led through a tube on the robotic arm towards the control box which incorporates a button so that the gripper can manually be switched between the open and closed state.

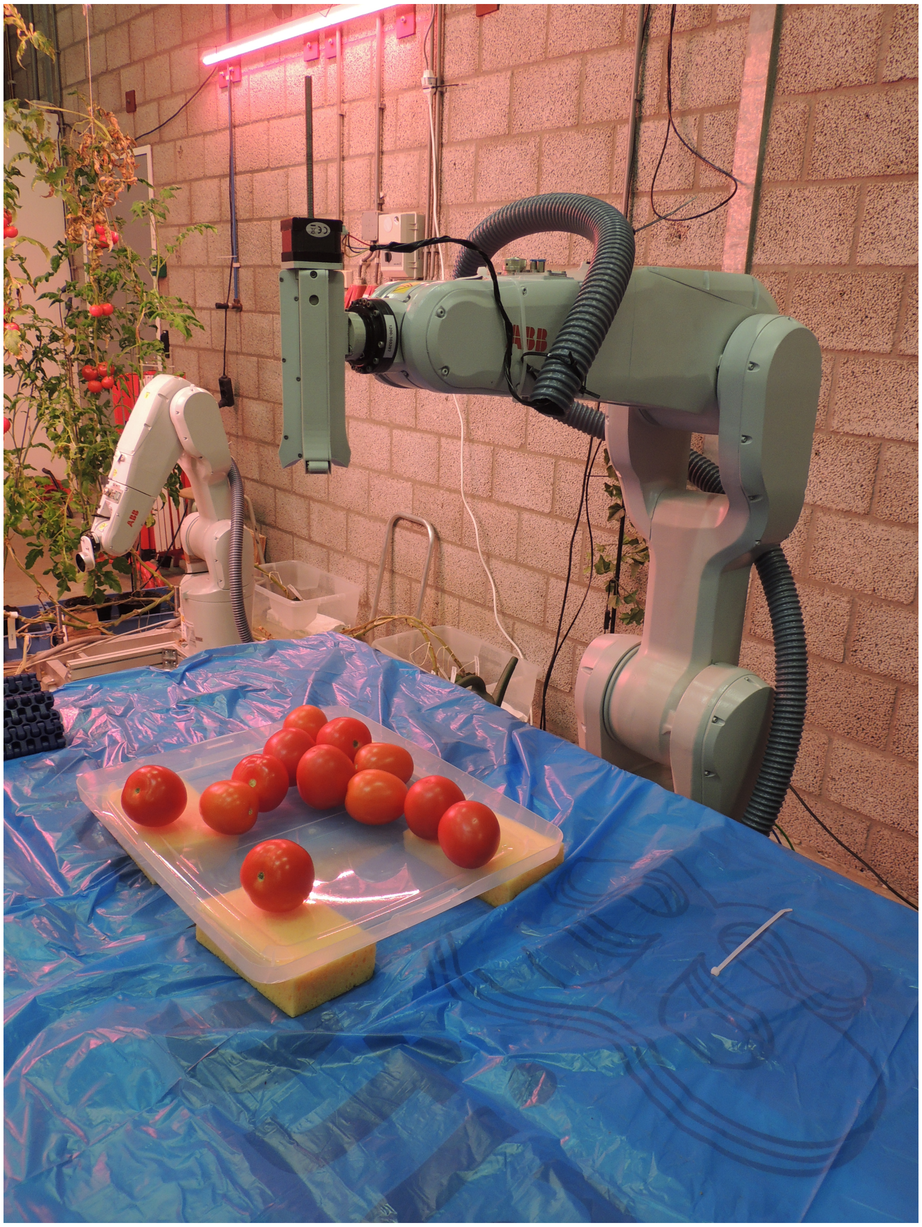

Figure 5.1: Setup of the robot arm and table with tomatoes. The tomatoes are placed on a lid with thick sponges underneath to prevent damage in case of invalid moves.

Figure 5.2: Overview of the setup, showing the camera placed above the tomatoes, and a storage table on the right, where the tomatoes will be deposited.

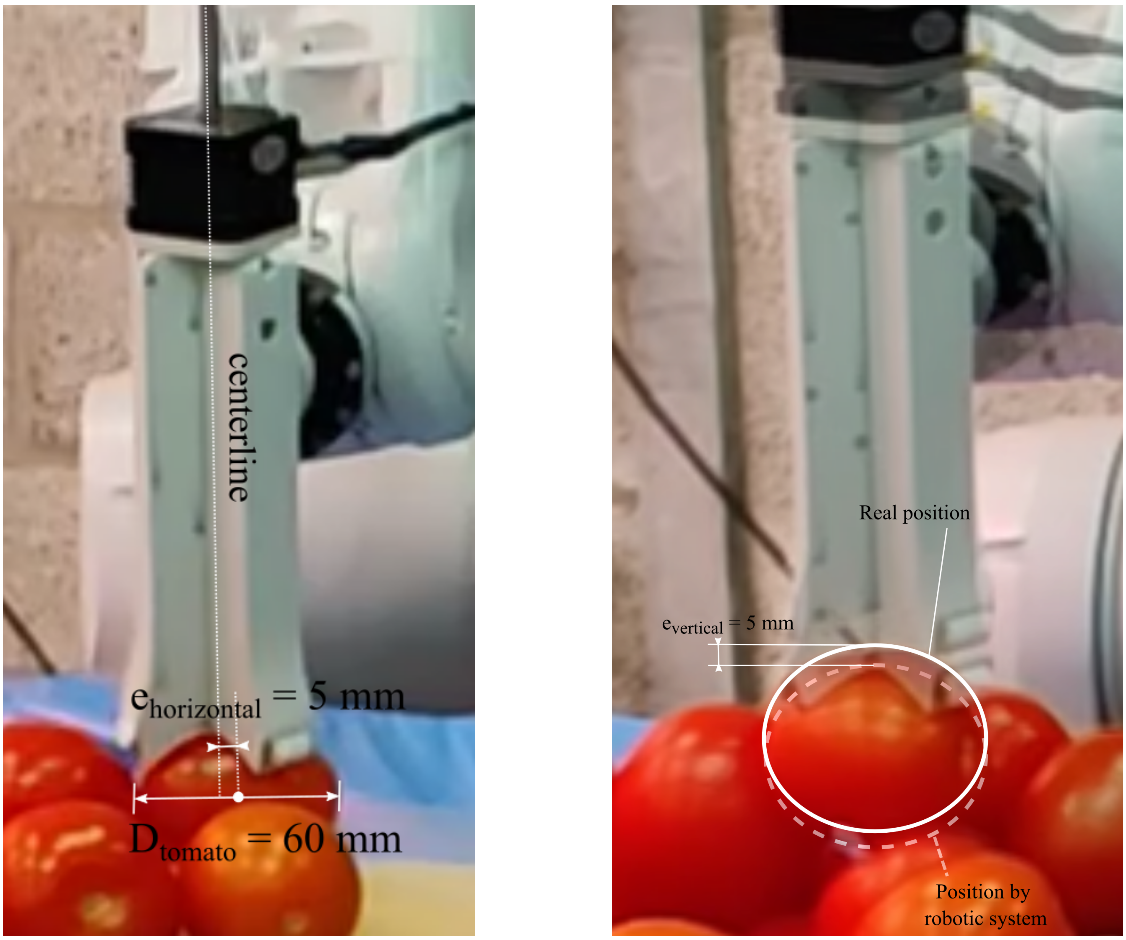

(a) (b)

Figure 5.3: Graphical estimation of the positioning error. (a) The horizontal error of between the gripper symmetry axis and the centroid of the tomato is estimated at 5 mm (b) the vertical error between the final object position after the gripper is erroneously positioned too low and the original object position is estimated at 5mm.

5.3.3 Tomato pile as a cluttered environment

The cluttered environment is simulated by a dense pile of objects, as shown in Figure 5.4. Objects used are Roma and Bunched tomatoes of varying size and weight. A sample of 50 tomatoes of these types was measured, leading to an average diameter of D_{tomato}= 62 $+/-$10 mm (95% confidence interval), an average heights of H_{tomato} = 60 $+/-$10 mm (95% conf.) and an average weight of 130 $+/-$40 gr (95% conf.). For complete data on the measured sample of tomatoes, see Appendix D. The pile of tomatoes is randomly stacked on a transparent plastic lid with an area of 40 x 35 cm. A 1.5 cm high rim around the lid keeps the pile from collapsing. Depending on the location in the pile, each tomato can be obstructed by other tomatoes from 0 up to 5 sides, being the top, right, left, front, and back sides. The bottom side is not taken into account, since the object is grasped vertically from above and will not interact with the bottom of the tomato. However, the bottom side is in principle generally supporting the weight of the object and therefore technically obstructed.

Figure 5.4: A cluttered and dense pile of 32 tomatoes, as used in the experiment.

5.3.4 Grasp planning and perception

The identification algorithm was estimated by eye to determine the object position with an uncertainty of up to +/- 5 mm in both horizontal and vertical directions. Using the positions of the tomatoes, the planning algorithm will try to pick a random tomato from the ones that can be confidently identified. This way, during the experiment, tomatoes with various levels of obstruction were picked. The identification algorithm is not programmed to recognize and avoid obstacles in the form of surrounding tomatoes. However, since the camera only uses a top view of the pile, obstruction of the object from the top will decrease the identification confidence so that these tomatoes will not be picked. This will inherently causes the robotic system to only pick tomatoes whose top surface are free. The lack of obstacle recognition also means that no pose planning could be used, meaning that the gripper was always placed vertically, and the rotation along the gripper symmetry axis was semi-random in the sense that it was not planned for the gripper task but simply constrained to a fixed angle with the arm resulting from the limited degrees of freedom of the robot arm.

Together, this relatively simple object recognition and path planning makes for an easily repeatable benchmark to compare performance differences between gripper designs in the future.

5.4 Results

During the experiment, 34 pick attempts were made, after which all 32 tomatoes were successfully grasped and moved to the storage table. A video of the experiment can be found here. In Table 5.1, the individual pick attempts performed in the video are given. For each pick, the attempt success (success/fail/invalid), the obstructed sides (1-5) and the time in the video were marked.

5.4.1 Invalid attempts

As can be seen in the comments in Table 5.1, there were two invalid grasp attempts due to errors that were not attributed to the gripper. First, on one occasion (attempt 22), the operator failed to engage the gripper timely, causing the gripper to not be fully engaged at the start of manipulation by at least 2 cm of finger length. However, the same tomato was picked up two attempts later, and the situation for that tomato had remained unchanged. This showed that the invalid attempt was not due to gripper performance.

The second problem that occurred was a programming error, in which the system reset itself midway through manipulation[1]. This caused an invalid attempt (attempt 34), where the robotic gripper released the tomato after picking it up, however the same tomato was picked up successfully at the next attempt, showing that this invalid attempt also could not be attributed to the gripper performance.

5.4.2 Obstructed sides

For each tomato, the number of obstructed sides were estimated by use of the videos and photos taken of the tomato pile during the experiment. The occurrence of different numbers of obstructed sides is shown in Figure 5.5. About 80% of the tomatoes had at least some level of obstruction, with more than 50% of the tomatoes having 2 or more surfaces obstructed. In 1 case was the picked tomato obstructed from all four sides.

5.4.3 Damage rate

After the experiment all 32 tomatoes that were initially in the pile were inspected for damage. The definition of damage was defined as a puncture of the skin, examples of which can be seen in Figures 5.6a and 5.6b. Small dents and lines where the skin was not punctured were not counted as damage, examples of which can be seen in Figures 5.6c and 5.6d.

In total, 3 tomatoes were found to have damage, two of them having a puncture of roughly 7 mm, and one having a gash of about 10 mm in length and 3 mm in width.

[1] During previous experiments, this issue was already discovered to happen after every 8 manipulations. This also is the reason that after every 8 tomatoes, the deposited tomatoes had to be removed manually, since the register keeping track of the deposited tomatoes also got reset causing collisions at the next tomato.

Table 5.1: Success and obstructed sides of the individual grasp attempts at the noted time stamps

Attempt #	**Attempt Success**	**Obstructed sides**	**Time**
1	Success	4	00:22
2	Success	0	01:20
3	Success	2	02:13
4	Success	3	03:00
5	Success	1	03:55
6	Success	3	04:48
7	Success	2	05:33
8	Success	1	06:20
9	Success	2	07:35
10	Success	1	08:42
11	Success	2	09:44
12	Success	2	10:40
13	Success	2	11:23
14	Success	3	12:05
15	Success	2	13:00
16	Success	3	14:00
17	Success	0	15:20
18	Success	2	16:20
19	Success	2	17:40
20	Success	0	18:25
21	Success	3	19:15
22	Invalid	2	20:00
23	Success	1	20:55
24	Succes	2	21:45
25	Succes	2	23:35
26	Succes	0	24:44
27	Succes	1	25:35
28	Succes	1	26:24
29	Succes	1	27:10
30	Succes	1	28:00
31	Succes	1	28:50
32	Succes	0	29:40
33	Invalid	0	30:36
34	Succes	0	32:00

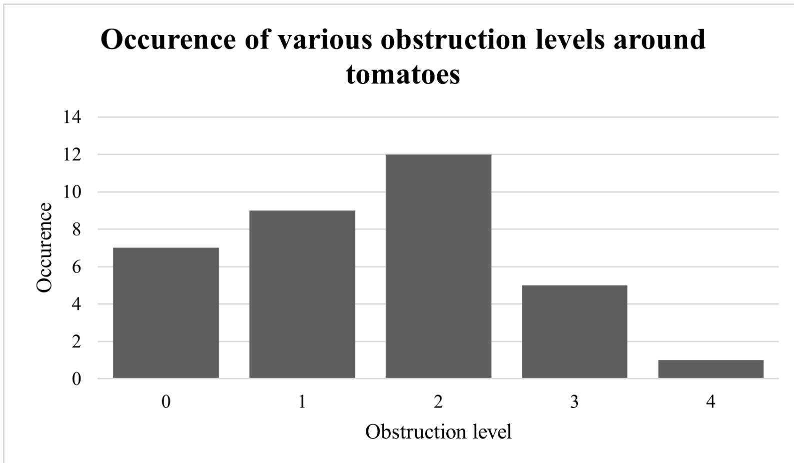

Figure 5.5: Histogram showing the occurrence of different levels of obstruction when grasping a tomato.

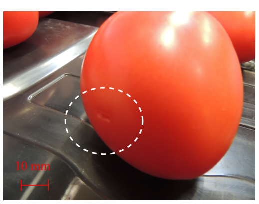

(a) Puncture of about 7 mm, counts as damage

(b) Gash of about 8x3 mm, counts as damage

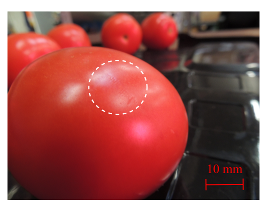

(c) Minor rippling of skin; does not count as damage

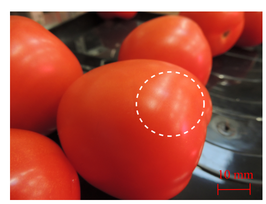

(d) Minor dents/lines; does not count as damage

Figure 5.6: Different examples of tomatoes that were or were not counted as ”damaged” during the grasp.

5.5 Discussions

In this section, the results of the practical experiment are explained. First, it is explained how successful the gripper was at grasping, and what this means for the gripper design. Explanations of the damages that occurred in same tomatoes, and the implications about the gripper design, are then given. Finally, the limitations of the gripper are explored by looking at additional experiments with varying accuracy of the robotic system, and different shapes of the objects.

5.5.1 Success rate

Considering only the valid grasp attempts, the gripper achieved a 100 % success rate during the manipulation of the pile, moving all 32 tomatoes in 32 valid attempts. Considering that this was achieved without any obstacle recognition or grasp planning considering of the surrounding clutter, this shows that the concept of the manoeuvering caging gripper makes grasping in clutter much simpler. Furthermore, the compliant object-following manoeuvre proved robust enough to the positioning inaccuracies present, which are comparable with state-of-the-art of object recognition.

5.5.2 Damage

Although the success rate in grasping was 100%, a small percentage of the tomatoes ended up damaged, the cause of which could not be identified. A possibility is that the damages are caused by interference with other parts of the gripper, like the sharp corners at the opening of the wrist channels, since at least one of the damages seemed to match up with one of these corners upon further inspection. This type of contact should not have occurred and may have been caused by an odd manoeuvre of the gripper during attempt 22, where the gripper collided with another tomato during object placement. In the future, other than reducing these unwanted contacts, smoothing the corners of the gripper or using a flexible soft material could reduce damage.

Furthermore, inspection for damage turned out to be prone to human errors. At inspection at least one damage was missed at first sight which was found later. Although the tomatoes were thoroughly checked after this, it suggests the possibility that not all tomatoes were damage-free before the experiment, which is likely since the tomatoes had already been used during integration and tuning of the robotic system, during which multiple collisions had occurred due to unplanned motions.

5.5.3 Limitations of the gripper

Since the gripper performed 100% successfully during the experiment, additional experiments were examined or carried out to find limitations to this successful performance.

Behaviour under positioning inaccuracies

First of all, a similar experiment to the experiment from 5.4 was done in which the perception system was not correctly calibrated and the horizontal positioning was off by up to 20 mm at times[2]. Furthermore, the height of the gripper was off by up to 10 mm as well. This caused the gripper fingers which were too far away from the objects centre to "bounce" off neighbouring

[2]These measurements are estimated from close-up video recordings of the experiments

tomatoes, and back into the target tomato. When reaching the target, the outside belt which should only make contact with the environment, made first contact with the object, and steered the finger back over the target tomato. This effect is shown in Figure 5.7.

With a properly calibrated perception, sufficient accuracy should easily be achievable so that this error does not occur. Still, to increase the robustness, a solution might be to alter the configuration of the rollers so that the inner belt will still contact the object first when this "bouncing" occurs, or even so that the first roller is free-wheeling so that it can follow which ever surface it contacts first. Furthermore, it must be noted that the opposite fingers, which were instead too close to the object centre, did not jam once, which suggests that a solution to increase robustness to misalignment might be found by bringing the exit points of the gripper fingers closer to the center of the wrist. However, this may increase the net force with which the gripper will push on an object at the start of engagement, since the fingers will start pressing on the objects top surface sooner. For some applications however, this might not necessarily be a problem.

Another important effect that became apparent is that the "cupped" shape of the wrist actually centers the object if the object is horizontally misaligned. If the environment has some compliance to allow for this re-alignment, pushing the wrist onto the object until it contacts, will thus decrease alignment issues. In the experiment of Section 5.4, the vertical positioning was accurate enough that the gripper would center the objects slightly upon approach, but would not damage them. To further improve vertical positioning and the centering of the wrist, it is possible to use a distance or contact sensor to detect when the gripper is positioned just above the object. For applications in which the environment is much more compliant, like when harvesting fruit from a plant, the gripper could instead be programmed to overreach by default, so that the object always ends up in contact and the plant provides the necessary slack for positioning uncertainties.

Behaviour under varying object size

The gripper was able to grasp any object in the provided set, which were all within a fairly well-defined range of sizes since they had already gone through the retail sorting process. To illustrate that the limits of the gripper lay much further, the gripper was also tested on two wildly different tomatoes, being a small bunch tomato of roughly 45 mm in diameter, and a large beefsteak tomato of roughly 85 mm in diameter. The compliant fingers were able to manoeuvre around both objects and provide a successful grasp. However, for the large tomato, some rippling of the skin occurred and the tomato tipped during the grasp, shown in Figure 5.8. This may have occurred due to the increased tension from over-extending the fingers. For the small tomato, the caging grasp did work well, but if the tomato had been placed in clutter, the same back-rolling effect from Figure 5.7 might occur. Still, this illustrates that the gripper has the potential to be very adaptive to different object sizes, given that the objects allow the additional stress, or that the environment is not too cluttered or is compliant enough to prevent the back-rolling effect from happening.

Behaviour with occluded objects

The last limitation of the gripper that should be mentioned is the level of occlusion until which it can safely grasp. If the gripper is applied vertically, and another tomato hangs over the target tomato at the position of one of the fingers, the gripper cannot be applied without colliding with the overhanging tomato, causing damage. Although no issues occurred during the experiment, there were two cases (attempt 1 and attempt 15) where the gripper fingers were seemingly only by chance

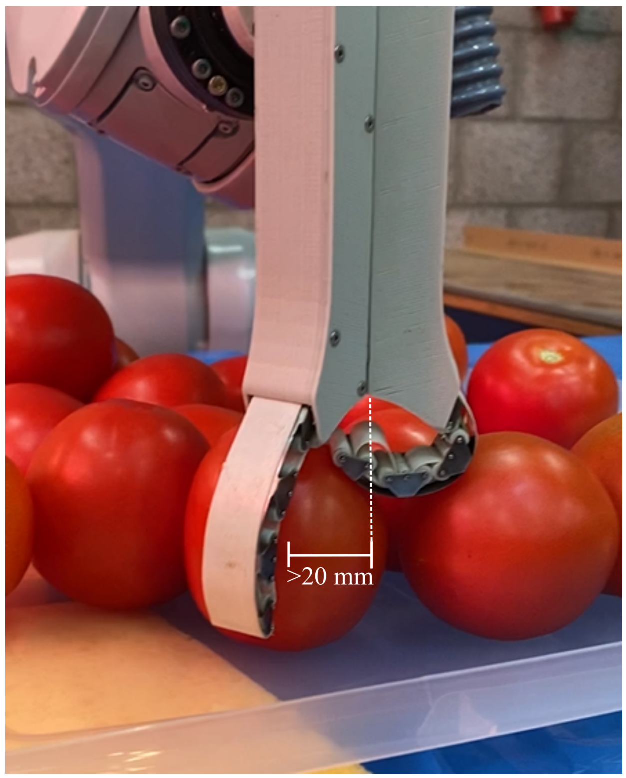

Figure 5.7: Figure showing the fail mechanism when the gripper positioning is too far off.

in a good position so that no collision occurred during approach of the gripper. Big steps could be taken to resolve this issue by some basic improvements in path planning and object recognition, so that a safe pose can still be applied even if an overhang is present.

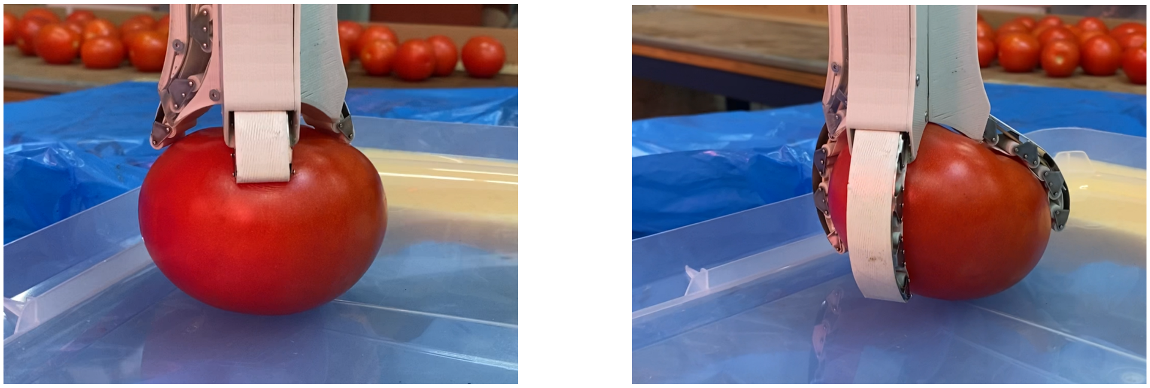

(a) Rippling

(b) Tipping

Figure 5.8: Grasp of a large (85 mm) beefsteak tomato and the resulting rippling (a) and tipping (b) of the tomato that occurred.

5.6 Conclusions

The conducted experiment showed that the gripper itself was 100% successful in grasping objects from a pile, most of which were obstructed from multiple sides. Furthermore, because the robotic system perception and path planning did not account for obstacle recognition or grasp pose planning, it is concluded that the resulting success can be attributed to the obstacle manoeuvering capabilities of the gripper itself. Because the used robotic system is well defined, and advanced object recognition and grasp poses were avoided, the experiment provides a good benchmark to compare how individual grippers perform in grasping in clutter. With the results for this gripper, one can first of all say that it will perform very well in clutter where the objects are obstructed from multiple sides, even if no obstacle recognition of advanced path planning is used. Furthermore, this shows that the gripper is not constraining the path planning on a specific grasp pose, meaning that with more advanced path planning, more difficult cases could also be solved.

Although the gripper successfully grasped and manipulated 100% of the objects from the pile, 3 damages occurred, of which the origin could not be confidently identified. Therefore, it is recommended that more testing is done to identify the causes and solve them by gripper redesign or employing more advanced planning.

Chapter 6

Conclusions and recommendations

Each of the chapters above independently had some main result: The existence of a gap in the state-of-the-art of grippers (Chapter 2), the most feasible strategy and concept for filling this gap (Chapter 3), the detailed design and verification of such a concept (Chapter 4) and finally the practical success of that concept (Chapter 5).

In this chapter, the higher level implications and conclusions when combining these chapters is given. Furthermore, research paths are given for further development of the inventions, as well as spin-off paths exploiting newly found opportunities.

6.1 Successful grasping of cluttered objects

Through the start of this research, several new ideas were proposed that were expected to improve grasping of agri-food objects in clutter. Below, it is explained how the research managed to show whether these ideas were correct, and how this resulting in a very successful gripper.

6.1.1 Caging gripper as a good choice for agri-food objects

During the literature review, the caging gripper was estimated to be inherently suitable for different difficult object characteristics. Therefore, because of the choice of a caging gripper, little attention was paid to the object characteristics. In fact, the resulting design would arguably have been almost the same for any other type of agri-food object. However, the gripper was highly successful in grasping tomatoes, which due to their delicate nature shows that the gripper can be considered to be relatively gentle. Therefore, it is concluded that the choice of a caging gripper in this case was indeed a good one.

6.1.2 Identified problems of grasping in clutter

In the literature review, the underlying problem of grasping in clutter was estimated to be the lack of space for the gripper, and the unpredictability of the hence required interactions with the clutter.

The two main problems of these disturbing interactions were found in Chapter 3, and two sub-strategies (minimizing space disturbance by object-following manoeuvering and minimizing friction by eliminating sliding) were identified to be the most feasible in solving these.

By actually producing a prototype of a gripper that implemented these strategies in Chapter 4, they were verified to minimize disturbance by eliminating friction forces and the net force on the object and environment during the grasp manoeuvre. More importantly, the idea that elimination of these disturbances during interaction would improve grasping was actually confirmed by applying the prototype to a practical case of grasping tomatoes. This showed that the problems of grasping in clutter have been correctly identified and that the proposed strategies are effective.

6.1.3 Improving grasping in clutter by redesign of the gripper

Finally, looking back at the first point where this research strayed from the beaten track, the most important new innovation of this research was to solve the interaction with clutter in the gripper design instead of using more advanced obstacle-recognizing perception and path planning algorithms. The high success rate of the gripper in a full robotic system, without using obstacle-recognition of the clutter, proved that this mechanical approach could drastically simplify the task of robotic grasping in cluttered environments. In the future, this may eliminate the need for ever more advanced algorithms or otherwise assist these algorithms in increasing the success rate of grasping even more complex cases.

6.2 Recommendations for future research

The gripper designed in this research, which incorporated a novel manoeuvering mechanism for the fingers, proved to minimize disturbances while still being able to provide ample stiffness for manipulation. In the practical case of grasping tomatoes, it has proved its worth. However, the opportunities for the findings of this research may be much wider, both for the specific gripper designed as well as the implementations and applications of the novel strategies and mechanisms that were found. Below, the different research paths for further developing the gripper and the underlying ideas and mechanisms are explored.

6.2.1 Other applications of the new gripper

The designed gripper is expected to work well for many difficult objects since it uses caging grasping, which is independent of friction and has no minimum pinch force. To explore this broad applicability, the gripper should be tested for many more agri-food objects, for instance, soft or slippery objects. The modular design also provides a good base for experimenting with different object shapes: By only changing the middle hub, a range of finger configurations can be obtained. For example, a parallel finger gripper could be used to grasp cylindrical objects (Figure 6.1a). In addition, more fingers could be used to increase the holding capabilities of heavy objects by dividing the force between more fingers, or by reducing the open space between the fingers (Figure 6.1b).

6.2.2 Other implementations of the new grasping principle

Although the new grasping principle has been shown to be effective, there are still some major obstacles that must be overcome to make this gripper industrially applicable. In the design of the prototype, little attention was paid to maintenance, reliability, cost, or industry-specific hygienic and safety standards. Although the concept proved reliable enough to carry out repetitive tests, other implementations of the object-following caging manoeuvre should be explored, for example, by going back to the eversion tube [Takahashi et al., 2021] by which the belt system was inspired. This eversion tube could be redesigned for increased stiffness for grasping, for instance, by increasing pressure, using a stiff backbone as in this concept, or by using variable stiffness methods like layer blocking or granular jamming. The eversion tube has the great advantage that it can be hermetically sealed and can consist of only one part. However, the mechanical behaviour of eversion tubes is still largely unknown, which means that steps need to be taken to describe the eversion mechanisms as well. Inspiration for other implementations can also be found in Chapter 3.

6.2.3 Other applications for the novel mechanical eversion mechanism

Currently, eversion mechanisms are mostly used for inspection [Takahashi et al., 2021], or some specific manipulations which do not require bending stiffness of the fingers [Blumenschein et al., 2020], since the inflated tubes buckle easily.

The novel adaptation of the eversion mechanism conceived for the prototype herein provides new opportunities. Since it employs only mechanical elements instead of pneumatics, together with a solid backbone, this mechanism can be designed to have a relatively high bending stiffness and axial stiffness compared to the soft pneumatics based eversion mechanisms. Furthermore, the use of a backbone provides design freedom to implement specific manoeuvres and propagation paths, like the object-following manoeuvre used in the gripper.

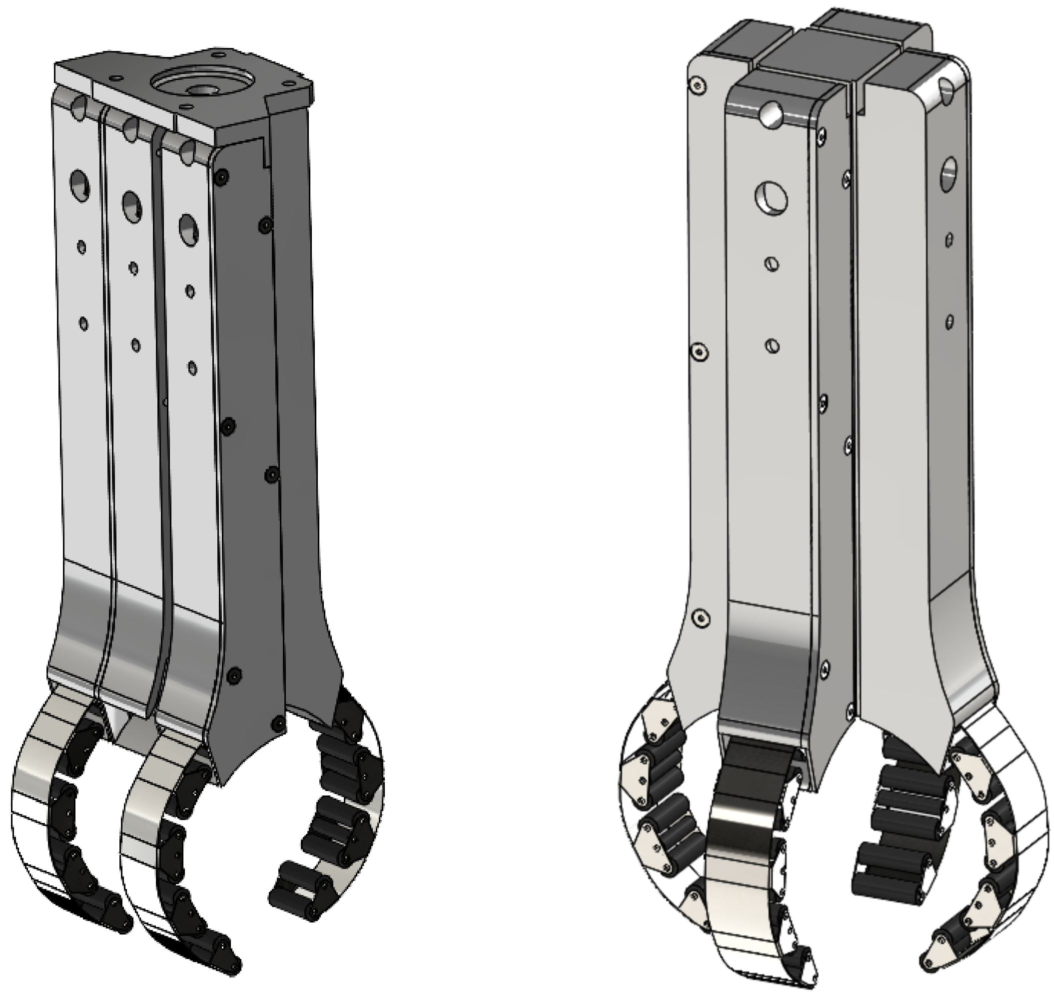

(a) (b)

Figure 6.1: Alternative gripper configurations, obtained by only redesigning the middle hub and attaching the finger modules

Bibliography

[Amend et al., 2012] Amend, J. R., Brown, E., Rodenberg, N., Jaeger, H. M., and Lipson, H. (2012). A Positive Pressure Universal Gripper Based on the Jamming of Granular Material. *IEEE Transactions on Robotics*, 28(2):341–350. Conference Name: IEEE Transactions on Robotics.

[Astrov and Leitner, 2021] Astrov, V. and Leitner, S. (2021). *How do Economies in EU-CEE Cope with Labour Shortages?* The Vienna Institute for International Economic Studies.

[Bac et al., 2017] Bac, C. W., Hemming, J., van Tuijl, B., Barth, R., Wais, E., and van Henten, E. J. (2017). Performance Evaluation of a Harvesting Robot for Sweet Pepper: Performance Evaluation of a Harvesting Robot for Sweet Pepper. *Journal of Field Robotics*, 34(6):1123–1139.

[Bac et al., 2016] Bac, C. W., Roorda, T., Reshef, R., Berman, S., Hemming, J., and van Henten, E. J. (2016). Analysis of a motion planning problem for sweet-pepper harvesting in a dense obstacle environment. *Biosystems Engineering*, 146:85–97.

[Baur et al., 2012] Baur, J., Pfaff, J., Ulbrich, H., and Villgrattner, T. (2012). Design and development of a redundant modular multipurpose agricultural manipulator. In *2012 IEEE/ASME International Conference on Advanced Intelligent Mechatronics, AIM 2012*, pages 823–830.

[Bicchi and Kumar, 2000] Bicchi, A. and Kumar, V. (2000). Robotic grasping and contact: a review. In *Proceedings 2000 ICRA. Millennium Conference. IEEE International Conference on Robotics and Automation. Symposia Proceedings (Cat. No.00CH37065)*, volume 1, pages 348–353 vol.1. ISSN: 1050-4729.

[Birglen, 2015] Birglen, L. (2015). Enhancing versatility and safety of industrial grippers with adaptive robotic fingers. In *2015 IEEE/RSJ International Conference on Intelligent Robots and Systems (IROS)*, pages 2911–2916.

[Blumenschein et al., 2020] Blumenschein, L., Coad, M., Haggerty, D., Okamura, A., and Hawkes, E. (2020). Design, Modeling, Control, and Application of Everting Vine Robots. *Frontiers in Robotics and AI*, 7.

[Breedveld, 2006] Breedveld, P. (2006). Development of a Rolling Stent Endoscope. In *The First IEEE/RAS-EMBS International Conference on Biomedical Robotics and Biomechatronics, 2006. BioRob 2006.*, pages 921–926. ISSN: 2155-1782.

[Breedveld et al., 2008] Breedveld, P., van der Kouwe, D. E., and van Gorp, M. A. J. (2008). Locomotion Through the Intestine by Means of Rolling Stents. In *ASME 2004 International Design*

Engineering Technical Conferences and Computers and Information in Engineering Conference, pages 963–969. American Society of Mechanical Engineers Digital Collection.

[Bulut and Conkur, 2021] Bulut, Y. and Conkur, E. S. (2021). A real-time path-planning algorithm with extremely tight maneuvering capabilities for hyper-redundant manipulators. *Engineering Science and Technology, an International Journal*, 24(1):247–258.

[Cao et al., 2019] Cao, X., Zou, X., Jia, C., Chen, M., and Zeng, Z. (2019). RRT-based path planning for an intelligent litchi-picking manipulator. *Computers and Electronics in Agriculture*, 156:105–118.

[Cheng et al., 2012] Cheng, F., Ji, W., Zhao, D., and Lv, J. (2012). Apple picking robot obstacle avoidance based on the improved artificial potential field method. In *2012 IEEE 5th International Conference on Advanced Computational Intelligence, ICACI 2012*, pages 909–913.

[Christiaensen et al., 2021] Christiaensen, L., Rutledge, Z., and Taylor, J. E. (2021). Viewpoint: The future of work in agri-food. *Food Policy*, 99:101963.

[Davidson et al., 2017] Davidson, J., Hohimer, C., Mo, C., and Karkee, M. (2017). Dual robot coordination for apple harvesting. In *2017 ASABE Annual International Meeting*.

[Davidson et al., 2016] Davidson, J. R., Silwal, A., Hohimer, C. J., Karkee, M., Mo, C., and Zhang, Q. (2016). Proof-of-concept of a robotic apple harvester. In *2016 IEEE/RSJ International Conference on Intelligent Robots and Systems (IROS)*, pages 634–639. ISSN: 2153-0866.

[de Gorter and Drabik, 2013] de Gorter, H. and Drabik, D. (2013). Biofuel Policies and Food Grain Commodity Prices 2006-2012: All Boom and No Bust? *AgBioForum*, 16:13.

[Do et al., 2020] Do, B. H., Banashek, V., and Okamura, A. M. (2020). Dynamically Reconfigurable Discrete Distributed Stiffness for Inflated Beam Robots. In *2020 IEEE International Conference on Robotics and Automation (ICRA)*, pages 9050–9056. ISSN: 2577-087X.

[D'Avella et al., 2020] D'Avella, S., Tripicchio, P., and Avizzano, C. A. (2020). A study on picking objects in cluttered environments: Exploiting depth features for a custom low-cost universal jamming gripper. *Robotics and Computer-Integrated Manufacturing*, 63:101888.

[Eastwood et al., 2020] Eastwood, K., Swarup, A., Francis, P., Alvar, A., Chen, H., Looi, T., Nagui, H., and Drak, J. (2020). A steerable neuroendoscopic instrument using compliant contact- aided joints and monolithic articulation. *Journal of Medical Devices, Transactions of the ASME*, 14(2).

[FESTO, nda] FESTO (n.d.a). Grippers and vacuum components. [Online; accessed Februari 20, 2022].

[FESTO, ndb] FESTO (n.d.b). Multi-choice gripper. [Online; accessed Februari 20, 2022].

[Fu et al., 2020] Fu, L., Majeed, Y., Zhang, X., Karkee, M., and Zhang, Q. (2020). Faster R–CNN–based apple detection in dense-foliage fruiting-wall trees using RGB and depth features for robotic harvesting. *Biosystems Engineering*, 197:245–256.

[Gama Melo et al., 2014] Gama Melo, E. N., Aviles Sanchez, O. F., and Amaya Hurtado, D. (2014). Anthropomorphic robotic hands: a review. *Ingeniería y Desarrollo*, 32(2):279–313.

[Gasparetto and Scalera, 2019] Gasparetto, A. and Scalera, L. (2019). From the Unimate to the Delta Robot: The Early Decades of Industrial Robotics: Proceedings of the 2018 HMM IFToMM

Symposium on History of Machines and Mechanisms. *History of Mechanism and Machine Science*, pages 284–295.

[Ge et al., 2019] Ge, Y., Xiong, Y., Tenorio, G., and From, P. (2019). Fruit Localization and Environment Perception for Strawberry Harvesting Robots. *IEEE Access*.

[Gifford, 1992] Gifford, R. C. (1992). *Agricultural Engineering in Development: Concepts and principles*. Food & Agriculture Org. Google-Books-ID: G6JkSfrmbF8C.

[Global, 2015] Global, D. (2015). Milking automation is gaining popularity.

[Gong et al., 2022] Gong, L., Wang, W., Wang, T., and Liu, C. (2022). Robotic harvesting of the occluded fruits with a precise shape and position reconstruction approach. *Journal of Field Robotics*, 39(1):69–84.

[Guo et al., 2010] Guo, J., Zhao, D.-a., Ji, W., and Xia, W. (2010). Design and control of the open apple-picking-robot manipulator. In *2010 3rd International Conference on Computer Science and Information Technology*, volume 2, pages 5–8.

[Hawkes et al., 2017] Hawkes, E. W., Blumenschein, L. H., Greer, J. D., and Okamura, A. M. (2017). A soft robot that navigates its environment through growth. *Science Robotics*, 2(8):eaan3028. Publisher: American Association for the Advancement of Science.

[He et al., 2021] He, C., Deng, C., Li, N., and Miao, Z. (2021). Design of Vision Control System of Tomato Picking Robot. In *Proceedings of the 40th Chinese Control Conference*, volume 2021-July, pages 4267–4271. ISSN: 1934-1768.

[Hemming et al., 2014] Hemming, J., Bac, C. W., and van Henten, E. J. (2014). A robot for harvesting sweet-pepper in greenhouses. *International Conference of Agricultural Engineering*, AgEng 2014 Zurich:8.

[Henselmans et al., 2019] Henselmans, P. W., Smit, G., and Breedveld, P. (2019). Mechanical Follow-the-Leader motion of a hyper-redundant surgical instrument: Proof-of-concept prototype and first tests. *Proceedings of the Institution of Mechanical Engineers, Part H: Journal of Engineering in Medicine*, 233(11):1141–1150. Publisher: IMECHE.

[Hertel et al., 2010] Hertel, T. W., Burke, M. B., and Lobell, D. B. (2010). The poverty implications of climate-induced crop yield changes by 2030. *Global Environmental Change*, 20(4):577–585.

[h+s Präzisionsfolien GmbH, 2017] h+s Präzisionsfolien GmbH (2017). Precision gauge strips precision foils special spring steel strips non-ferrous metal foils. [Online; accessed Februari 20, 2022].

[Huang et al., 2020] Huang, W., Xu, Z., Xiao, J., Hu, W., Huang, H., and Zhou, F. (2020). Multimodal Soft Robot for Complex Environments Using Bionic Omnidirectional Bending Actuator. *IEEE Access*, 8:193827–193844. Conference Name: IEEE Access.

[IFT, 2022] IFT (2022). Robotics on the Rise in the Food Industry.

[Jha et al., 2020] Jha, R., Vishvachi, Lang, W., and Jedermann, R. (2020). B4.5 Sensory Options for Earthquake Victim Recovery. *SMSI 2020 - Sensors and Instrumentation*, pages 125–126.

[Ji et al., 2016] Ji, W., Qian, Z., Xu, B., Tao, Y., Zhao, D., and Ding, S. (2016). Apple tree branch segmentation from images with small gray-level difference for agricultural harvesting robot. *Optik*, 127(23):11173–11182.

[Jianjun et al., 2012] Jianjun, Y., Chun, X., Chuanyu, W., Mittal, G., and Yang, S. (2012). Quick motion path plan for joint-robot to pick tomato under free-obstacle. *Applied Mechanics and Materials*, 229-231:2225–2228. ISBN: 9783037855102.

[Jidong et al., 2016] Jidong, L., De-An, Z., Wei, J., and Shihong, D. (2016). Recognition of apple fruit in natural environment. *Optik*, 127(3):1354–1362.

[Joffe et al., 2019] Joffe, B., Walker, T., Gourdon, R., and Ahlin, K. (2019). Pose estimation and bin picking for deformable products. *IFAC-PapersOnLine*, 52(30):361–366.

[Khatib, 1985] Khatib, O. (1985). Real-time obstacle avoidance for manipulators and mobile robots. In *1985 IEEE International Conference on Robotics and Automation Proceedings*, volume 2, pages 500–505.

[Kootstra et al., 2021] Kootstra, G., Wang, X., Blok, P. M., Hemming, J., and van Henten, E. (2021). Selective Harvesting Robotics: Current Research, Trends, and Future Directions. *Current Robotics Reports*, 2(1):95–104.

[Lacquey, nd] Lacquey (n.d.). Underactuated gripper. [Online; accessed Februari 20, 2022].

[Lee et al., 2013] Lee, D.-Y., Jung, G.-P., Sin, M.-K., Ahn, S.-H., and Cho, K.-J. (2013). Deformable wheel robot based on origami structure. In *2013 IEEE International Conference on Robotics and Automation (ICRA)*, pages 5612–5617.

[Lee et al., 2019] Lee, G., Choi, Y., Lee, T., Lim, K. S., Shin, J., Kim, T., Kim, H., Koo, B.-K., Kim, H., Lee, J., Ahn, K., Lee, E., Lee, M. S., Jin, J., Yang, H. S., Won, P., Mo, S., Kim, N., Jeong, M., and Choi, M. (2019). Nature-inspired rollable electronics. *NPG Asia Materials*, 11:67.

[Li et al., 2022] Li, T., Feng, Q., Qiu, Q., Xie, F., and Zhao, C. (2022). Occluded Apple Fruit Detection and Localization with a Frustum-Based Point-Cloud-Processing Approach for Robotic Harvesting. *Remote Sensing*, 14(3):482. Number: 3 Publisher: Multidisciplinary Digital Publishing Institute.

[Li et al., 2013] Li, Z., Li, P., Yang, H., and Liu, J. (2013). Internal mechanical damage prediction in tomato compression using multiscale finite element models. *Journal of Food Engineering*, 116(3):639–647.

[Lien, 2013] Lien, T. (2013). Gripper technologies for food industry robots. In *Robotics and Automation in the Food Industry*, pages 143–170. Elsevier.

[Lin et al., 2021] Lin, G., Zhu, L., Li, J., Zou, X., and Tang, Y. (2021). Collision-free path planning for a guava-harvesting robot based on recurrent deep reinforcement learning. *Computers and Electronics in Agriculture*, 188:106350.

[Lin et al., 2011] Lin, P., Abney, K., and Bekey, G. (2011). Robot ethics: Mapping the issues for a mechanized world. *Artificial Intelligence*, 175(5):942–949.

[Ma et al., 1994] Ma, S., Hirose, S., and Yoshinada, H. (1994). Development of a hyper-redundant multijoint manipulator for maintenance of nuclear reactors. *Adv. Robotics*.

[Marel, nd] Marel (n.d.). Marel singlefeed. [Online; accessed Februari 20, 2022].

[Mazzolai et al., 2019] Mazzolai, B., Mondini, A., Tramacere, F., Riccomi, G., Sadeghi, A., Giordano, G., Del Dottore, E., Scaccia, M., Zampato, M., and Carminati, S. (2019). Octopus-Inspired

Soft Arm with Suction Cups for Enhanced Grasping Tasks in Confined Environments. *Advanced Intelligent Systems*, 1(6):1900041.

[Mnyusiwalla et al., 2020] Mnyusiwalla, H., Triantafyllou, P., Sotiropoulos, P., Roa, M. A., Friedl, W., Sundaram, A. M., Russell, D., and Deacon, G. (2020). A Bin-Picking Benchmark for Systematic Evaluation of Robotic Pick-and-Place Systems. *IEEE Robotics and Automation Letters*, 5(2):1389–1396. Conference Name: IEEE Robotics and Automation Letters.

[Moli, 2018] Moli, X. (2018). Real-time construction of fruit tree model based on image. *Paper Asia*, 1(Compendium5):16–19.

[Nemlekar et al., 2021] Nemlekar, H., Liu, Z., Kothawade, S., Niyaz, S., Raghavan, B., and Nikolaidis, S. (2021). Robotic Lime Picking by Considering Leaves as Permeable Obstacles. In *2021 IEEE/RSJ International Conference on Intelligent Robots and Systems (IROS)*, pages 3278–3284. 2021 IEEE/RSJ International Conference on Intelligent Robots and Systems (IROS). ISSN: 2153-0858.

[Pettersson et al., 2010] Pettersson, A., Davis, S., Gray, J., Dodd, T., and Ohlsson, T. (2010). Design of a magnetorheological robot gripper for handling of delicate food products with varying shapes. *Journal of Food Engineering*, 98(3):332–338.

[Popov et al., 2017] Popov, D., Klimchik, A., and Mavridis, N. (2017). Collision detection, localization classification for industrial robots with joint torque sensors. In *2017 26th IEEE International Symposium on Robot and Human Interactive Communication (RO-MAN)*, pages 838–843. ISSN: 1944-9437.

[Robotiq, nd] Robotiq (n.d.). More than just a parallel gripper. [Online; accessed Februari 20, 2022].

[Sadeghi et al., 2017] Sadeghi, A., Mondini, A., and Mazzolai, B. (2017). Toward Self-Growing Soft Robots Inspired by Plant Roots and Based on Additive Manufacturing Technologies. *Soft Robotics*, 4(3):211–223. Publisher: Mary Ann Liebert, Inc., publishers.

[Sarabu et al., 2019] Sarabu, H., Ahlin, K., and Hu, A.-P. (2019). Graph-based cooperative robot path planning in agricultural environments. In *2019 IEEE/ASME International Conference on Advanced Intelligent Mechatronics, AIM 2019*, volume 2019-July, pages 519–525.

[Scarfe et al., 2009] Scarfe, A., Flemmer, R., Bakker, H., and Flemmer, C. (2009). Development of an autonomous kiwifruit picking robot. In *4th International Conference on Autonomous Robots and Agents, ICARA 2009*, pages 380–384.

[Schunk, nd] Schunk (n.d.). Angular gripper swg. [Online; accessed Februari 20, 2022].

[SepúLveda et al., 2020] SepúLveda, D., Fernández, R., Navas, E., Armada, M., and González-De-Santos, P. (2020). Robotic Aubergine Harvesting Using Dual-Arm Manipulation. *IEEE Access*, 8:121889–121904. Conference Name: IEEE Access.

[Silwal et al., 2017] Silwal, A., Davidson, J. R., Karkee, M., Mo, C., Zhang, Q., and Lewis, K. (2017). Design, integration, and field evaluation of a robotic apple harvester. *Journal of Field Robotics*, 34(6):1140–1159. _eprint: https://onlinelibrary.wiley.com/doi/pdf/10.1002/rob.21715.

[SINTEF Raufoss Manufacturing, nd] SINTEF Raufoss Manufacturing (n.d.). Needle gripper. [Online; accessed Februari 20, 2022].

[Tadokoro et al., 1999] Tadokoro, S., Verhoeven, R., Hiller, M., and Takamori, T. (1999). A portable parallel manipulator for search and rescue at large-scale urban earthquakes and an identification algorithm for the installation in unstructured environments. In *Proceedings 1999 IEEE/RSJ International Conference on Intelligent Robots and Systems. Human and Environment Friendly Robots with High Intelligence and Emotional Quotients (Cat. No.99CH36289)*, volume 2, pages 1222–1227 vol.2.

[Takahashi et al., 2021] Takahashi, T., Tadakuma, K., Watanabe, M., Takane, E., Hookabe, N., Kajiahara, H., Yamasaki, T., Konyo, M., and Tadokoro, S. (2021). Eversion Robotic Mechanism With Hydraulic Skeletonto Realize Steering Function. *IEEE Robotics and Automation Letters*, 6(3):5413–5420. Conference Name: IEEE Robotics and Automation Letters.

[Tian et al., 2016] Tian, J. J., Bryksa, B. C., and Yada, R. Y. (2016). Feeding the world into the future – food and nutrition security: the role of food science and technology. *Frontiers in Life Science*, 9(3):155–166. Publisher: Taylor & Francis _eprint: https://doi.org/10.1080/21553769.2016.1174958.

[Van Henten et al., 2010] Van Henten, E. J., Schenk, E. J., van Willigenburg, L. G., Meuleman, J., and Barreiro, P. (2010). Collision-free inverse kinematics of the redundant seven-link manipulator used in a cucumber picking robot. *Biosystems Engineering*, 106(2):112–124.

[Wang et al., 2019a] Wang, X., Zhang, Q., Shen, D., and Chen, J. (2019a). A Novel Rescue Robot: Hybrid Soft and Rigid Structures for Narrow Space Searching. In *2019 IEEE International Conference on Robotics and Biomimetics (ROBIO)*, pages 2207–2213.

[Wang et al., 2019b] Wang, Y., Ju, F., Yun, Y., Yao, J., Wang, Y., Guo, H., and Chen, B. (2019b). An inspection continuum robot with tactile sensor based on electrical impedance tomography for exploration and navigation in unknown environment. *Industrial Robot: the international journal of robotics research and application*, 47(1):121–130. Publisher: Emerald Publishing Limited.

[Wang et al., 2020] Wang, Z., Or, K., and Hirai, S. (2020). A dual-mode soft gripper for food packaging. *Robotics and Autonomous Systems*, 125:103427.

[Wang et al., 2017] Wang, Z., Torigoe, Y., and Hirai, S. (2017). A Prestressed Soft Gripper: Design, Modeling, Fabrication, and Tests for Food Handling. *IEEE Robotics and Automation Letters*, 2(4):1909–1916. Conference Name: IEEE Robotics and Automation Letters.

[Xiong et al., 2020a] Xiong, Y., Ge, Y., and From, P. J. (2020a). Push and Drag: An Active Obstacle Separation Method for Fruit Harvesting Robots. In *2020 IEEE International Conference on Robotics and Automation (ICRA)*, pages 4957–4962. ISSN: 2577-087X.

[Xiong et al., 2021] Xiong, Y., Ge, Y., and From, P. J. (2021). An improved obstacle separation method using deep learning for object detection and tracking in a hybrid visual control loop for fruit picking in clusters. *Computers and Electronics in Agriculture*, 191:106508.

[Xiong et al., 2020b] Xiong, Y., Ge, Y., Grimstad, L., and From, P. (2020b). An autonomous strawberry-harvesting robot: Design, development, integration, and field evaluation. *Journal of Field Robotics*, 37(2):202–224.

[Xue, 2017] Xue, H. (2017). Design of an embedded system for a fruit- and vegetable-picking robot based on genetic algorithm and EDA technology. *Agro Food Industry Hi-Tech*, 28(1):1992–1996.

[Yang et al., 2020] Yang, C., Xiong, L., Wang, Z., Wang, Y., Shi, G., Kuremot, T., Zhao, W., and Yang, Y. (2020). Integrated detection of citrus fruits and branches using a convolutional neural network. *Computers and Electronics in Agriculture*, 174.

[Zhang et al., 2016] Zhang, S., Yuan, T., Wang, D., Zhang, J., and Li, W. (2016). Structure optimization and path planning of tomato picking manipulator. In *9th International Symposium on Computational Intelligence and Design, ISCID 2016*, volume 2, pages 356–360.

[Zhong et al., 2019] Zhong, G., Hou, Y., and Dou, W. (2019). A soft pneumatic dexterous gripper with convertible grasping modes. *International Journal of Mechanical Sciences*, 153-154:445–456.

Appendix A

Calculation of bending strain in thin films

For calculating the maximum strain in curvature of a thin film, formulae A.1 can be used, where the required parameters are shown in Figure A.1.

$$\eta_{max} = \frac{L_{strain} - L_{neutral}}{L_{neutral}} = \frac{t_{backbone}}{2R_{neutral}} \tag{A.1}$$

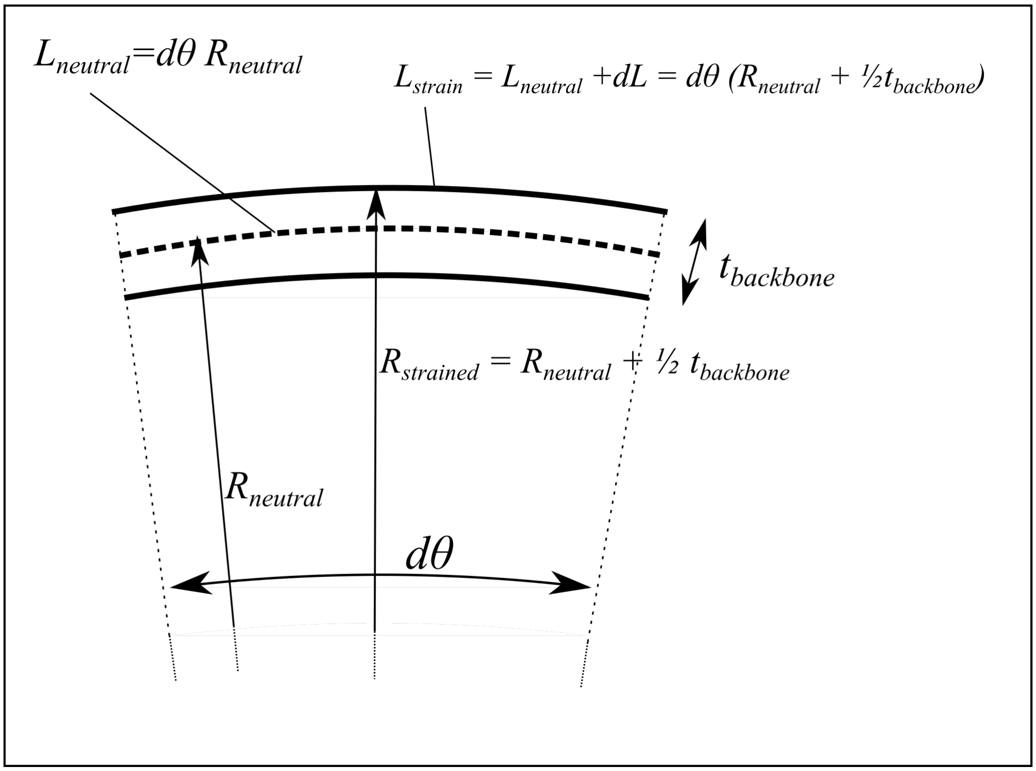

Figure A.1: Curvature and deformation of a thin film in bending

Appendix B

Calculation of belt tension loss through a series of rollers

```
@author: bartf
"""
def calc_fout(Fin, mueff, phi):
    Fw = 2*sind(phi/2)*Fin*mueff
    Fout = Fin-Fw
    return Fout

import numpy as np
sind = lambda degrees: np.sin(np.deg2rad(degrees))
cosd = lambda degrees: np.cos(np.deg2rad(degrees))

Daxle = 0.5
Dlargeroller = 5
Dsmallroller = 3

musteel = 0.45
muback = 0.6

mul= musteel*Daxle/Dlargeroller
mus = musteel*Daxle/Dsmallroller

Fbelt = 4.5
phi_tip = 225
phi_pushout = 45
phi_pullin = 90

phi_back = 90
```

```
philist = [phi_tip ,phi_pushout ,phi_pullin ,phi_pushout ,phi_pushout ,phi_pullin ,phi_pushout ,p
mulist = [mul,mul,mus,mul,mul,mus,mul,mul,mus,mul]

Flist = [0,0,0,0,0,0,0,0,0,0,0]
Flist[0] = Fbelt


for i in range(0,len(philist)):
    Fnew = calc_fout(Flist[i],mulist[i],philist[i])
    Flist[i+1] = Fnew


Fspareout = calc_fout(Fbelt,mul,phi_tip)*np.exp(-muback*phi_back/360*2*3.14)
```

Appendix C

Bending spring steel sheet-metal

Issues with bending spring steel

Sheet-metal can be used to be complex monolithic 3D parts, especially when bending and creasing is used. However, forming spring-steel sheet-metal proves a difficult task, since there is a large amount of spring-back present, something which is inherent to the desired material properties of spring steel. Spring-back results in the bend being less steep than desired, a solution for which is compensating by bending further than the desired angle.

Due to the steep stress strain curve of spring steel, spring steel has a very short plastic deformation range before fracture, while having a large amount of spring-back. This means that depending on the bending radius and bending angle, material failure will occur before the angle of bending at which spring-back is compensated. There are several solutions to solve this problem so that the part can still be made:

- **Increase bending radius:** With a higher bending radius, the required plastic strain will be divided over a longer length of material. However, the problem might occur that impossibly large spring-back compensation (e.g. $> 180\ ^{\circ}$) would be required. Furthermore, the design or available tools may not allow for an increased bending radius.
- **Decreased bending angle:** A discrete version of increasing the bending radius, by dividing the bend over more bends. Depending on the part this might be a feasible design change.
- **Annealing before, and re-heat-treating after forming:** If heat-treating methods are available, the part can formed in its annealed state, and heat-treated to steep the spring-steel curve afterwards.
- **Local heat-treating at bends:** Another option is to locally treat the material at the points where it must be bend. Although this can be a delicate process, when using thin spring steel sheet it is possible to locally heat the spring steel at for instance mounting tabs which must be bent but do not locally require the spring steel steep curve. This way, the monolithic spring steel part can steel have non-homogeneous material properties.

Local heat-treating

For prototyping purposes, the local heat-treating can prove a useful solution. An example of a part treated this way, is given in Figure C.1. The used spring steel sheet metal material is 0.2mm thick, and the overall length is about 120mm.

The part is to be used in a mechanical gripper, where the backbone should remain flexible for a compliant grip, while the tabs need to be bent and have no special requirements for the material properties. Therefore, it was decided to locally heat treat the part using a small gas torch (e.g. one used for kitchen purposes). Each tab was locally heat treated at its end until it was red hot. By touch, the temperature of the backbone was checked to remain cool enough (anything beyond 60 °C will not be comfortable to hold for more than a second) so that no permanent changes to the material properties occur.

The process proved to be sufficient for prototyping the designed part, used repeatedly in a gripper. It is recommended to test the method on a few extra parts, and also test the part before use. Other than that the method might prove useful if implemented at an industrial level, using local heating techniques like acoustic or laser heating.

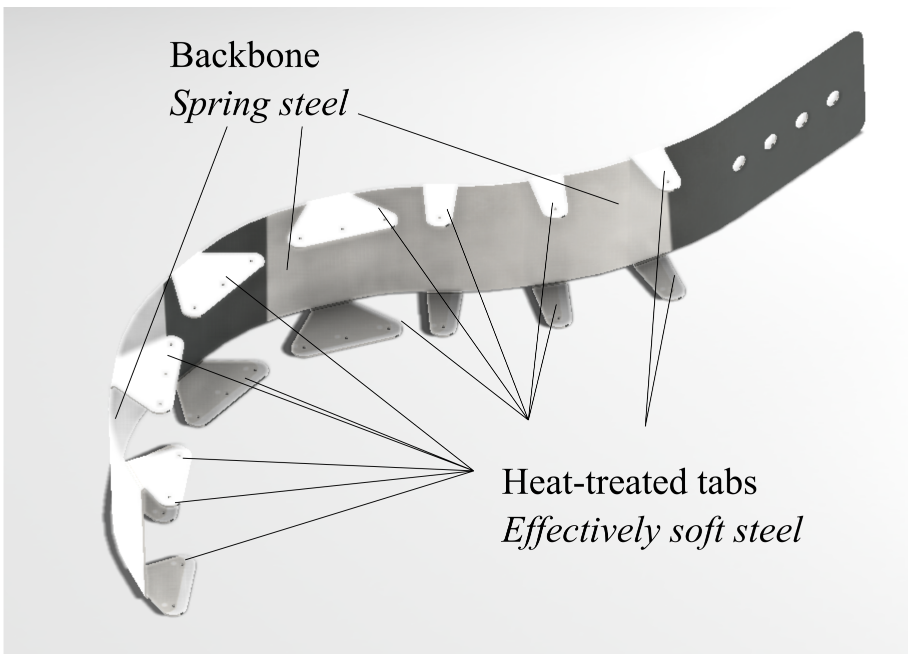

Figure C.1: Spring steel part, bent by locally heating the tabs that are to be bent.

Appendix D

Measurements on Sample Population

A set of tomatoes of the same types and source as used in the practical experiments, were measured using a caliper (1 mm precision) and scale (1 gr precision). The data are shown in Table D.1. The height and diameter of the tomatoes were measured separately, the results of which are plotted in Figure D.1. Furthermore, the weight of the tomatoes was measured. The results are shown in Figure D.2. A mix of Roma and Bunched tomatoes were used. As can be seen, Roma tomatoes on average have a larger height than width, while for Bunched tomatoes the opposite is true. The mean dimensions of the tomatoes are: $H_{tomato} = 61$ mm +/- 10 (95% conf.) and $W_{tomato} = 60$ mm +/- 10 (95% conf.)

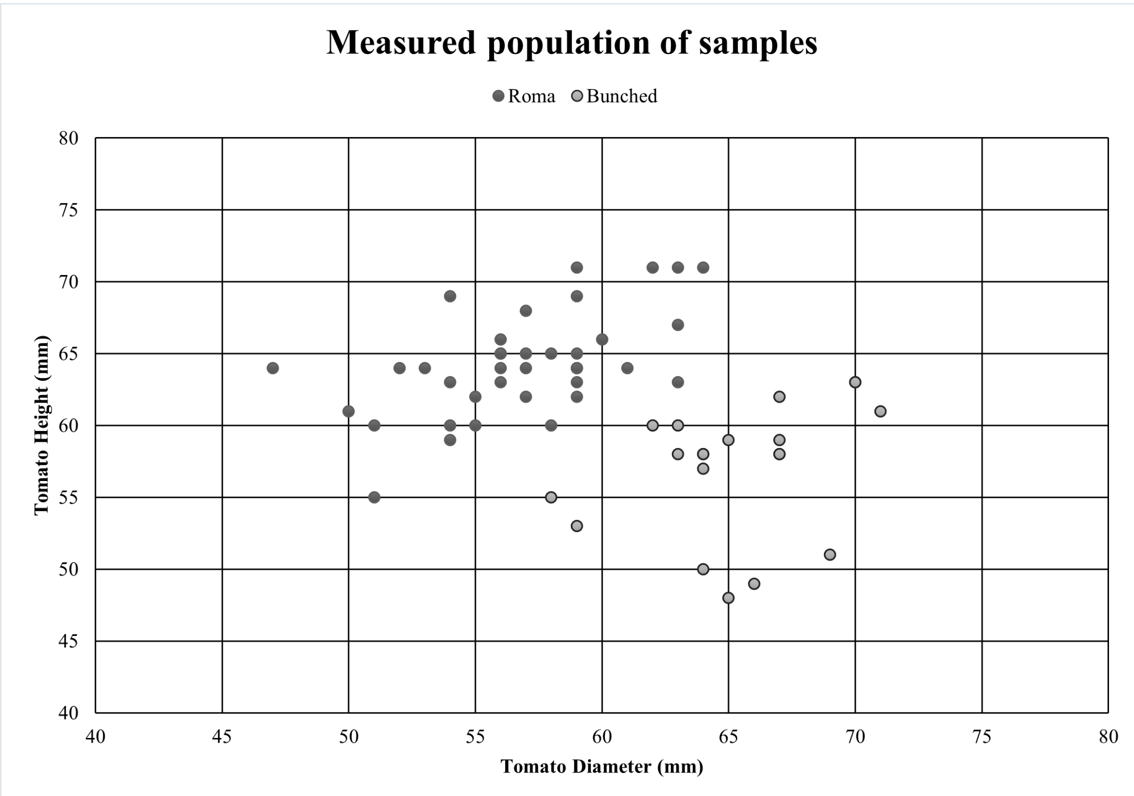

Figure D.1: Scatter plot showing dimensions of the population of tomatoes that were used in the practical experiments.

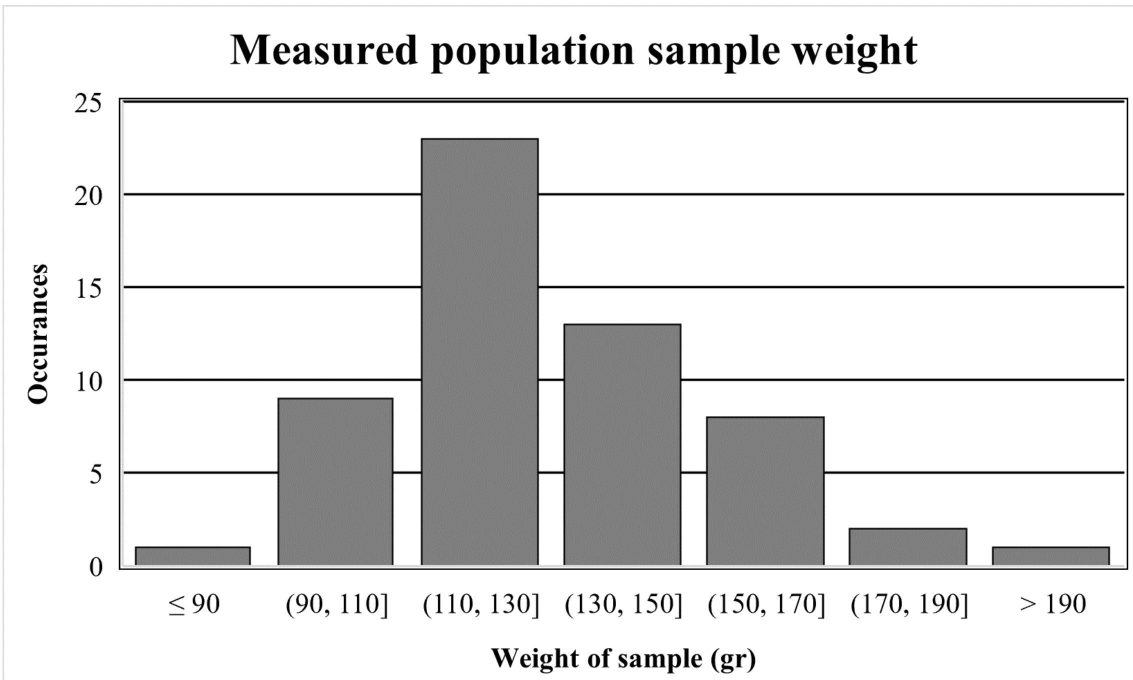

Figure D.2: Histogram showing weight of the population of tomatoes that were used in the practical experiments.

Table D.1: Measurements on tomatoes used in a practical experiment with a robotic tomato gripper

Sample#	**Weight (gr)**	**Heigth (mm)**	**Width (mm)**	**Type**
1	116	59	54	Roma
2	124	66	56	Roma
3	160	71	62	Roma
4	134	64	59	Roma
5	124	69	54	Roma
6	106	63	54	Roma
7	117	65	57	Roma
8	119	65	59	Roma
9	110	63	56	Roma
10	120	71	59	Roma
11	118	68	57	Roma
12	126	62	59	Roma
13	109	60	55	Roma
14	148	69	59	Roma
15	155	71	64	Roma
16	150	66	60	Roma
17	163	67	63	Roma
18	163	71	63	Roma
19	128	64	59	Roma
20	131	63	59	Roma
21	130	60	58	Roma
22	130	64	56	Roma
23	139	63	63	Roma
24	121	64	57	Roma
25	138	64	61	Roma
26	128	65	58	Roma
27	120	65	56	Roma
28	113	60	54	Roma
29	128	65	56	Roma
30	113	62	57	Roma
31	104	62	55	Roma
32	105	64	53	Roma
33	104	64	47	Roma
34	87	55	51	Roma
35	102	64	52	Roma
36	92	60	51	Roma
37	93	61	50	Roma
38	192	63	70	Tros
39	190	61	71	Tros
40	171	63	70	Tros
41	159	62	67	Tros
42	128	60	62	Tros
43	159	58	67	Tros
44	113	55	58	Tros
45	153	59	67	Tros
46	149	60	63	Tros
47	151	58	67	Tros
48	128	48	65	Tros
49	136	49	66	Tros
50	126	50	64	Tros
51	116	53	59	Tros
52	141	51	69	Tros
53	140	59	65	Tros
54	134	58	64	Tros
55	130	58	63	Tros
56	134	58	64	Tros
57	139	57	64	Tros
Mean	131	62	60	
Max	192	71	71	
Min	87	48	47	

Appendix E

Force response of a rubberband

A rubberband can be characterized by its force response. It is valueable to use the elongation as a measure, since this generalizes the results for any length of rubberband. For measuring, a springscale with a precision of 5 grams, and a caliper with a precision of 1mm was used. However, measuring the length of the rubberbands free length L_0 was hard to do accurately, so the uncertainty should be interpreted with caution. The measured length L_0 was determined to be 56 mm. Using this L_0, the rubberbands force response dependign on a certain elongation was measured, as is plotted in Figure E.1. The measured forces correspond to an increasing load, so when unloading, lower forces at the same elongation are expected due to hysteresis.

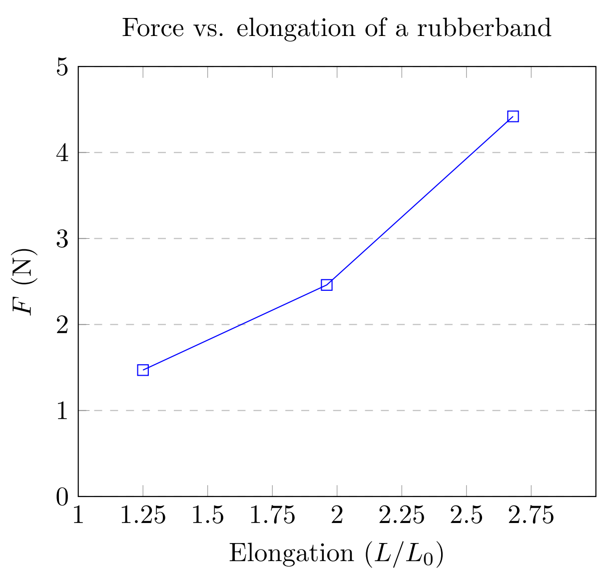

Figure E.1: Force response of a rubberband loop with a free length of $L_0 = 56$ mm.

Appendix F

Lasercutting Parameters

The spring steel backbone was cut using a CO2 laser CNC cutter, suitable for metal cutting, with a total available power of 1 kilowatt. For cutting spring steel sheet, it is important to make sure the material does not overheat which will change the material properties. For reference, the used settings in this research are shown in Figure F.1

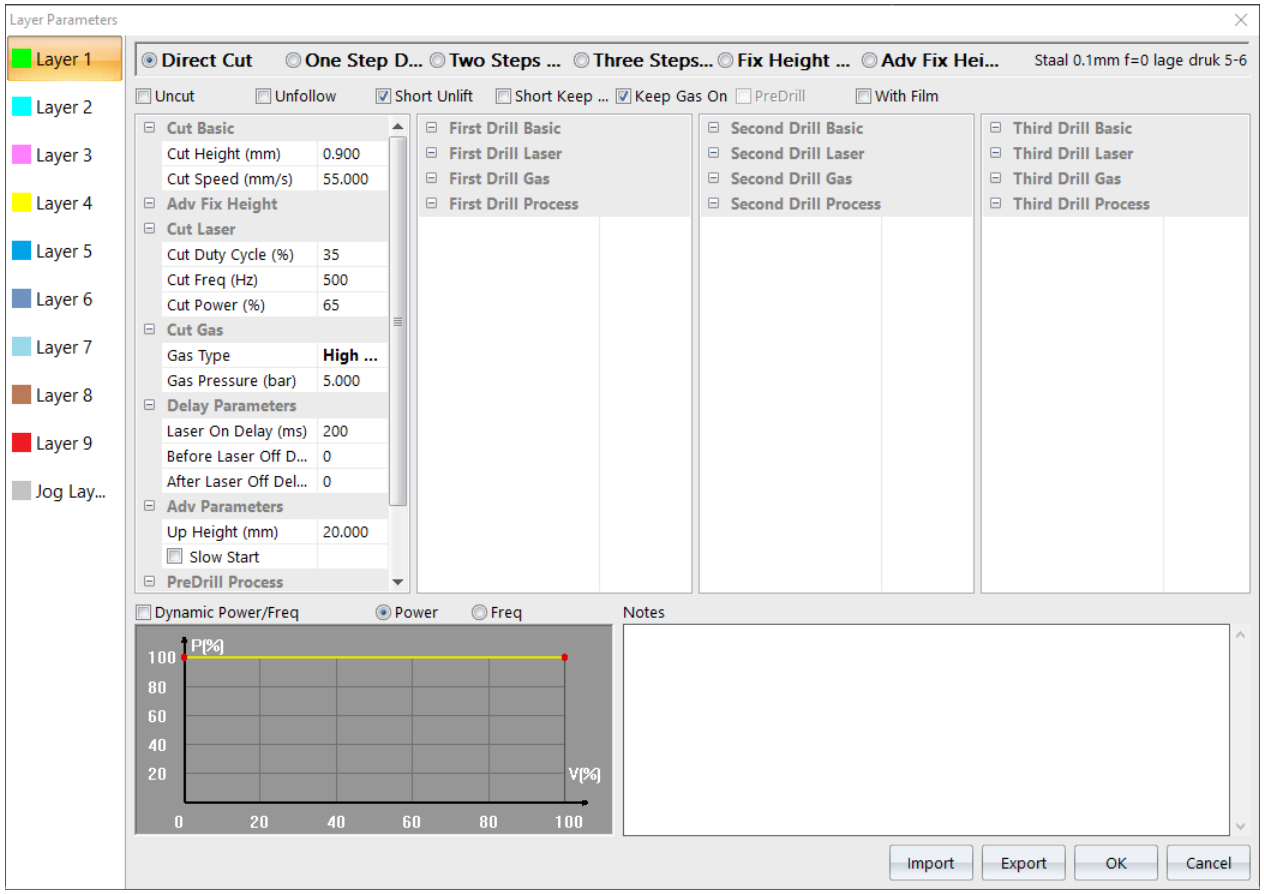

Figure F.1: Used parameters for lasercutting 0.2 mm spring steel sheet

Appendix G

Stills from finger motion

To verify that the finger propagates forwards along the object surface during the grasp manoeuvre, a video was shot showing a sideways view of one of the gripper finger. The video was shot from a 2 m distance with a high zoom, to minimize perspective distortion. In Figure G.1 to Figure G.5, different intermediate states during the grasp manoeuvre are shown. In each still, the final state of the finger is traced in red, showing that during motion, the finger stays closely within the outward bound of the final finger state. The

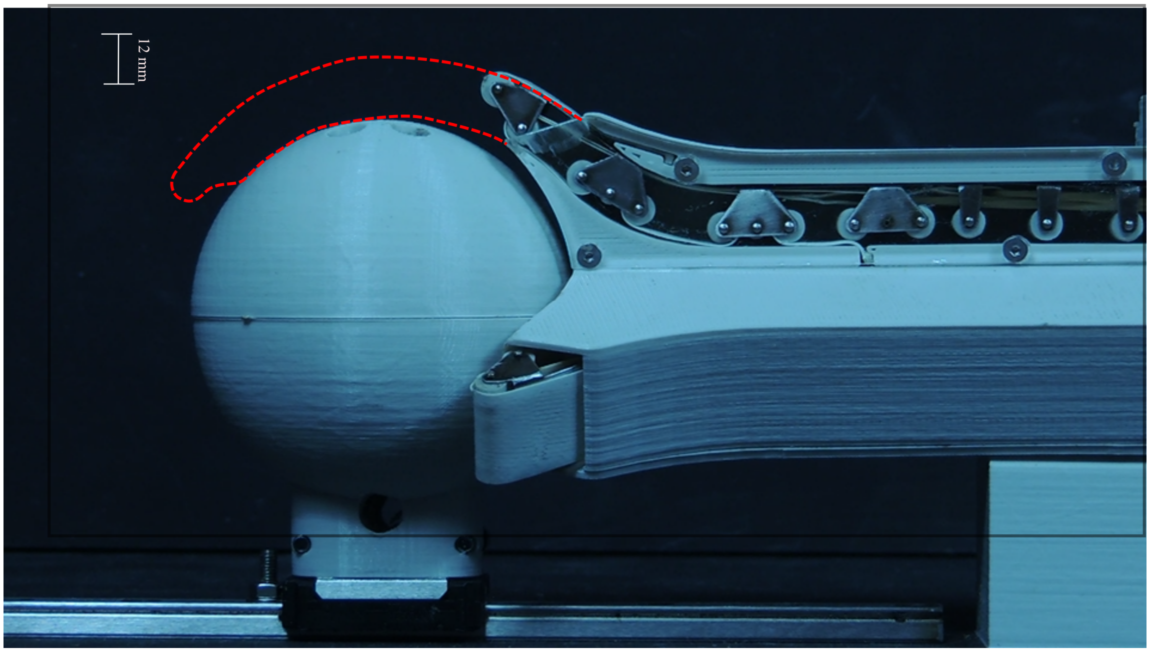

Figure G.1: Intermediate state of grasping. In red, the final finger state is traced.

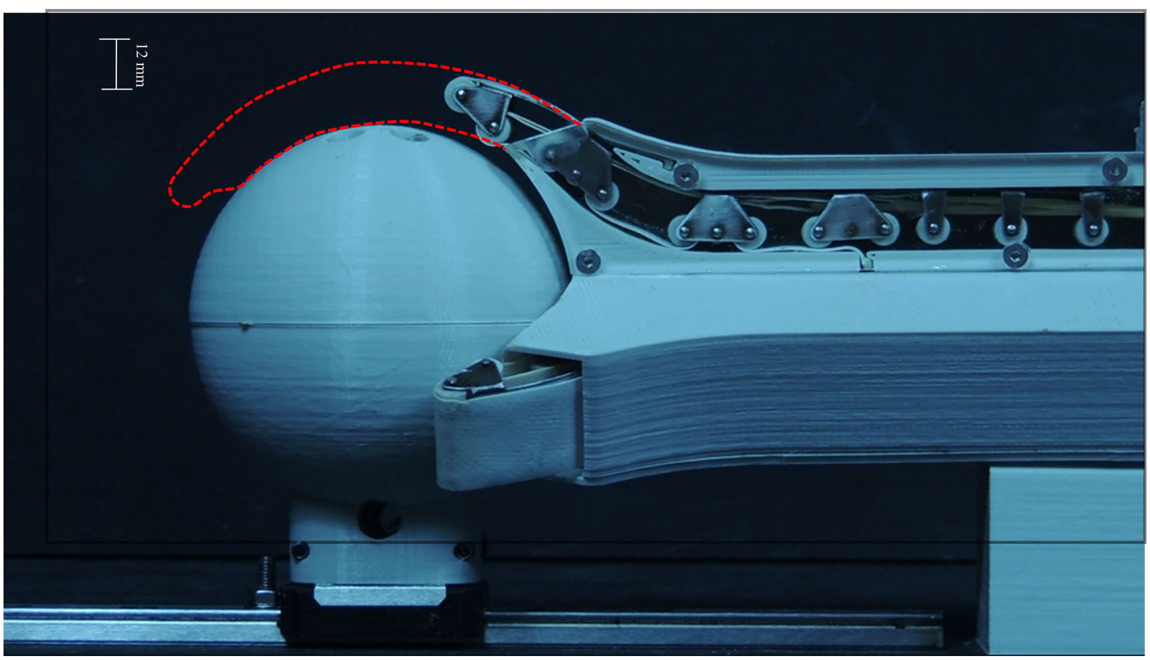

Figure G.2: Intermediate state of grasping. In red, the final finger state is traced.

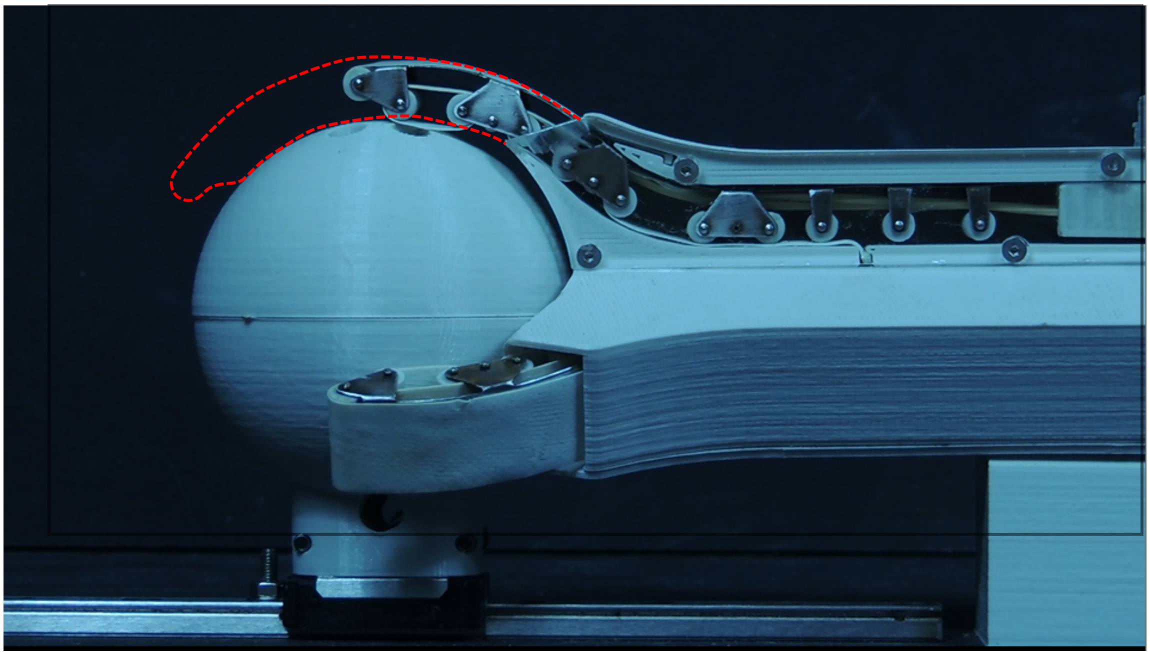

Figure G.3: Intermediate state of grasping. In red, the final finger state is traced.

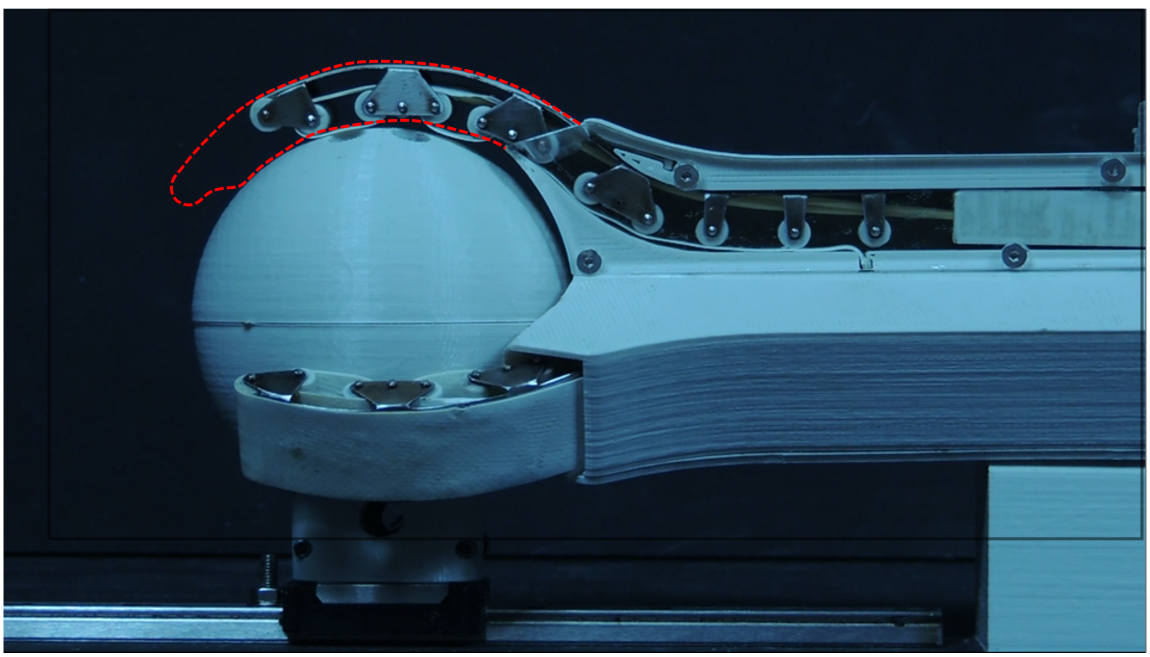

Figure G.4: Intermediate state of grasping. In red, the final finger state is traced.

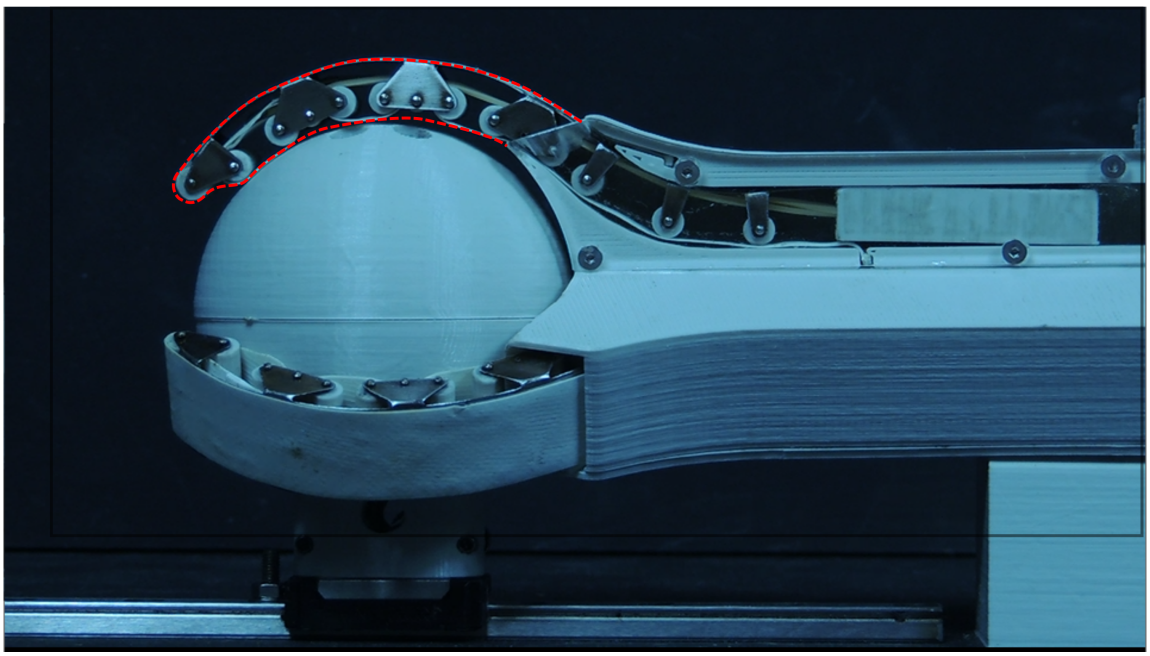

Figure G.5: Final state of grasping. In red, the final finger state is traced.

Appendix H

Calibration of measurement setups

Calibration of friction setups

The measurement setup, shown in Figure 4.17, was calibrate to determine the effective spring coefficients κ_L and κ_R, and the offset-angles $\theta_{0,L}$ and $\theta_{0,R}$, so that the rotation $\delta\kappa$ can be calculated.

For calibration of each of the cylinders, a thread was wrapped around the cylinder and a spring scale connected suspended above the setup vertically. Then, the force on the spring scale was increased in steps of 25 gr up to 200 gr, noting the measured angle θ corresponding to each force. To get an idea of the effects of friction, the force was then decreased by steps of 25 gr and the corresponding angles were noted again. The measurement data is shown in Table H.1 and H.2.

To find the relationship between the angle and force of each cylinder, the data is plotted in Figures H.1 and H.2. Friction is seen to be very low, by the fact that for a rising and falling force, the resulting angles barely differ. In black, the linear regressions used to estimate the setup behaviour are given, which by the R of 0.9983 and 0.9897 are considered sufficiently accurate.

From the equations of the linear regressions, the offset θ_0 of each cylinder can be calculated by setting each equation equal to zero, as below, in which y is the force and x is the corresponding θ:

$$y = ax + b = 0 \tag{H.1}$$

$$x = -b/a \tag{H.2}$$

...resulting in $\theta_{0,L} = 1.28$ degrees and $\theta_{0,R} = 0.18$ degrees. Furthermore, the effective spring coefficients κ_L and κ_R can be calculated by dividing the a terms of both equations by the radius R = 30 mm of the cylinder, to obtain $\kappa_L = 0.642$ mNm/degree and $\kappa_R = 0.666$ mNm/degree.

Calibration of net force setup

For the net force setup, a similar method was used as in the friction setups, where a spring scale was used to apply an increasing force to the object on the slider. The measurement data of the

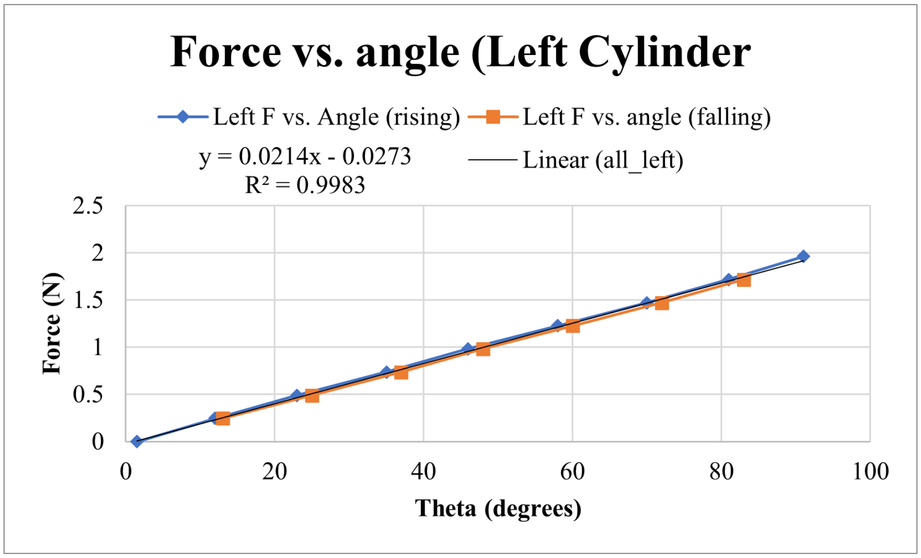

Figure H.1: Graph of the calibration measurement of the left cylinder of the friction measurement setup. The measurements with rising and decreasing force F_L are shown in different colors, and the fitted regression of all data points is given.

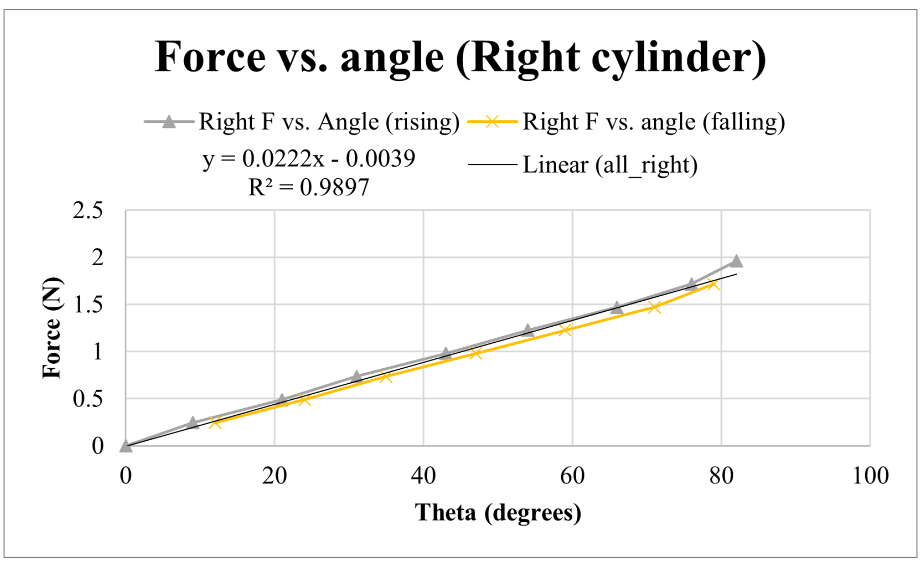

Figure H.2: Graph of the calibration measurement of the left cylinder of the friction measurement setup. The measurements with rising and decreasing force F_R are shown in different colors, and the fitted regression of all data points is given.

Table H.1: Measurement data for the calibration force loop for the left cylinder.

θ_L	F_L **(gr)**	F_L **(N)**
1.5	0	0
12	25	0.24525
23	50	0.4905
35	75	0.73575
46	100	0.981
58	125	1.22625
70	150	1.4715
81	175	1.71675
91	200	1.962
83	175	1.71675
72	150	1.4715
60	125	1.22625
48	100	0.981
37	75	0.73575
25	50	0.4905
13	25	0.24525

force vs. the measured position are given in Table H.3.

To obtain the relation between position and force applied, the data is plotted in Figure H.3. The resulting linear regression approximating the spring system is given in black.

From the equation, the offset position can be calculated as $u_0 = 39.6$ mm. Furthermore, the effective spring coefficient is equal to: $k_{eff} = |a| = 18.75$ N/mm.

Table H.2: Measurement data for the calibration force loop for the right cylinder.

θ_R	F_R (gr)	F_R (N)
0	0	0
9	25	0.24525
21	50	0.4905
31	75	0.73575
43	100	0.981
54	125	1.22625
66	150	1.4715
76	175	1.71675
82	200	1.962
79	175	1.71675
71	150	1.4715
59	125	1.22625
47	100	0.981
35	75	0.73575
24	50	0.4905
12	25	0.24525

Table H.3: Measurement data for calibrating the net force measurement setup. The force was increased and then decreased, and the corresponding position u measured.

u (mm)	**F (gr)**	**F (N)**
39.5	0	0.00
39	10	0.10
38.75	20	0.20
38.25	30	0.29
37.5	40	0.39
37	50	0.49
36.5	60	0.59
37	50	0.49
37.5	40	0.39
38	30	0.29
38.5	20	0.20
39	10	0.10
39.75	0	0.00

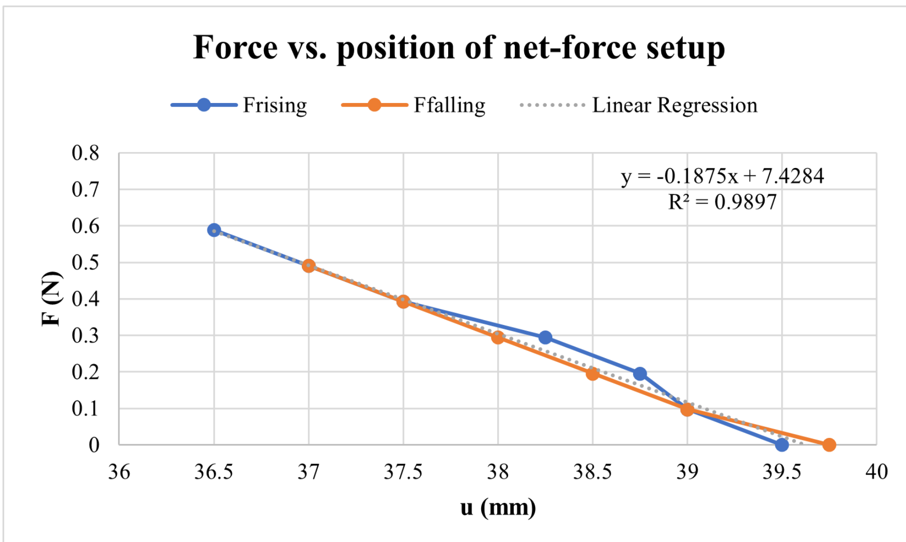

Figure H.3: Graph of the calibration measurement of the net force measurement setup. The measurements with rising and decreasing force F are shown in different colors, and the fitted regression of all data points is given.

Appendix I

Measurement of belt friction on a single roller

When rolling a belt over a roller, the main friction contribution was expected to be the rolling friction of the roller. This roller friction was expected to be $\mu_{eff} = 0.05$. However, in practice, belt friction was much higher, and the belt refused to fully retract, meaning that at the last few rollers, the belt was hanging loose. Such behaviour can only be explained by the presence of an additional friction force which is not dependent on belt tension, meaning that the friction force would be better described by the following equation:

$$F_w = F_N \mu_{eff} + F_{w,c} \tag{I.1}$$

Where $F_{w,c}$ is an additional, constant friction force. To verify the presence of $F_{w,c}$, the friction of the belt over a single roller is measured. This is done by wrapping a belt over a single roller and adding a weight of m_T to one end of the belt, so that that end of the belt is under tension of $F_T = m_T g$. Then, by mounting a spring scale on the other end, the difference between the forces required to pull and slack the belt over the roller can be measured, which is roughly equal to twice the friction force F_w present in the roller and belt together. By varying the weight m_T, the friction F_w for different belt tensions F_T, and fitting a linear linear approximation to the points, the coefficients for equation I.1 can then be estimated. In Figure I.1, this plot is shown:

As can be seen, the friction is indeed much higher than when taking the friction component term alone, and a large constant term of $F_{w,c} = 0.23$ N is present. A likely cause for this friction term, is the deformation of the belt when it conforms to the roller radius. This seems likely because the belt thickness is relatively high compared to the roller radius of 2.5mm ($t_{belt}/R_{roller} = 15\%$). For industrial conveyors for instance, this is generally closer to 2-5%.

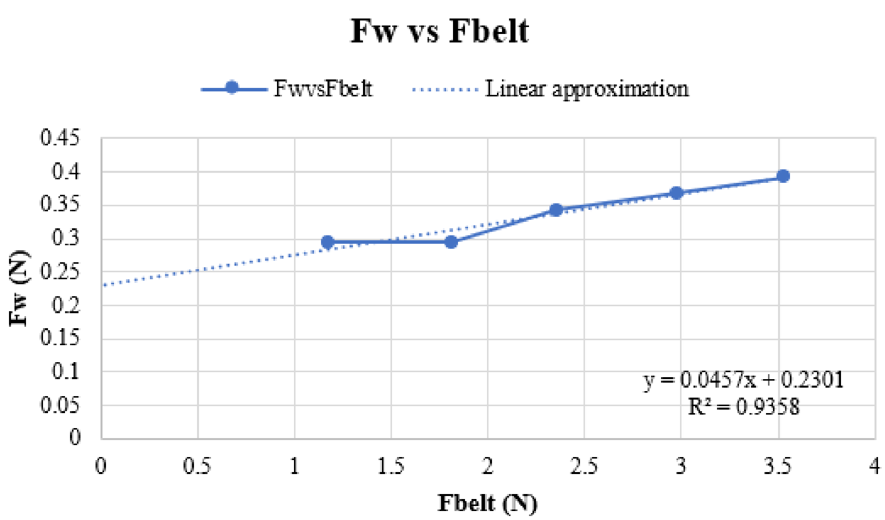

Figure I.1: Plot of the measured friction F_w for a single roller, wrapped 180°around a 5 mm roller, for varying belt tensions F_{belt}.

Design and validation of a manoeuvering caging gripper for grasping in cluttered environments

A mechanical approach to grasping in cluttered environments

1st Bart Friederich
Department of High-Tech Engineering
Technical University of Delft
Delft, The Netherlands
B.Friederich@student.tudelft.nl

2nd Ad Huisjes
Department of High-Tech Engineering
Technical University of Delft
Delft, The Netherlands
A.E.Huisjes@tudelft.nl

3rd Just Herder
Department of High-Tech Engineering
Technical University of Delft
Delft, The Netherlands
J.L.Herder@tudelft.nl

***Abstract*—This research proposes and validates a novel grasping principle to be able to set caging grasps in cluttered environments. A prototype is designed making use of manoeuvering fingers which propagate along the object surface and are covered with everting belts to minimize slip and thus friction forces on the object and environment. Using several lab setups, it is shown that the designed gripper fingers closely follow spherical objects, and do so while exerting only negligible normal and friction forces on the object or surrounding clutter. Furthermore, the gripper is validated with a robotic system in a practical test case of grasping tomatoes from a dense cluttered pile. The gripper successfully grasped 100% of the objects without any control effort in terms of clutter avoidance and grasp pose control. This shows that this novel strategy for setting a caging grasp makes grasping difficult objects in cluttered environments robust and highly successful.**

***Index Terms*—gripper, grasping, clutter, manoeuvering, eversion, frictionless, compliant, adaptive, agri-food**

I. Introduction

A. Background

Robotic grasping and manipulation of agri-food objects is a complex task, in part due to the uncertainties in shape and position, and the combinations of difficult properties (e.g. roughness, slipperiness, softness or fragility) of organic objects. A wide range of gripper types exists, from suction cup grippers [Mantriota, 2007], to granular jamming grippers [Brown et al., 2010] and parallel grippers [Ciocarlie et al., 2014], each of which is suitable for a different variety of objects. An especially interesting gripper type is the caging gripper, which makes use of form closure using 4 or more frictionless contacts to constrain the object [Bicchi and Kumar, 2000]. Because cage grasping does not rely on friction forces, it can work regardless of the friction coefficient of the object surface, and since there is no minimal normal force required to establish friction, the forces on the object need not exceed the objects mass and acceleration forces. Furthermore, to accommodate shape variety and divide forces over different contacts, grippers with underactuated [Meijneke et al., 2011] and compliant fingers [Crooks et al., 2017] have been designed which are already widely used in the agri-food industry.

Together, these caging grippers provide a promising and universal solution for manipulating agri-food objects. However, in practice, success rates are still low in more complex tasks where environments near the object are cluttered, like selective harvesting and picking unsingularized objects. These low success rates can be partly explained by the fact that caging grippers are inherently unsuitable for objects in cluttered environments, since application of such a gripper requires almost all surfaces of the object to be free from obstacles. Hence, in literature on selective harvesting systems, collisions due to the gripper size [Silwal et al., 2017] and the unreachability of certain fruits in clutters [Bac et al., 2017] [Davidson et al., 2016] are quoted as reasons for failure. Since these problems first arise at implementation of the gripper in a robotic system, the solutions in state-of-the-art research are sought in advanced planning and obstacle recognition while still trying to avoid contact with the obstacles [Silwal et al., 2017] or obstacle-interactive strategies to separate the object and obstacles [Xiong et al., 2020] [Páll and Brock, 2021].

Unlike these control-side approaches, we present a mechanical approach by redesigning the gripper for use in cluttered environments. The proposed gripper uses a new strategy for setting a caging grasp which eliminates unwanted interaction with the environment and actually uses interaction to manoeuvre. Implementing such a gripper in a robotic system will be simpler and higher success rates may be achieved.

B. Novel approach for setting a caging grasp

The proposed approach minimizes interaction with the clutter in two steps. First, since displacements on the object or clutter during the grasp manoeuvre may cause damage or miss grasps, the gripper should ideally exercise minimal displacements on the object and the environment during the manoeuvre. Most existing caging grippers engage with pivoting joints or prismatic joints so that during the grasp manoeuvre empty space is created between object and environment, in addition to the thickness of the fingers. This research proposes compliant gripper fingers which engage by an object-following forward-propagating manoeuvre, so that the environment only has to be displaced by the finger thickness.

Second, during the insertion of the gripper fingers between the object and clutter, friction forces will emerge due to sliding at the contact surfaces. These forces may also cause damage or unwanted displacement. This problem may be reduced by minimizing friction of the gripper surface by low-friction material or by using free-rolling contacts. Better yet, we propose a more effective solution by actively keeping the contact surfaces of the gripper still with respect to the object and environment (zero-slip), which eliminates friction forces from emerging at all.

C. Research structure

Through the rest of this paper, a prototype will be designed and tested to show that this approach of minimizing clutter interaction in the grippers design indeed makes cage grasping in cluttered environments simple and successful. Since the performance of a gripper is dependent on many factors at once, a high success rate of a gripper in a practical experiment would not show whether the proposed new design features are responsible for improvement. Therefore, several lab experiments as well as a practical experiment will be carried out, verifying the presence and improvements of individual design features, but also showing the performance of the gripper as a whole. This combination of lab and practical experiments thus substantiates the claim that the designed features perform as intended and are responsible for the grippers success.

The Methods section starts off with the functional design of the prototype, as well as an analysis of the expected behaviour. Then, the four lab experiments used for individually verifying the four main design features of the gripper are described. The Methods section finishes with the description of the practical experiment, which includes a fully working robotic system. In the Results section, the measurements of the individual design features are shown and, where applicable, plotted against expected or benchmark values. Furthermore, the results of the practical experiment are given. Finally, the interpretation of the research results and the conclusions that can be drawn are given in the Discussions and Conclusions sections.

II. Methods

A. Functional design

The gripper was designed which based on four main functions. First of all, like any caging gripper, the gripper fingers required *structural stiffness* so that forces at the contact points can be transferred to the gripper wrist. The main innovation of this research was the implementation of two new functions, being the *object-following propagation* of the fingers, and the *slip elimination* at the contact surfaces of the fingers. An extra function, *initial finger guiding*, followed from the object-following manoeuvre, and is necessary to guide the finger before it touches the object. In Figure 1, the gripper design is shown. The individually labeled parts perform the four gripper functions as follows:

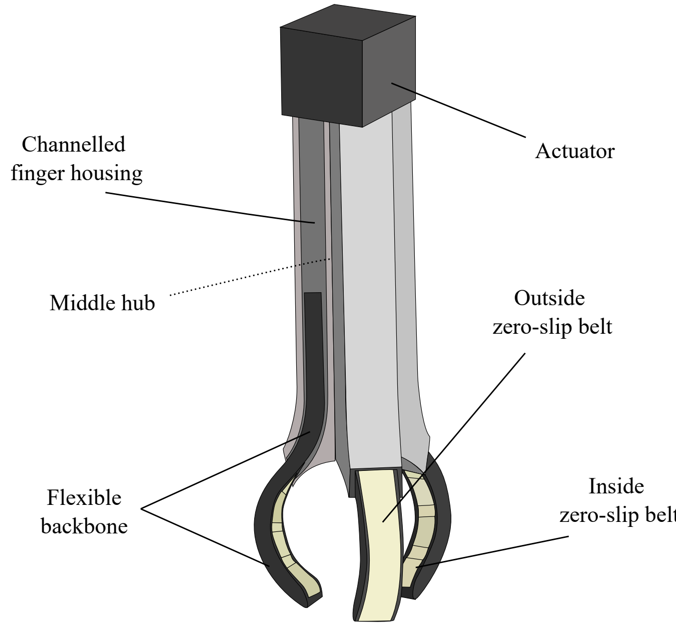

Fig. 1. Schematic drawing of the three fingered gripper, consisting of three finger modules and an actuator connected by a middle hub (hidden behind finger modules).

- *Object-following propagation*
  Each finger has a 150 mm long "flexible backbone" which provides axial stiffness to the finger during propagation. It was pre-shaped to the expected curvature of the object surface, but due to its flexibility it can adapt to the actual object shape. The backbone propagates from or retracts into the 3D-printed "channeled finger housing" by use of the linear stepper "actuator". To minimize the initial footprint and thus obstacle-free space required on the object, the three fingers approach the object in an S-shape path from a coincident axis at the wrist in which they are stored.
- *Initial finger guiding*
  To ensure that the fingers do not push the object away at initial contact, the ends of the "channeled finger housing" curve outward so that the fingers engage the object surface tangentially. After leaving the channel, the backbones bend back to their pre-curved shape, thereby following the object.
- *Slip elimination*
  To eliminate relative motion and accompanying friction forces between the gripper finger contact surfaces and the object / clutter, "zero-slip belts", which were 3D printed in TPU, cover the finger contact surfaces. They evert (roll out) from the finger tip with the opposite velocity of propagation of the fingers, thereby actively eliminating slip. The use of these belts was a mechanical adaptation from existing eversion mechanisms [Takahashi et al., 2021] [Hawkes et al., 2017], where pneumatics and 3D tensions in the tubes were taken over by plastic rollers, rubberbands and the backbone, as illustrated in Figure 2.

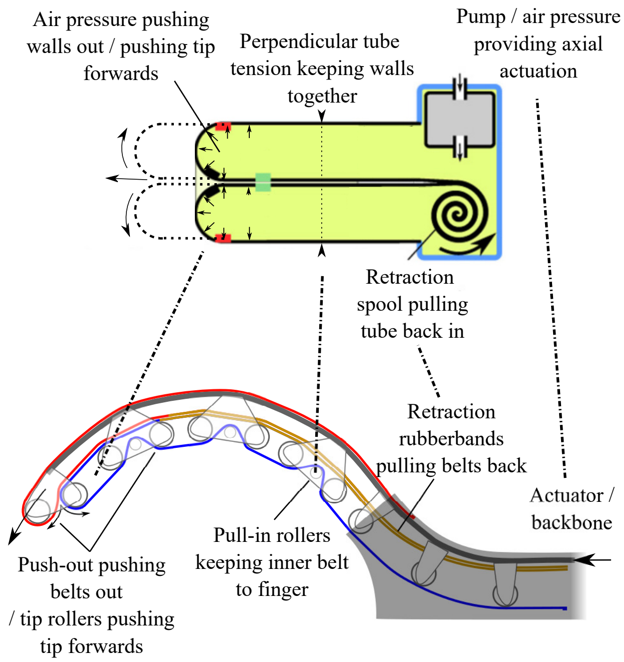

Fig. 2. Schematic showing how each individual element of the original pneumatic eversion mechanism (adapted from [Hawkes et al., 2017]) is substituted by mechanical elements.

- *Structural stiffness*
  The bending stiffness of the gripper finger is formed by a combination of the compressive stiffness of the "flexible backbone" on the outside of the finger and the tensile stiffness of the "zero-slip belts" on the inside of the fingers, comparable to the tendons of the human hand, as illustrated in Figure 3. Additionally, the backbone provides torsional stiffness to the finger.

B. Mechanical analysis of holding force

A critical parameter for a caging gripper is its ability to lift and manipulate objects with a holding force F_{hold} through the stiffness of its caging structure. For the purposes of the practical case of manipulating tomatoes, the holding force should at least equal the maximum object weight of 1.8 N (see Section II-D). Hence, each finger should have a vertical reaction force of at least 0.6 N to be able to lift the tomatoes. The reaction force of each finger was estimated both analytically and by simulation.

A rough analytical estimate was done by using the moment balance around the first point where the backbone emerges from the wrist, marked as the pivotting point P in Figure 4. For determining a safe minimum of the holding force, only one contact point at the tip of the gripper was assumed, and which was modelled as frictionless. The moment caused by $F_{contact}$ acting at a distance $R_{contact}$ from P, is here opposed by the force $F_{tendons}$ acting at a net distance $R_{tendons}$ from P. Herein, the force $F_{tendons}$ is caused by the belts acting as tendons between the moving parts of the gripper finger, as illustrated in Figure 3. Finally, considering that the contact

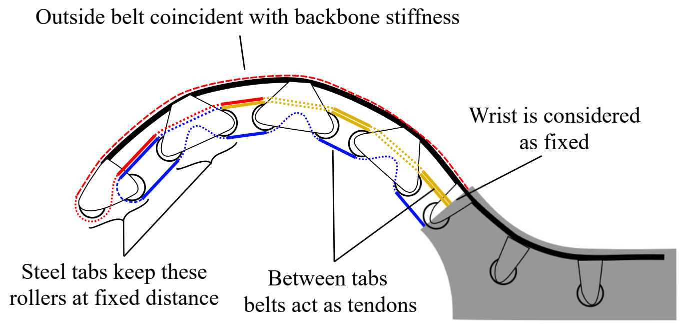

Fig. 3. Certain belt sections act as tendons by pulling rollers together, while other sections can be neglected because the much stiffer backbone/tabs prevents them from doing work. Between each of the four tabs and the wrist, 3 belts act in parallel, each exerting 3 N with a total of $F_{tendons}$ = 9 N.

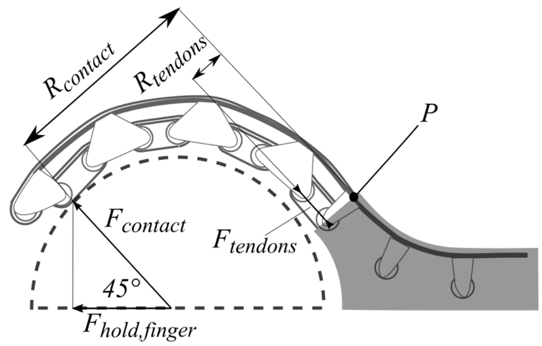

Fig. 4. Relevant geometry and forces for to analytically determine the holding force of a single gripper finger by use of moment balance around P.

force is at an angle of 45° with the grippers symmetry axis, the effective component $F_{hold,finger}$ which keeps the object from being pulled out, is then given by Equation 1. Substituting the values for the gripper design, which are $F_{tendons}$ = 9 N, $R_{tendons}$ = 6 mm and $R_{contact}$ = 42 mm, the holding force is estimated to be at least $F_{hold,finger}$ = 0.9 N or $F_{hold,analytical}$ = 2.7 N for the gripper in total.

$$F_{hold,finger} = \sin(45)\frac{F_{tendons}R_{tendons}}{R_{contact}} \tag{1}$$

In addition, a simulation using finite element analysis (FEA) was performed to obtain a more advanced estimation. In the FEA model, all four tendons were simulated by applying constant attractive forces between the rollers, as opposed to the analytical model, which only considered the first (but most critical) tendons. The object was simulated by a half cylinder with a diameter of D = 60 mm, and the contact was modeled as a non-penetrable frictionless contact. Using a non-linear analysis, the tendon forces were increased to $F_{tendons}$ = 9 N, at which point the reaction force on the object in the axial direction of the gripper was $F_{hold,finger}$ = 0.97 N or $F_{hold,FEA}$ = 2.91 N for the gripper in total. Together with the analytical estimate of 2.7 N, this gives an indication of the minimal holding force that is expected when measuring the holding force later.

C. Measurements

To verify the performance of the four main gripper functions, individual experiments were carried out for each function. Below, measurement setups, and measurement plans are given according for each function. The individual performance metrics of the experiments are italicized.

1) Object-following propagation → deviations (mm): The finger should propagate along the object without *deviations* to minimize the spatial perturbation of the environment to the finger thickness. This was verified graphically by taking a video from the side-view of one finger during the grasping of an object with a size of D_{mean} = 60 mm. By overlaying stills at different points of the video, deviations from the object surface and from the final state of the finger could be graphically compared.

2) Slip elimination → friction force F_{fric} (N) and perturbations $\Delta\theta$ (deg): Due to the zero-slip belts, any *friction forces* and *perturbations* from pushing the gripper between an object and obstacle should have been eliminated. To verify this, a measurement setup was made which can be used to measure both the friction force and the perturbation (rotation) by a simple finger, as shown in Figure 5. Two cylinders were used to simulate an object and obstacle. Using ball bearings, the cylinders could freely rotate on axles which were mounted on individual free running carriages on a linear slider. The carriages were held together with an extension spring to simulate a force pushing an obstacle and object together, with an effective force of 7 N when the cylinders were separated by the nominal finger thickness of 12 mm. The cylinders were kept in a neutral position with an effective torsion spring coefficient of κ_{obst} = 0.64 mNm/degree for the obstacle cylinder, and κ_{obj} = 0.66 mNm/degree for the object cylinder. To achieve a constant proportional torsion stiffness, a combination of two opposing extension springs acting at a radius of 12 mm from the cylinder axle was used. The rotation of each cylinder could be read using graduated arcs and indicators mounted to the cylinders and carriages respectively, with a precision of +/− 0.5 degrees.

To obtain the maximum perturbation $\Delta\theta$ of the cylinders, the finger was inserted using a linear actuator and the maximum rotation was read from the indicators. Next to this perturbation, the maximum friction force that was exerted could also be calculated. This was done by finding the moment required to rotate the cylinder, which was centered by the effective torsion spring coefficients κ, using Hooke's Law: $T_{cyl} = \kappa\Delta\theta$, which can then be converted to a friction force acting at the cylinders surface: $F_{fric} = \kappa\Delta\theta/R_{cyl}$. This way, the experiment gave a measure for both the friction force exerted, as well as the perturbation (rotation) of the object/environment. As a benchmark, two additional fingers were made and tested, one being a solid straight finger, and one being an S-path following finger *without* zero-slip belts. These were printed from the same material as the belts of the zero-slip finger, so that differences could not be attributed to potential differences in friction coefficients.

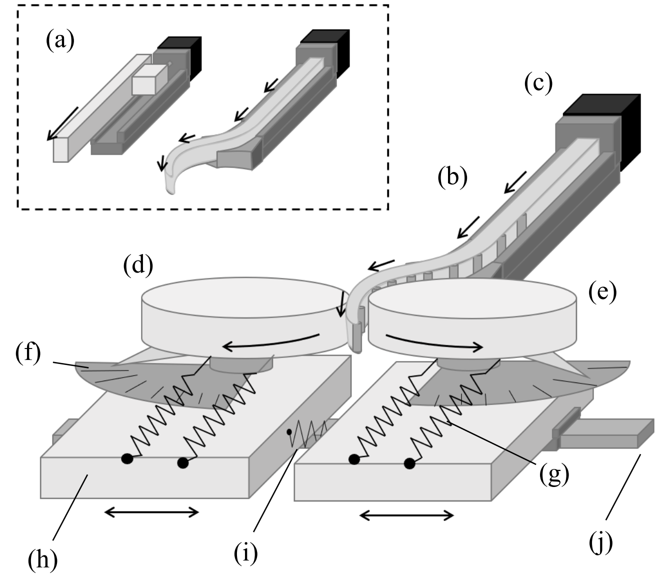

Fig. 5. Schematic of the setup for measuring friction of the gripper finger. Indicated are: (a) straight and object-following bench mark gripper fingers (b) zero-slip finger (c) linear actuator (d) rotatable obstacle cylinder (e) rotatable object cylinder (f) indicators and graduated arcs (g) opposing springs keeping the cylinders in neutral position (h) sliding carriages on to which the cylinder axles and spring are mounted (i) extension spring pulling the cylinders together (j) linear rail for carriages.

3) Initial finger guiding → net force F_{net} (N): The curved wrist channel should ensure that no excessive *net force* is exerted on the object during the grasp manoeuvre. To verify this, a setup was made consisting of a spherical object of D_{mean} = 60 mm on a linear slider, held in a neutral position by two opposing springs with an effective spring coefficient of k_{eff} = 0.19 N/mm, as seen in Figure 6. The gripper was then mounted in line with the slider, with a distance of 2 mm to the object surface, measured from the center of the wrist. Then, by engaging the gripper multiple times, the maximum perturbation Δu from the initial position of the object could be measured, with a precision of +/− 0.25 mm. Finally, using Hooke's law, the magnitude of the net force exerted on the object could be determined as $|F_{net}| = k_{eff}\Delta u$.

4) Structural stiffness → holding force F_{hold} (N): Due to the structural stiffness of the fingers, the gripper has a certain *holding force*, an estimation of which was already given analytically and using FEA in Section II-B. To measure the holding force in practice, a setup was made where the gripper was mounted vertically upward, and an object with diameter D_{mean} = 60 mm and mass m_{obj} = 50 g was placed in the gripper after which the gripper was closed. Using a spring scale, the object was pulled vertically upwards until grip was lost. Using a recording of the experiment, the maximum exerted force by the spring scale could be read with a precision of +/− 25 g, or about +/− 0.25 N. After correction for the objects weight of m_{obj} = 0.5 N, the maximum reaction force (holding force) exerted by the gripper could then be determined.

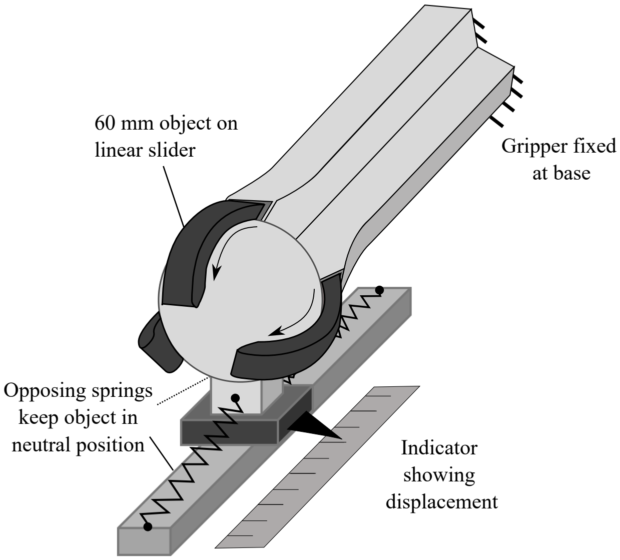

Fig. 6. Setup used for measuring the net force. Using the effective spring coefficient of the two opposing springs and the displacement of the object, the net force exerted by the gripper can be determined.

D. Practical experiment

To verify the performance of the gripper and the newly introduced features as a whole, the gripper was integrated into a fully working robotic system. The setup is shown in Figure 7. The gripper was then applied to the practical case of grasping random tomatoes from a cluttered pile of 32 tomatoes. In a sample population of 50 such tomatoes, their average diameter and height were measured to be 60 +/− 10 mm, and their mass was 130 +/− 40 g. The robotic system consisted of an ABB IRB 1200 robotic arm, controlled and guided via ROS which performed object recognition and position estimation using stereo image sensing. Other than the target object position, no high-level processing was used to avoid the surrounding clutter, such as obstacle recognition or grasp pose planning.

During the experiment, at each grasp attempt, the algorithm chose a target based on the accuracy of the object recognition, meaning that only objects that were roughly free from the top surface could be picked. However, the side surfaces of the target could still be obstructed by surrounding tomatoes. After choosing a target, the robot positioned the gripper vertically, with the center of the gripper wrist at the estimated center of the tomato. The positioning had an accuracy of +/− 5 mm in horizontal and vertical directions. Then, the grasp manoeuvre (propagation of the fingers) was performed and the object was moved to the deposit table and released. This process was repeated until all the tomatoes were removed from the pile. By analyzing the video material of the experiment, the percentage of successful grasps could be calculated. Furthermore, by visual inspection, the percentage of tomatoes that had been damaged could be calculated.

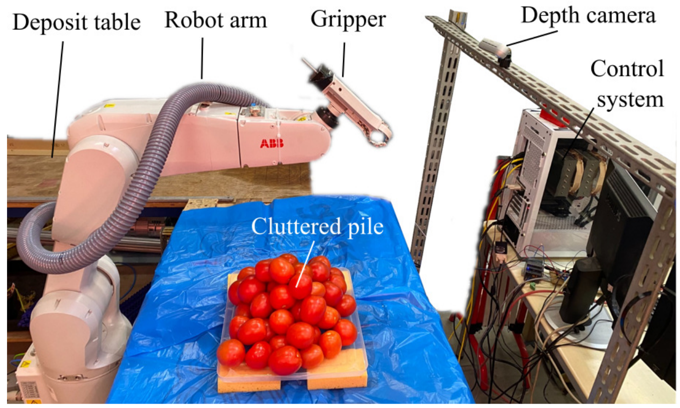

Fig. 7. Practical experiment of grasping tomatoes from a pile, consisting of approximately 4 layers of tomatoes.

III. Results

A. Measurements

In Figure 8, different intermediate positions of the gripper during propagation are overlayed and the final position of the finger was traced. The finger properly propagated forward and did not deviate from the final position during the motion. It closely followed the surface of the object and did not deviate from the thickness of the finger, except for the initial 10 mm after exiting the wrist where it deviated by 3 mm.

The results of the friction measurement are shown graphically in Figure 9 for the obstacle and object. The plotted results can be interpreted as the caused perturbations (rotations) by looking at the left axis $\Delta\theta$, but also as the derived friction forces that were exerted by looking at the appropriately scaled right axis $F_{friction}$. By comparing the resulting perturbation/friction with the benchmark fingers, the designed gripper is seen to decrease the exerted friction force by at least 91% for the obstacle, and at least 98% for the object contact.

The net force exerted during a grasp was measured to be 0.1 N, where the measurement results of 10 consecutive measurements were consistent within the precision of the measurement setup of +/− 0.04 N.

Finally, the holding force was measured as F_{hold} = 3.7 N, as plotted in Figure 10. For comparison, the analytical and FEA estimations are plotted, showing that they underestimated the holding force by 27% and 13%, respectively.

B. Practical experiment

During the experiment, the gripper performed 100% successfully: All 32 tomatoes were moved in exactly 32 valid grasp attempts taken by the robotic system. Two additional attempts were disregarded, since in these cases the robotic system rather than the gripper failed: In once case the operator failed to timely start the grippers actuation and in the other case the robotic system reset during manipulation. After the experiment, 3 tomatoes were found to have punctures in the skin. Tomatoes with minor deformations were not considered damaged. Examples of two damaged tomatoes are given in Figure 11.

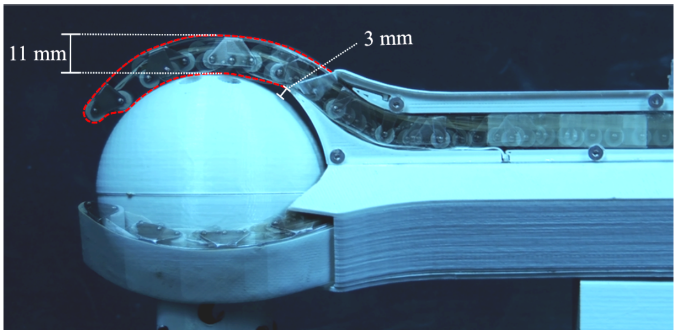

Fig. 8. Overlayed intermediate states of finger engagement, showing that finger propagates forwards within bounds of finger thickness.

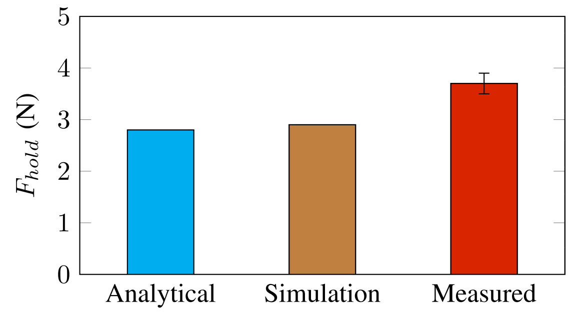

Fig. 10. Measured holding force F_{hold}, compared to the analytical and FEA estimations. The measured value represent the mean of 7 repetitions, with the standard deviation indicated by the error bars. .

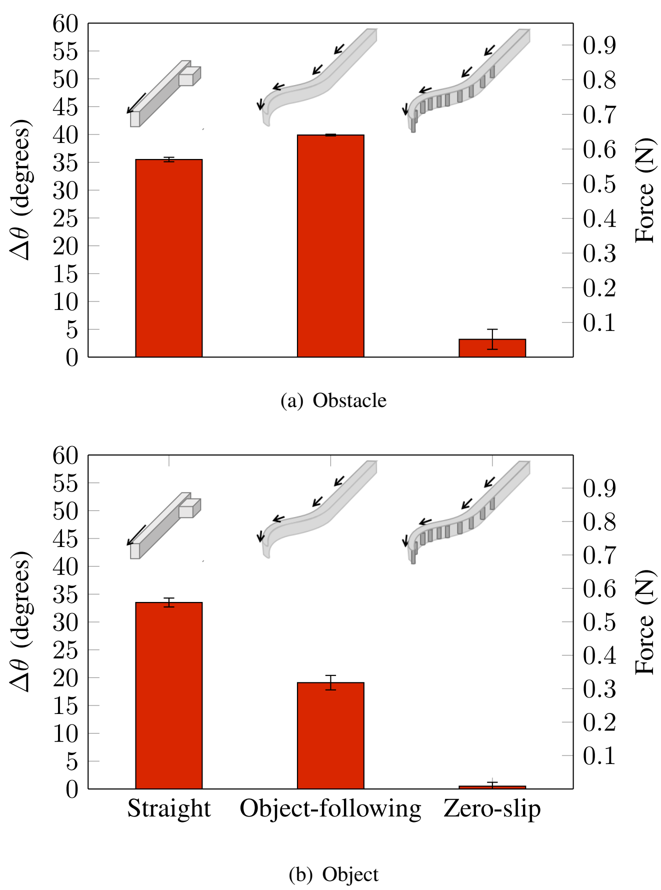

Fig. 9. Rotation / friction force exerted on the (a) obstacle and (b) object cylinder during insertion of different fingers. The plotted values represent the mean of 11 repetitions of each experiment, with the standard deviation indicated by the error bars.

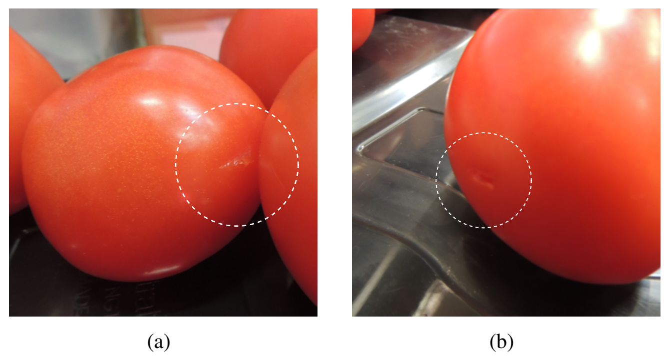

Fig. 11. Examples of damages, where the skin was punctured.

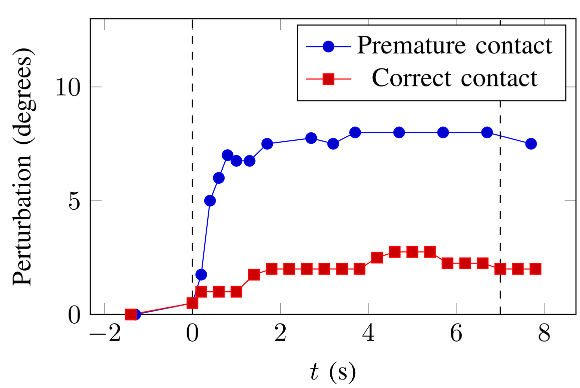

Fig. 12. Perturbation of the obstacle cylinder plotted against the time t (s), where t = 0 s corresponds to the first moment of contact and t = 7 s corresponds to the end of engagement.

IV. Discussion

A. Measurements

The functions were individually tested using several performance metrics. Figure 8 showed that the fingers closely follow the object, which means that the displacement of the obstacles will be limited to approximately the thickness of the finger of 11mm, so any unnecessary displacements are eliminated. Only a small initial deviation of about 3 mm occurs, which gradually decreases to zero at the first 10 mm of the manoeuvre. This is not considered a major problem since the obstacles are the least critical near the top of the object.

As expected, the perturbations (rotations) and friction forces that occurred when the finger was inserted between an obstacle and an object were almost eliminated, with a decrease of 97% at the object surface, and 92% at the obstacle surface. The slightly higher rotation/friction at the latter may be explained by the fact that in the experiment, the finger was retracted while still in contact with the obstacle, which prevented the outside belt from fully retracting. This caused the belt to contact the obstacle prematurely at the next engagement. Figure 12 clearly illustrates this by showing the rotation of the obstacle cylinder during engagement of the finger. A large initial rotation is seen to occur only during initial contact when the outer belt prematurely contacts the obstacle.

The net force that the gripper exerts was measured to be about 0.1 N. Compared to both the expected weight of the objects (m_{obj} = 0.18 N) and the holding force (F_{hold} = 3.7 N), it is orders of magnitude smaller. This indicates that the net force will not damage the object. Furthermore, because of this low push-out force, the gripper could be useful for harvesting operations where objects are suspended from branches, which may easily be perturbed.

The holding force of the gripper was measured to be 3.7 N, or about 200% of the maximum expected object weight. Considering that generally, agri-food objects have the same density close to that of water, the gripper holding force is therefore expected to be sufficient for most agri-food objects of within the maximum diameter for which the gripper was designed. Compared to the analytical and FEA estimations, the grasp force in practice was at least 27% higher, which means that the estimations give a safe minimum for the holding force that will be achieved in practice. An explanation for the differences may be that the estimations assumed frictionless contact, so that the friction between finger and object in practice would have contributed to a higher grasp force. Next to that, due to friction in the belt guidance, the tension in the tendons is in practice expected to be higher than the rubber band tension, thereby increasing the structural stiffness of the fingers.

B. Practical experiment

The practical experiment resulted in an unusually high success rate of the gripper of 100%. From video footage analysis, it was estimated that at least 80% of the tomatoes were obstructed from at least one side by another tomato when grasped. Because the success rate of grasping in clutter was not yet addressed in existing research on grippers, no quantitative comparison of the success rate could be done. Still, it clearly shows the grippers feasibility, especially considering the fact that until now, obstructed objects were generally considered unreachable for caging grippers. Although the success rate was clearly very high, the pile size was limited, so 100% success cannot be guaranteed with larger tests. For instance, during additional testing, it was found that in some edge cases, the gripper could collide with obstacles or would not properly manoeuvre between object and obstacle, especially when the gripper alignment error was excessive. Still, the integration of the gripper with the robotics system was simple in the sense that no obstacle recognition or grasp pose planning was required, showing that the gripper greatly simplifies the task of grasping in clutter.

After the experiment, 3 tomatoes were found to have minor damages. It was not possible to determine during which grasp attempts these damages had occurred or if they were already present before the experiment had started. Considering that the other 94% of the tomatoes were not damaged, the damages may be specific cases in which unintended contact occurred, for example between the edges of the wrist and the object. These unwanted contacts can most likely be resolved by further improvement of the gripper or control system.

C. Future research and uses

Although the designed prototype performed reliably in the lab and practical experiments, it is suggested that new implementations of forward propagating fingers with slip elimination should also be explored, to reduce the complexity of the gripper and to conform to industry standards by making the design less prone to damage and hygienic issues.

The gripper was already tested on tomatoes, which are soft, irregular in size and shape, and easily damaged, showing that the gripper can solve very difficult grasp cases. In the future, the gripper should be tested on a wider variety of objects to further show the wide applicability of the caging gripper, for instance its ability of grasping very slippery or very soft objects, as well as a wider range of sizes and shapes.

Although the results only prove the success of the gripper and the finger mechanism for the specific task of grasping tomatoes from a pile, the implications of the results of this research lie much wider. The grippers ability to grasp partially obstructed objects with little exerted forces, combined with the general ability of caging grippers to grasp difficult objects, in principle makes the gripper suitable for a wide range of tasks which could thus far not be reliably performed with existing grippers. Many examples can be found in the agri-food industry alone, like the bin-picking of slippery and fragile objects like chicken fillets, or the selective harvesting of high-value fruits like tomatoes.

Furthermore, the belt-based adaption of the eversion mechanism, which was invented for the fingers of the gripper, is the first of its kind in the sense that is uses a rigid backbone. This way, it can exert significant manipulative forces by use of moments and axial force, as opposed to the pneumatic eversion mechanisms of previous researches, which are limited by the buckling of the pneumatic columns. This addition of these manipulative functions to the eversion mechanism, opens up a range of possibilities for manipulation tasks in cluttered environments where disturbance or damage to the surroundings causes problems, like in invasive surgery or even rescue operations in earthquake rubble.

V. Conclusions

This research presented a new strategy for obtaining a caging grasp in clutter, which used forward propagating fingers with everting belts to manoeuvre along the object and between surrounding clutter. The gripper was applied to a practical test case of picking and placing tomatoes, and from the 100% success rate of the gripper, it can be concluded that this new strategy is indeed a feasible solution.

The first part of the research consisted of a combination of lab experiments to verify the individual functions that were proposed to minimize displacement and forces on the object and surrounding obstacles. It was shown that the forward propagating fingers closely follow the objects surface, with a maximum deviation of 3 mm. The designed zero-slip belts, which were a mechanical adaptation of existing pneumatic eversion mechanisms, were shown to reduce friction forces and perturbations to be applied to the object and surrounding obstacles by at least 92%. Furthermore, unlike pneumatic eversion mechanisms, the gripper fingers had considerable structural stiffness, which was shown by the high holding force of the gripper of 3.7 N.

Next to these lab experiments, a practical experiment was performed to show the effectiveness of the gripper as a whole, by grasping tomatoes from a pile. The hitherto unseen success rate of 100% showed that with the proposed new strategy for setting a caging grasp by manoeuvering along the object, high success rates could be achieved without requiring obstacle recognition or grasp pose planning.

Although the gripper proved its effectiveness in the practical test case of grasping tomatoes from a pile, more research is needed to see how well the gripper can be applied to the variety of object types in agrifood industry. Furthermore, new implementations of the forward propagating, zero-slip fingers should be explored to reduce complexity and to conform to industry standards of reliability and hygiene.

Overall, the research provided a new insight into the task of grasping, by including the context of clutter already in the stage of the gripper design. By redesigning the gripper to handle interaction with clutter, implementation into a robotic system can be much simpler, and higher grasp success rates may be achieved. Finally, the designed adaptation of the eversion mechanisms combined its manoeuvering capabilities in clutter with the ability to provide manipulations. This opens up a new range of tasks that robots will be able to perform in clutter.

References

[Bac et al., 2017] Bac, C. W., Hemming, J., van Tuijl, B., Barth, R., Wais, E., and van Henten, E. J. (2017). Performance Evaluation of a Harvesting Robot for Sweet Pepper: Performance Evaluation of a Harvesting Robot for Sweet Pepper. *Journal of Field Robotics*, 34(6):1123–1139.

[Bicchi and Kumar, 2000] Bicchi, A. and Kumar, V. (2000). Robotic grasping and contact: a review. In *Proceedings 2000 ICRA. Millennium Conference. IEEE International Conference on Robotics and Automation. Symposia Proceedings (Cat. No.00CH37065)*, volume 1, pages 348–353 vol.1. ISSN: 1050-4729.

[Brown et al., 2010] Brown, E., Rodenberg, N., Amend, J., Mozeika, A., Steltz, E., Zakin, M., Lipson, H., and Jaeger, H. (2010). Universal robotic gripper based on the jamming of granular material. *Proceedings of the National Academy of Sciences of the United States of America*, 107(44):18809–18814.

[Ciocarlie et al., 2014] Ciocarlie, M., Hicks, F. M., Holmberg, R., Hawke, J., Schlicht, M., Gee, J., Stanford, S., and Bahadur, R. (2014). The Velo gripper: A versatile single-actuator design for enveloping, parallel and fingertip grasps. *The International Journal of Robotics Research*, 33(5):753–767. Publisher: SAGE Publications Ltd STM.

[Crooks et al., 2017] Crooks, W., Rozen-Levy, S., Trimmer, B., Rogers, C., and Messner, W. (2017). Passive gripper inspired by *Manduca sexta* and the Fin Ray® Effect. *International Journal of Advanced Robotic Systems*, 14(4):172988141772115.

[Davidson et al., 2016] Davidson, J. R., Silwal, A., Hohimer, C. J., Karkee, M., Mo, C., and Zhang, Q. (2016). Proof-of-concept of a robotic apple harvester. In *2016 IEEE/RSJ International Conference on Intelligent Robots and Systems (IROS)*, pages 634–639. ISSN: 2153-0866.

[Hawkes et al., 2017] Hawkes, E. W., Blumenschein, L. H., Greer, J. D., and Okamura, A. M. (2017). A soft robot that navigates its environment through growth. *Science Robotics*, 2(8):eaan3028. Publisher: American Association for the Advancement of Science.

[Mantriota, 2007] Mantriota, G. (2007). Theoretical model of the grasp with vacuum gripper. *Mechanism and Machine Theory*, 42(1):2–17.

[Meijneke et al., 2011] Meijneke, C., Kragten, G., and Wisse, M. (2011). Design and performance assessment of an underactuated hand for industrial applications. *Mechanical Sciences*, 2(1):9–15.

[Páll and Brock, 2021] Páll, E. and Brock, O. (2021). Analysis of Open-Loop Grasping From Piles. In *2021 IEEE International Conference on Robotics and Automation (ICRA)*, pages 2591–2597. ISSN: 2577-087X.

[Silwal et al., 2017] Silwal, A., Davidson, J. R., Karkee, M., Mo, C., Zhang, Q., and Lewis, K. (2017). Design, integration, and field evaluation of a robotic apple harvester. *Journal of Field Robotics*, 34(6):1140–1159. _eprint: https://onlinelibrary.wiley.com/doi/pdf/10.1002/rob.21715.

[Takahashi et al., 2021] Takahashi, T., Tadakuma, K., Watanabe, M., Takane, E., Hookabe, N., Kajiahara, H., Yamasaki, T., Konyo, M., and Tadokoro, S. (2021). Eversion Robotic Mechanism With Hydraulic Skeletonto Realize Steering Function. *IEEE Robotics and Automation Letters*, 6(3):5413–5420. Conference Name: IEEE Robotics and Automation Letters.

[Xiong et al., 2020] Xiong, Y., Ge, Y., and From, P. J. (2020). Push and Drag: An Active Obstacle Separation Method for Fruit Harvesting Robots. In *2020 IEEE International Conference on Robotics and Automation (ICRA)*, pages 4957–4962. ISSN: 2577-087X.